ROLES OF HFQ-DEPENDENT SRNAS IN *E. AMYLOVORA* REGULATION OF VIRULENCE

By

Jeffrey Kent Schachterle

A DISSERTATION

Submitted to
Michigan State University
in partial fulfillment of the requirements
for the degree of

Genetics – Doctor of Philosophy

2019

ABSTRACT

ROLES OF HFQ-DEPENDENT SRNAS IN *E. AMYLOVORA* REGULATION OF VIRULENCE

By

Jeffrey Kent Schachterle

Erwinia amylovora is the causative agent of fire blight disease of apple and pear trees, causing annual losses of over 100 million USD in the USA. *E. amylovora* cells are disseminated to new hosts by insects, wind, and rain, and then invade susceptible tissues and migrate systemically throughout the host, requiring coordinate regulation of several virulence factors, including production of the exopolysaccharides amylovoran and levan, biofilm formation, flagellar motility, and type III secretion. Complex regulatory mechanisms have evolved in *E. amylovora* that occur at the transcriptional, post-transcriptional, and post-translational levels to control these virulence factors. In my work, I analyze the role of small RNAs (sRNAs) as post-transcriptional regulators of virulence-associated traits in *E. amylovora*.

The Hfq chaperone protein stabilizes sRNAs in the cell, allowing them to interact with and regulate mRNA targets. An *hfq* mutant differs from wild-type cells in several virulence-associated phenotypes including production of the exopolysaccharides amylovoran and levan, biofilm formation, flagellar motility, and type III secretion. *E. amylovora* encodes at least 40 Hfq-dependent sRNAs; in my work, I have systematically made deletion mutants of each sRNA singly, as well as constructed inducible expression vectors for each sRNA. Screening of this sRNA library has shown that several sRNAs contribute to regulation of each virulence phenotype, indicating complex regulation of the traits assessed. Of particular interest, the ArcZ sRNA regulates several of the virulence-associated traits we have assessed, and an *arcZ* deletion mutant loses virulence in both immature pear and apple shoot infection models.

Flagellar motility, which enables *E. amylovora* cells to swim through flower nectar to invade natural openings in host flowers, is regulated by ArcZ. We have shown that ArcZ regulates motility by

regulating the flagellar transcription factor FlhD at both the transcriptional and post-transcriptional levels. Because the ArcZ regulation of FlhD at the transcriptional and post-transcriptional levels has a contradiction in sign, we searched for additional layers of regulation between ArcZ and FlhD. We did so by conducting a transposon screen in the *arcZ* mutant background for suppressor mutants that restored flagellar motility. This screen yielded as the most common suppressor mutation the leucine responsive regulator protein (Lrp), a global transcription factor known for regulation of amino acid metabolism. We have found that Lrp not only acts as a regulator of flagellar motility between ArcZ and FlhD, but that it also reverses the regulatory effects of *arcZ* deletion on amylovoran and levan production, as well as biofilm formation. Our work shows that Lrp is a novel virulence regulator that plays an important role in regulating several virulence-associated traits in conjunction with the sRNA ArcZ.

Transcriptomic comparison between the *arcZ* mutant and wild-type cells confirmed that ArcZ regulates several genes known to also be regulated by Lrp, and also indicated that ArcZ regulates several genes involved in mitigating the threat of reactive oxygen species, including genes encoding a catalase, a thiol-peroxidase, and a peroxiredoxin. We found that catalase makes the greatest contribution to diminishing the threat of exogenous hydrogen peroxide. Additional analysis suggests that ArcZ participates in regulation with an oxidative sensing transcription factor network that includes the transcription factors ArcA, Fnr, and Fur.

This work shows that several sRNAs make small contributions to virulence trait regulation, and that a few sRNAs, like ArcZ, make major contributions to *E. amylovora* virulence. ArcZ regulates several virulence-associated traits through the global transcription factor Lrp, which we have found to be a novel virulence regulator. ArcZ also regulates genes involved in mitigating the threat of reactive oxygen species, which can protect *E. amylovora* cells from host defenses during infection. Thus, ArcZ plays an integral role in modulating phenotypic expression during fire blight disease progression that enables *E. amylovora* to successfully colonize and infect host plants. Mechanistic understanding of *E. amylovora* gene regulation moves us closer to understanding weaknesses that can be exploited for development of novel disease control strategies.

ACKNOWLEDGEMENTS

Greatest and most sincere thanks to my wonderful wife, Elizabeth, and to my awesome boys, Samuel and Richard. Thanks for making every day exciting and worthwhile!

Thanks to George Sundin and all Sundin lab members past and present, as well as several other MSU colleagues for help, support, and friendship along the way.

Acknowledgement of and gratitude for the National Science Foundation Graduate Research Fellowship program. This material is based upon work supported by the National Science Foundation Graduate Research Fellowship under Grant No. DGE1424871.

TABLE OF CONTENTS

LIST OF TABLES

LIST OF FIGURES

CHAPTER 1

The roles of sRNAs as post-transcriptional regulators in phytopathogenic bacteria

I. Post-transcriptional control in bacteria

The ever-changing arms race between phytopathogenic bacteria and their hosts requires pathogens to have rapidly evolving mechanisms for regulation of virulence traits that allow them to overcome host defenses, acquire nutrients, and disseminate to new hosts (1-3). Although traditional views of gene regulation focused on transcription factors that regulate transcription of target genes through protein-nucleic acid interactions, more recent work has shown that in addition to transcription factor control of these traits, additional layers of control are present that regulate the phenotypic output after transcription has occurred. In recent years, both post-transcriptional and post-translational control have grown as fields of studies. One set of regulatory molecules that regulates these host-pathogen interactions is that of small non-coding RNAs (sRNAs) (4). There has been much recent attention to the roles of microRNAs in eukaryotic systems and their role in mediating interactions between pathogens and hosts. MicroRNAs play important roles in host regulation of defense and microRNAs are also used by some fungal pathogens as effector molecules to manipulate host defenses (5). However, the role of sRNAs in bacterial pathogens has grown in recent years and concise reviews summing up the current state of research on sRNAs and their roles in phytopathogenic bacteria are lacking. It is the intent of this review to outline the current status of sRNA research in phytopathogenic bacteria, discuss the many sRNAs that have been identified, the characterization of these sRNAs, and the state of research into the molecular mechanisms of these sRNAS in regulation of their target genes.

Mechanisms of post-transcriptional control in bacteria

Once an RNA has been transcribed, additional factors that influence how long it persists in the cytoplasm as well as how quickly and how many times it is translated if it is protein

coding. These post-transcriptional regulatory mechanisms can be grouped into three main classes based on the molecule interacting on the RNA molecule: protein-RNA interactions, small molecule-RNA interactions, and RNA-RNA interactions.

Post-transcriptional control through protein-RNA interactions can be exerted by a protein sequestering, stabilizing, or degrading a target RNA molecule. The RNA binding protein CsrA (or RsmA) binds to target RNAs harboring appropriate motifs and sequesters the ribosome binding site preventing translation. The ability of CsrA to regulate target RNAs is modulated by the antagonizing small RNAs CsrB and CsrC (6). RNA degrading ribonucleases (RNases) hydrolyze the phosphodiester backbone of RNA molecules in a sequence-signal dependent manner (7). Although bacterial genomes typically encode several RNAses, it is typical that 3 of these are essential: RNase E, RNase P, and oligoribonuclease (Orn) (8). RNase E is typically associated with sRNAs (9), but studies are limited due to its essentiality. Additional post-transcriptional regulatory interactions between protein complexes and RNAs include the role of ribosome translational rate on nascent RNA secondary structure and the inhibition or formation of termination or anti-termination structures in the target RNA (10). This type of regulation is impacted by nutritional status of the cell as based on charged tRNA abundance as in the case of the tryptophan leader peptide (11), and can also be impacted by rare codon usage in the coding region (12).

In addition to protein-RNA interactions, several small molecules can impact RNA molecules post-transcriptionally by affecting the secondary structure of the RNA molecule. In riboswitches, small molecules bind directly to specific structural motifs or aptamers to alter the folding or conformation of the RNA molecule, resulting in altered stability or translation. Small molecules with known binding aptamers include metals, such as manganese (13), amino acids,

such as glycine (14), and other small metabolites, such as cyclic-di-GMP (15). In addition to small molecules binding directly to aptamers, RNA structure and folding can be affected by changes in ionic availability and general stress (16), as well as by changes in temperature (17). These changes to RNA secondary structure can all play a role in affecting RNA interactions with ribosomes, other proteins, and other cell components leading to post-transcriptional regulation of RNAs containing specific structures. Although such regulatory roles may be unpredictable using current computational approaches, patterns suggest that the roles of these conditions in post-transcriptional regulation have evolved to maximize bacterial fitness (16).

RNA molecules regulate each other through base-pairing interactions that are often imperfect and interrupted. However, the secondary structure of each RNA molecule in the interaction could allow for regions of the RNA molecules that are distant to each other in the primary sequence of the RNA molecule to be close together in three-dimensional space (18). Similar to RNA-protein interactions and small molecule-RNA interactions, RNA-RNA interactions exert regulatory effects by altering secondary structure or by altering RNA interactions with protein structures such as ribosomes or RNAses. Because of the short and imperfect base-pairing between sRNAs and target RNAs, chaperone proteins often play critical roles in stabilizing sRNAs and sRNA-target complexes (19-22).

II. Small RNAs of phytopathogenic bacteria and their roles

Phytopathogenic bacteria use small RNAs to regulate several diverse phenotypes. Efforts, primarily in the past decade, have been made to identify and characterize non-coding RNA elements in phytopathogenic bacteria, with particular emphasis on sRNAs that are transcribed from intergenic regions and act in trans on target RNAs and proteins.

One of the most studied sRNA systems in plant pathogenic bacteria is the Csr/Rsm system in which the protein CsrA (or RsmA) acts as a global post-transcriptional regulator, and one or more sRNAs (CsrB and CsrC or RsmB and RsmC) act to sequester CsrA and prevent it from binding to target mRNAs (6). The virulence-associated phenotypes regulated by Csr/Rsm systems, including underlying mechanisms, have been studied in detail in many plant pathogens and reviews of this work are available (23, 24), and thus will not be considered in detail here, but rather the focus will be recent efforts to identify and characterize the roles of other sRNAs and sRNA systems in phytopathogenic bacteria.

Identification of novel sRNAs

sRNA identification studies have resulted in the identification of thousands of putative sRNAs in phytopathogenic bacteria. These sRNAs are identified using a variety of methods, and a summary of sRNA identification studies in phytopathogenic bacteria is found in Table 1.1. Early identification methods relied heavily on computational prediction (25-29)and in some cases microarray signal data from probes matching intergenic regions (30). Additionally, generation and sequencing of cDNA libraries was also used. More recent studies utilize variations of high-throughput sequencing to acquire deep sequencing data from ribosomally depleted total RNA (RNAseq), size-selected small RNAs (sRNAseq), or enzymatically treated differential RNAs (dRNAseq; for transcription start site mapping). The number of sRNAs identified by any one study ranges from seven sRNAs (31); when cDNA library sequencing was the approach) to 1108 sRNAs (32); using an RNAseq approach), which is illustrative of the wide range in the sensitivity of these methods. However, even in studies that utilize RNAseq, several studies identified fewer than 50 sRNAs (33-36), which is further indicative of additional

variations including differences in stringency utilized in each study for selection of thresholds that distinguish putative sRNAs from noise or artefacts (37).

Some sRNA identification studies were limited to certain classes of sRNAs and ignored all others. For example, of two sRNA identification studies in *E. amylovora* one utilized a computational approach and identified 10 sRNAs based on similarity to previously identified sRNAs in other organisms (38), and the other utilized an sRNAseq approach and identified 40 sRNAs (39). Both studies, however, limited their identification to intergenic sRNAs dependent on the chaperone protein Hfq. These numbers of identified sRNAs contrast starkly with the hundreds of sRNAs identified in studies that are inclusive of any class of sRNA.

In sRNA identification, some genera are well studied, and others are quite limited. For example, both *Agrobacterium* and *Xanthomonas* have had multiple high-throughput sequencing studies conducted identifying more than one thousand putative sRNAs in each of these genera (32, 40-44). However, on the understudied end, *Ralstonia* and *Xylella* have only had computational searches for putative sRNAs conducted and lack experimental discovery and validation (45, 46). For these, and other phytopathogenic bacteria lacking sRNA identification, experimental work to identify and validate sRNAs is certainly warranted. Additional phytopathogenic genera lacking sRNA identification include *Pantoea*, *Clavibacter*, and *Dickeya*. Although *Pseudomonads* are well studied in general, the diversity of plant pathogenic *Pseudomonads* merits further experimental work to identify sRNAs in this genus, as the only sRNA identification completed was tangentially noted in a transcriptomic study (47). Other phytopathogenic bacteria that have experimentally identified sRNAs do not at present require further identification but now need characterization of the roles of the identified sRNAs.

Initial characterization of sRNAs is often computational to separate sRNAs into different classes. The broadest separation is between antisense sRNAs and intergenic sRNAs. In this separation it is typically assumed that antisense sRNAs are cis-acting with a single target, and that intergenic sRNAs are trans-acting with potential to interact with one or up to several RNA targets (48, 49). In phytopathogenic bacteria, sRNA identifications (that differentiate between antisense and intergenic sRNAs) have ranged from three to 83 percent of sRNAs identified being classified as antisense, with median of 39 percent (Table 1.1). Additional common characterization of sRNAs include characterization of sRNA length, GC content, and free-energy of predicted secondary structure (34). It is clear that these metrics can be easily generated for all identified sRNAs, but until further work is conducted to associate these metrics with functional characteristics of sRNAs, they are of limited utility. Additional classifications can be predicted based on sRNA sequence and structure, such as ability to interact with RNA binding proteins or chaperones.

An initial limitation following computational characterization of sRNAs is validation of sRNAs. No standardized criteria are followed, leading to sRNA identification studies using validation methods that are limited to comparison to other studies/species, comparison to the Rfam database (50), reverse-transcriptase PCR validation, and northern blot validation. In most sRNA studies, far fewer sRNAs are validated than are identified, resulting in an initial bottleneck in sRNA research (Figure 1.1).

Table 1.1 Studies to identify sRNAs in phytopathogenic bacteria

Genus	Organism	Method	sRNAs identified	Reference
Acidovorax				
	A. avenae	RNAseq	118	(37)
Agrobacterium				
	A. fabrum	RNAseq	1108	(32)
	A. tumefaciens	dRNAseq	228	(41)
	A. tumefaciens	sRNAseq	16	(36)
	A. tumefaciens	RNAseq	475	(40)
Burkholderia				
	B. cenocepacia	Microarray	91	(30)
	B. cenocepacia	Hfq-pull down	24	(67)
	B. cenocepacia	RNAseq	41	(33)
	B. cenocepacia	Computational	17	(26)
	B. cenocepacia	Computational	213	(25)
	Burkholderia spp.	Computational	29	(46)
Erwinia				
	E. amylovora	sRNAseq	40	(39)
	E. amylovora	Computational	10	(38)
Pectobacterium				
	P. carotovorum	Computational	26	(27)
	P. carotovorum	Computational	27	(28)
	P. atrosepticum	RNAseq	31	(34)
Pseudomonas				
	P. syringae (DC3000)	RNAseq	140	(47)
Ralstonia				
	R. solanacearum	Computational	193	(46)
Xanthomonas				
	X. campestris (Xcc)	Computational	176	(29)
	X. campestris (Xcc)	RNAseq	24	(35)
	X. campestris (Xcc)	cDNA library	7	(31)
	X. campestris (Xcc)	dRNAseq	907	(42)
	X. campestris (Xcv)	dRNAseq	23	(81)
	X. oryzae (Xoo)	cDNA library	856	(43)
	X. oryzae (Xoo)	sRNAseq	601	(44)
Xylella				
	X. fastidiosa	Computational	34	(45)

Functional characterization of sRNAs

The identification of thousands of sRNAs in phytopathogenic bacteria suggests that sRNAs must be playing critical roles for bacteria to invest in their transcription. Although certain sRNAs have been validated, such as CsrB/RsmB, that play major roles, most identified sRNAs are not validated and even fewer have any known function. This presents a further constriction of the bottleneck between sRNA identification and biological roles for sRNAs (Figure 1.1). Despite the limited number of functionally characterized sRNAs, several of those tested play important roles in regulation of virulence and virulence-associated traits.

sRNAs that bind to protein targets

In *Pseudomonas syringae* pv. tomato DC3000, the Crc protein acts as a post-transcriptional regulator playing an important role in catabolite repression (51). Two small RNAs, CrcX and CrcZ, will bind to Crc to sequester it and inhibit its post-transcriptional regulatory effects (52, 53). Double deletion mutants lacking *crcX* and *crcY* have growth defects compared to wild-type and the defects are most dramatic with arabinose or mannitol as carbon source. This suggests that the sRNA regulation of Crc and its post-transcriptional regulatory activity are very similar to the Csr/Rsm system in that sRNAs sequester a protein to have ultimate effects on carbon metabolism.

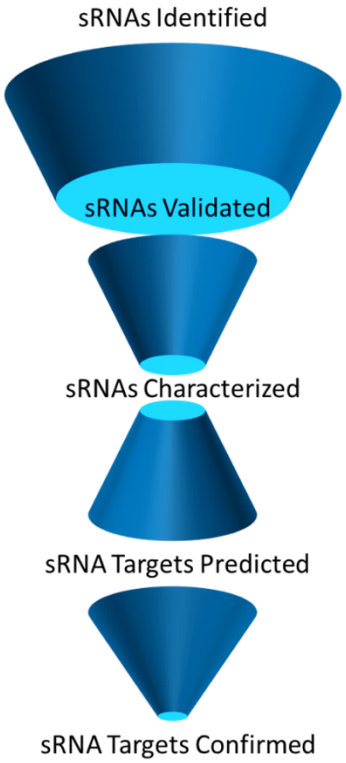

Figure 1.1: High-throughput sequencing and computational power have led to identification and/or prediction of thousands of sRNAs in phytopathogenic bacteria. A conceptual representation of the challenging bottlenecks in current sRNA research. To date, over 3500 sRNAs have been identified across all phytopathogenic bacteria. Depending on the study, up to 25 percent of identified sRNAs are validated but only 31 sRNAs (less than 1%) have reported phenotypic roles. For each sRNA, hundreds of sRNA targets may be predicted computationally, with most being false-positives. Identifying true sRNA targets and thus beginning to link sRNAs mechanistically to phenotype is far more difficult. The two main bottlenecks being faced in sRNA research for phytopathogenic bacteria are currently sRNA phenotypic characterization and mechanistic characterization (target confirmation).

Another unique interaction between an sRNA and a protein is in the case of the ToxIN toxin-antitoxin system of *Pectobacterium carotovorum* (54). In this system the sRNA ToxI will bind to the ToxN toxin protein and act as an antitoxin. In this way the ToxI sRNA acts as a post-translational repressor of the ToxN toxin activity. Although toxin-antitoxin systems are known to have pleiotropic effects with poorly understood mechanisms (55), this type of interaction suggests that anti-toxin sRNAs like ToxI regulate a single target to modulate activity, but do not play roles as global regulators.

sRNAs that interact by base-pairing

Most identified sRNAs act as post-transcriptional regulators by RNA-RNA base-pairing interactions. Despite the imperfections in base-pairing between sRNAs and cognate targets, several attempts have been made to computationally predict targets of specific sRNAs (56-59). These approaches are usually based only on genome sequence, with more advanced prediction tools utilizing sequence data for related organisms to compare conservation of the sRNA and putative targets to inform prediction of conserved targets. Although improvements have been made, attempts to predict sRNA base-pairing targets result primarily in generation of a list of putative targets, most of which are false-positives, each of which must be validated experimentally (60). For this reason, sRNA prediction may result in several candidate targets, but the number of specific targets identified is quite limited (Figure 1.1). Because of this challenge, specific sRNAs of interest are typically first characterized for the phenotypes affected by deletion or over-expression of the sRNA, and further experimentation is necessary to identify and validate targets one by one. Here, the current status of sRNA functional characterization in phytopathogenic bacteria is presented by phytobacterial genus, and a summary of characterized sRNAs is found in Table 1.2.

Agrobacterium

Some of the most advanced characterizations of specific sRNAs have been conducted in the genus *Agrobacterium*. In *A. fabrum*, the RNA1111 sRNA transcribed from the Ti plasmid has been identified, which when knocked out results in formation of fewer tumors compared to wild-type (32). No such effect on aggressiveness was observed when RNA1111 was over-expressed in wild-type *A. fabrum* cells. Comparative transcriptomics between wild-type and *RNA1111* mutant cells, coupled with sRNA target predictions have identified several candidate targets of RNA1111, but these have yet to be confirmed. In *A. tumefaciens*, the sRNAs AbcR1 and PmaR have been well characterized. Infection with a *pmaR* deletion mutant resulted in more tumors per plant relative to wild-type (61). In addition to its role as a negative regulator of virulence, PmaR also acts as a negative regulator of motility. Proteomic comparison between wild-type and *pmaR* mutant cells identified 10 proteins with altered abundance, whose transcripts were confirmed to be direct targets of PmaR. Site-directed mutagenesis identified key bases in PmaR important in direct binding to distinct targets involved in growth and motility. The sRNA AbcR1 was initially identified for its similarity to known sRNAs in *Sinorhizobium meliloti* (62). In *A. tumefaciens*, AbcR1 acts as a regulator of ABC-transport systems (63, 64). Initially characterized for its role in regulating uptake of the plant defense signaling molecule GABA (65), AbcR1 has since been confirmed to bind directly to mRNAs of 14 different ABC transporter operons (63). AbcR1 has also been demonstrated to rely on the chaperone protein Hfq for stability, as the half-life of AbcR1 is reduced four-fold in *hfq* mutant cells. For both PmaR and AbcR1 which both have known direct targets, the candidate direct targets were initially identified using a proteomic approach and then subsequently confirmed.

Burkholderia

In *Burkholderia*, all efforts to characterize specific sRNAs have been conducted in *B. cenocepacia*, which can behave as an opportunistic human pathogen or as an onion pathogen (66). Thus far, phenotypic effects have been shown for MtvR, h2cR, ncS27, and ncS35. MtvR, a trans-acting sRNA, and h2cR, an antisense sRNA, were both reported to affect virulence by regulating *hfq1* or *hfq2*, respectively (67-69). However, two of these studies have since been retracted and the effects of these sRNAs have yet to be confirmed in subsequent studies (70, 71). The sRNAs ncS27 and ncS35 both act as repressors of growth (33, 72). Target predictions for ncS27 suggest its effects on growth are likely due to regulation of carbon metabolism and iron homeostasis (33). Transcriptomic comparison of an *ncS35* mutant to wild-type indicated that several metabolic genes are affected by ncS35, but more details and specific targets have yet to be determined (72). No reports have been made as to whether ncS27 or ncS35 affect virulence.

Table 1.2 sRNAs of phytopathogenic bacteria with characterized phenotypes

Genus	Organism	sRNA	Role	Confirmed Targets[a]	References
Agrobacterium					
	A. fabrum	RNA1111	Virulence	N	(32)
	A. tumefaciens	AbcR1	ABC transporter regulation	Y	(63), (64), (65)
		PmaR	Cell Wall, Motility	Y	(61)
Burkholderia					
	B. cenocepacia	MtvR	Virulence, regulation of hfq translation	Y	(69)
		h2cR	Virulence	Y	(68)
		ncS27	Growth, carbon metabolism	N	(33)
		ncS35	Growth, general metabolism	N	(72)
Dickeya					
	D. dadantii	ArcZ	Virulence, type III secretion, pectate lyase	Y	(76)
Erwinia					
	E. amylovora	ArcZ	Virulence, Amylovoran (EPS), Biofilm, Motility	Y	(38), (39)
		Hrs21	Virulence	N	(39)
		OmrAB	Amylovoran (EPS), Motility	N	(39)
		RmaA	Amylovoran (EPS), Motility	N	(39)
		RprA	Virulence	N	(38)
Pectobacterium					
	P. atrosepticum	RyhB2	sdhCDAB inverse correlation	N	(34)
	P. carotovorum	ArcZ	Virulence	N	(28)
		RprA	Protease, cellulase, and pectate lyase activity	N	(78)
		SraG	Virulence	N	(78)
		ToxI	Antitoxin of ToxN	Y	(54)
Pseudomonas					
	P. syringae	CrcX/Z	Regulate carbon metabolism and catabolite repression by binding to Crc	Y	(53)
		PrrF1/2	Iron and T3SS associated	N	(47)
Xanthomonas					
	X. campestris (Xcc)	sRNAXcc-15, 16, 28	Virulence (triple deletion mutant)	N	(35)
	X. campestris (Xcv)	sX12	Virulence	N	(81)
		sX13	Virulence and T3SS	Y	(82)
	X. oryzae (Xoo)	sRNA-Xoo1, Xoo3, Xoo4	Protein abundance by 2-DGE	N	(43)
		trans217	Virulence and T3SS	N	(44)
		trans3287	Virulence	N	(44)

[a]Targets are only considered confirmed if experimental evidence indicates a directly interaction

Dickeya

Although sRNA studies in *Dickeya* spp. are primarily focused on the Csr/Rsm system, a comparative genomics study in *Dickeya solani* found that a low-virulence strain had a point-mutation in *arcZ* (73). The authors of the study speculated that the mutation in *arcZ* could contribute to virulence because ArcZ is known to regulate virulence-associated traits in several species (38, 39, 74, 75). A recent study in *D. dadantii* also found that an *arcZ* mutant lost virulence (76). Furthermore, the *arcZ* mutant had reduced expression of type III secretion system genes and reduced pectate lyase activity. It was determined that ArcZ directly interacts with mRNA of the transcription factor PecT, and the authors suggest that this interaction with PecT explains the observed effects of ArcZ on virulence-associated traits.

Erwinia

In *Erwinia amylovora* specific phenotypes have been associated with the Hfq-dependent sRNAs ArcZ, Hrs21, OmrAB, RmaA, and RprA (38, 39). Deletion of *arcZ*, *omrAB*, or r*maA* reduced motility (39). Loss of *omrAB* or *rmaA* resulted in increased production of the exopolysaccharide amylovoran. The *arcZ* deletion mutant produced less amylovoran, yet had increased crystal violet staining in a biofilm assay, which was shown to be due to surface hyper-attachment and not formation of mature biofilm. ArcZ was also found to be critical for elicitation of hypersensitive response in non-host tobacco. Loss of *arcZ, hrs21*, or *rprA* resulted in a reduction in virulence on immature pears (38, 39). Because virulence is a complex trait and only ArcZ has been found to affect known virulence-associated traits, this suggests that Hrs21 and RprA must affect virulence through some yet to be characterized mechanism. It is noteworthy that prior to the work contained herein, none of these sRNAS have confirmed direct targets linking them to the associated phenotypes.

Pectobacterium

The soft-rot pathogens of the genus *Pectobacterium* have had sRNAs characterized. The *P. atrosepticum* sRNA RyhB2 is induced under starvation conditions and its abundance has an inverse correlation with abundance of transcripts from the *sdhCDAB* operon (34). In other *Enterobacteriaceae*, RyhB directly interacts with transcripts of the *sdhCDAB* operon (77), and the inverse correlation between RyhB2 and *sdhCDAB* abundance suggests that a similar relationship may exist in *P. atrosepticum*. In *P. carotovorum*, the ToxI sRNA is known to interact directly with ToxN protein as a post-translational antitoxin molecule (54). Furthermore, in *P. carotovorum*, deletion mutants of the sRNAs *arcZ* and *sraG* have reduced virulence compared to wild-type (28, 78). In *Yersinia*, the mRNA of a protein of unknown function is a direct target of SraG, but no phenotypic role has been assigned (79). Thus, the role of SraG in virulence in *P. carotovorum* represents the only known phenotypic function, although the mechanism remains uknown. RprA of *P. carotovorum* is regulated by the global regulator RcsB, and acts as an activator of extracellular enzyme activity, including protease, cellulase, and pectate lyase activities (78). RprA activation of protease activity requires functional flagellar master regulators FlhD and FlhC, suggestive of the fact that RprA has flagellar-associated targets, as has been found in other *Enterobacteriaceae* (80).

Pseudomonas

Although much work has been conducted on the roles of sRNAs in animal pathogenic *Pseudomonads*, studies in plant pathogenic *Pseudomonads* remain quite limited. The iron associated sRNAs PrrF1 and PrrF2 (homologs of RyhB and RyhB2 of the Enterobacteriaceae) are expressed in association with genes harboring binding motifs for the ferric uptake regulator (Fur) transcription factor. In transcriptome analysis, PrrF2 clustered closely with transcripts

coding for the type III secretion system (47). This is consistent with findings that RyhB is associated with type III secretion system. Although these correlations have been found, no studies have specifically characterized the roles of these or other sRNAs in phytopathogenic *Pseudomonads*.

Xanthomonas

In *Xanthomonas campestris* pv. campestris, the sRNAs sRNAXcc-15, sRNAXcc-16, and sRNAXcc-28 were found to be regulated by the RpfF/RpfC system (35). Single deletion mutants of these sRNAs had no effect, but a triple sRNA deletion lacking all three lost virulence in a Chinese radish model of infection, suggesting that these sRNAs may have similar or overlapping sroles allowing for functional redundancy.

In *Xanthomonas campestris* pv. vesicatoria, two sRNAs with roles in virulence have been identified, sX12 and sX13 (81, 82). Transcription of sX12 is dependent on the transcription factor HrpX, a regulator of the type III secretion system. An *sX12* mutant has reduced symptom development when inoculated on a susceptible pepper line (81). Additionally, the *sX12* mutant elicited a reduced hypersensitive response on resistant pepper leaves, suggesting a role in regulation of the type III secretion system, but no differences were detected in abundance of T3SS apparatus proteins in *sX12* cells compared to *X. campestris* pv. vesicatoria wild-type cells. Mutants lacking the sRNA *sX13* also exhibit reduced virulence on susceptible pepper and reduced hypersensitive response on resistant pepper (82). An *sX13* mutant has reduced expression of several type III secretion system components, suggesting that sX13 is a general regulator of the T3SS. It was determined that sX13 does not depend on the chaperone protein Hfq for stability nor function. The sRNA sX13 has 3 stem-loops structures in the predicted secondary structure, each of which is C-rich in the loop region that would be free for base-

pairing. Introduction of point-mutations to these loops had severe effects on sX13 function, suggesting these accessible loops are critical for sX13 interaction with regulatory targets.

In *Xanthomonas oryzae* pv oryzae (Xoo), the small RNAs sRNA-Xoo1, sRNA-Xoo3, and sRNA-Xoo4 have been characterized by proteomic comparison of single sRNA deletion strains to *X. oryzae* oryzae wild-type by two-dimensional gel electrophoresis (43). Excision of protein spots with altered abundance and subsequent identification by mass spectrometry resulted in the identification of several proteins with abundance affected by each sRNA, but further work is needed to determine whether these proteins represent direct targets of these sRNAs, or whether the altered abundance is due to indirect effects. Similarly, phenotypic or physiological roles for these sRNAs remain unknown. Additional sRNAs have been identified in Xoo that have significant virulence phenotypes resulting from deletion (44). These sRNAs, trans217 and trans3287, when knocked out result in a losses of virulence, hypersensitive response and effector secretion, as well as altered HrpX/Y expression. However, these sRNAs overlap protein-coding genes with structural roles in the type III secretion system, rendering knockout mutant analysis ineffective for differentiating between roles of the sRNA and roles of the overlapping protein-coding genes. Further work is needed to positively connect these sRNAs with the type III secretion and virulence phenotypes.

Challenges to sRNA characterization

A major challenge that continues to face sRNA characterization is that efforts are typically focused on few sRNAs because time- and labor-intensive approaches are being utilized. In this way, some sRNAs are selected for screening and are utilized until an sRNA affecting virulence or pathogenicity is found, at which point research efforts are focused on that single sRNA. In order to fully understand the overall roles of sRNAs in phytopathogenic bacteria,

development of high-throughput methods is needed to accelerate this work. This will require both improved methods for generating strains for testing (mutants or expression strains) and higher-throughput methods for assessment of phenotypes of interest. In such efforts, research on sRNAs will be aided by other studies in virulence regulation as sRNAs are better incorporated to existing genome annotations so that other genetic screens and transcriptomic studies will begin to correlate identified sRNAs with traits of interest.

Characterization of RNA chaperone proteins

One way to accelerate characterization of sRNAs is to be able to test whole classes of mutants at once. This is being completed in several phytopathogenic bacteria by targeting the chaperone protein Hfq. Because Hfq acts to stabilize its interacting sRNAs, an *hfq* deletion mutant should result in the phenotype of a functional knockout or knock-down of all Hfq-dependent sRNAs. Thus, any phenotype affected by loss of *hfq* should be affected by at least one Hfq-dependent sRNA. In this way, several sRNA-regulated phenotypes are being identified, leaving the responsible sRNA to be identified.

For nearly all bacterial strains tested, deletion of *hfq* results in loss of virulence with the exception of *Xanthomonas campestris* (*Xcv*) and *Xanthomonas oryzae* (*Xoo*) (Figure 1.2) (43, 82). Because virulence is a complex phenotype with contributions from multiple virulence-associated traits, several additional traits have been linked to *hfq*. Loss of *hfq* results in reduced motility and exopolysaccharide production for all phytopathogenic bacteria for which these phenotypes have been tested in the *hfq* mutant (Figure 1.2). Several plant pathogenic bacteria rely on secretion systems to manipulate host cells, and Hfq has been found to be important for type III secretion in *Dickeya dadantii* (76) and *Erwinia amylovora* (39) and type VI secretion in *Pectobacterium carotovorum* (28) but Hfq was found to have no effect on the *A. tumefaciens*

type IV secretion system (63). In *E. amylovora*, loss of *hfq* resulted in increased crystal violet staining compared to wild-type in a biofilm assay, which was determined to be due to surface hyper-attachment by *hfq* mutant cells, and not formation of mature biofilms (39). In *P. carotovorum*, however, an *hfq* mutant has reduced crystal violet staining compared to wild-type cells in a biofilm assay (28).

In several species, loss of *hfq* results in an *in vitro* growth defect. Phytopathogenic bacteria with growth defects in the *hfq* mutant included *A. tumefaciens* (63), *X. oryzae* (*Xoo*) (43) and *B. glumae* (83). Deletion mutants lacking *hfq* in *E. amylovora* and *X. campestris* (*Xcc*) had no growth defects under the conditions tested (38, 84). For *A. tumefaciens* and *B. glumae*, the growth defect may explain a portion of the reduction in virulence. Interestingly *X. oryzae* (*Xoo*) had a growth defect in one media type (PSA), but not another (MMX), and loss of *hfq* does not reduce virulence (43). This suggests that the MMX media type may be a better representation of *in planta* growth, or that compensatory mechanisms prevent growth defects in the *hfq* mutant from resulting in reduced virulence.

Because each phytopathogenic bacteria infects distinct hosts and occupies distinct niches, each pathogen has its own specially evolved repertoire of virulence factors that enables it to succeed. Hfq plays an important role in regulating several of these specialized virulence traits. In *Xanthomonas campestris* (*Xcc*), loss of *hfq* affected several secreted extracellular enzymes including protease, amylase, and cellulase (84). Similarly, the ability of the *hfq* mutant to cope with salt stresses was compromised. In the soft-rot pathogens *Dickeya dadantii* and *Pectobacterium carotovorum*, loss of *hfq* also reduced secreted cell-wall degrading enzyme activity (28, 76). In *Burkholderia glumae*, secreted enzymes, such as metalloprotease were

unaffected by loss of *hfq1* or *hfq2*, but production of the phytotoxin toxoflavin was lost in the *hfq1* mutant (83). Virulence-associated traits affected by *hfq* are summarized in Figure 1.2.

In addition to Hfq, an additional sRNA chaperone protein, ProQ has been recently described, and more sRNA chaperones likely exist (49). Although these additional RNA chaperones are functionally uncharacterized to date in any phytopathogenic bacteria, the approach of knocking out the chaperone has thus far identified several phenotypes regulated by Hfq (and Hfq-dependent sRNAs). This same approach promises to be an effective and efficient starting point for characterizing the functional roles of sRNAs associated with these novel RNA chaperones.

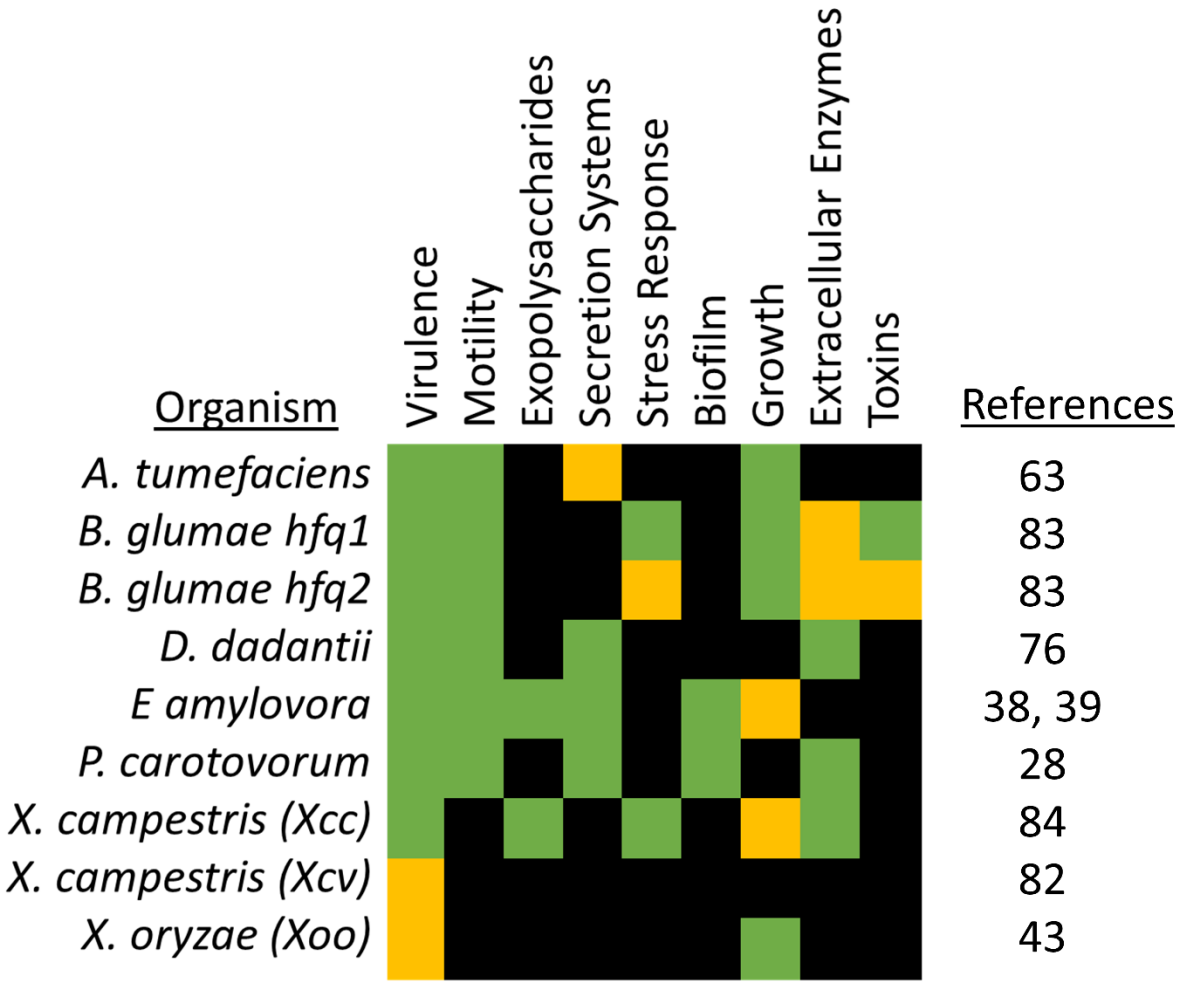

Figure 1.2: Traits known to be affected by Hfq in plant pathogenic bacteria. Green indicates that the trait was tested and *hfq* deletion resulted in an impact on the trait compared to wild-type. Yellow indicates that the trait was tested but that *hfq* deletion had no effect. Black indicates that the indicated trait was not tested or not reported.

III. Characterization of Hfq-dependent sRNAs in *Erwinia amylovora*

Because of the large number of sRNAs identified in phytopathogenic bacteria, the objective of this research is to characterize virulence-associated phenotypes associated with many identified sRNAs and to elucidate underlying mechanisms of regulatory control by identifying targets and uncovering regulatory pathways involved in sRNA regulation of virulence traits.

Rationale for use of *E. amylovora* as study model

Erwinia amylovora, the fire blight pathogen, is an ideal model for the functional study of sRNAs, as it is an economically important problem. Each year, fire blight causes losses of greater than $100 million USD in the United States alone (85). Despite more than a century of research into pathogen biology and control strategies, it persists as an ongoing challenge to growers. Increased understanding of the genetic mechanisms underlying disease development and regulation is essential for development of novel fire blight control strategies (86). In this way, sRNA research can provide a more complete understanding of how *E. amylovora* cells fine-tune regulation in response to the host environment.

As a pathogen, *E. amylovora* utilizes several well characterized virulence factors to successfully infect hosts. Motility enables the bacterial cells to migrate to susceptible host tissues (87, 88). *E. amylovora* produces three main exopolysaccharides, amylovoran (89), levan (90), and cellulose (91), which facilitate biofilm formation and protection from host defenses and other environmental threats (92, 93). To suppress host defenses, *E. amylovora* utilizes a type III secretion apparatus to deliver effector proteins directly to the host cell cytoplasm (94-96). Appropriate expression and control of these virulence-associated traits during disease

development are critical for bacterial success across the cell- and tissue-types encountered during systemic infection of a host.

For research on characterization of Hfq-dependent sRNAs as virulence regulators, *E. amylovora* is an ideal model because several roles for Hfq have been determined already (38, 39). An *E. amylovora hfq* mutant is impacted in each of the major virulence traits, including production of the exopolysaccharides amylovoran and levan, biofilm formation, flagellar motility and type III secretion. Additionally, sRNA identification studies in this pathogen have specifically sought to identify Hfq-dependent sRNAs, rather than all sRNAs. Of the 42 Hfq-dependent sRNAs identified in *E. amylovora*, 26 sRNA deletion mutants have been generated and have been partially characterized (38, 39). This resulted in the finding of 5 sRNAs with roles in virulence or modulation of virulence-associated traits. As not all sRNA deletion mutants have been generated, there remain additional sRNAs to be characterized by chromosomal deletion, and none of the Hfq-dependent sRNAs have been analyzed for phenotypic effects upon overexpression (Figure 1.3). This suggests that several previously unknown relationships between Hfq-dependent sRNAs and virulence associated traits may be uncovered by systematically studying deletion and overexpression of each sRNA.

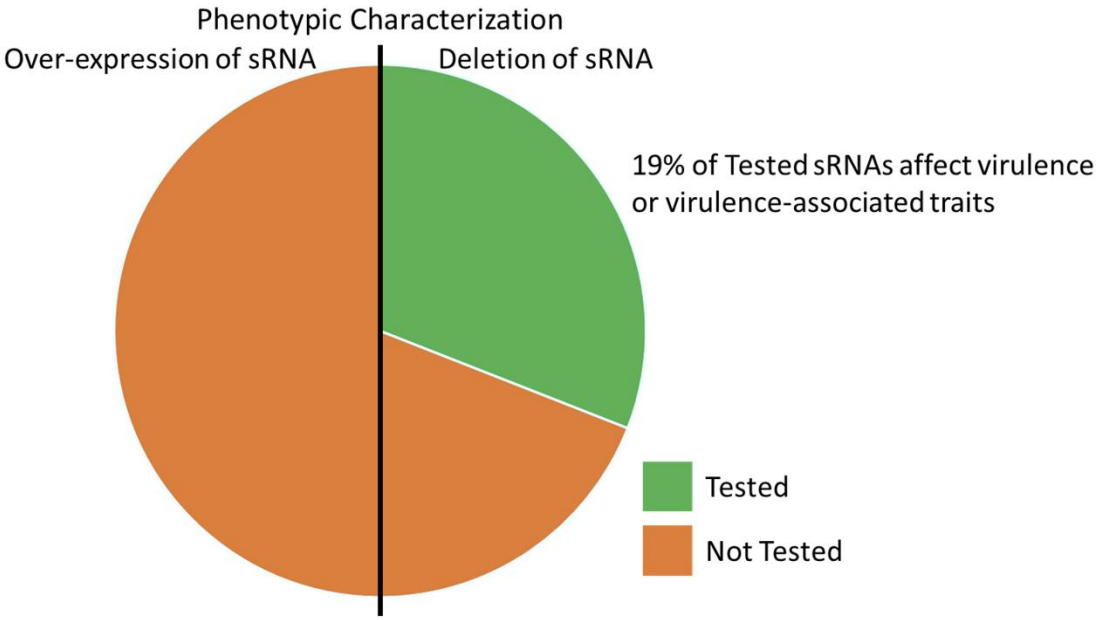

Figure 1.3: *E. amylovora* is an ideal system for testing the roles of sRNAs. 62% of known Hfq-dependent sRNAs have been phenotypically tested using deletion mutants. Of these 19% affect virulence or virulence associated traits. None of these sRNAs have been tested for phenotypic effects when over-expressed. If the rate of 19% is representative of all, by screening the remaining sRNAs we expect to find an additional 11 sRNAs phenotypically linked to virulence-associated traits.

Because *E. amylovora* is closely related to other *Enterobacteriaceae* (including important plant pathogens and human/animal pathogens), there are several benefits to using *E. amylovora* as a model. It is possible that for conserved sRNAs, regulatory roles and mechanisms may also be conserved. For this reason, the findings from studying sRNA regulation of virulence in *E. amylovora* may also contribute to understanding of virulence regulation in several other enteric pathogens. Additionally, like other *Enterobacteriaceae, E. amylovora* is genetically tractable and many genetic manipulation methods are effective. In contrast to human or animal pathogenic members of *Enterobacteriaceae*, study of infection by *E. amylovora* can be conducted using the primary host without the concern of using animals for testing.

The main aim of this study is to characterize virulence-associated roles of Hfq-dependent sRNAs in *E. amylovora* and elucidate mechanisms underlying how sRNAs are regulating associated phenotypes. Critical to this aim is leveraging high-throughput approaches and technologies such as high-throughput phenotyping and sequencing, and for the discovery and characterization of novel sRNA-phenotype and sRNA-target relationships.

Goals of this study

To characterize the virulence associated roles of Hfq-dependent sRNAs in *E. amylovora* efforts are focused on accomplishing the following goals.

Goal 1: Functionally characterize *E. amylovora* sRNAs and their roles in virulence-associated trait regulation. To accomplish this goal, a library of sRNA single-deletion mutants and overexpression strains has been generated and assessed for several phenotypes.

Goal 2: Determine mechanisms of regulation for select sRNA-virulence-trait combinations. A focus on flagellar motility and the sRNA ArcZ has uncovered several novel post-transcriptional regulatory roles for this sRNA.

Goal 3: Utilize transcriptomic analysis for discovery of novel sRNA-virulence trait associative relationships. High-throughput RNA sequencing of the *E. amylovora* wild-type and Δ*arcZ* mutant strains has revealed novel virulence roles of this sRNA and putative underlying molecular mechanisms.

The work to accomplish these goals through the characterization of virulence-associated phenotypic and mechanistic roles of sRNAs in *E. amylovora* and resultant findings are herein presented and discussed.

Conclusion

Although extensive work has been conducted to identify sRNAs in phytopathogenic bacteria, work to characterize the roles and mechanisms of the identified sRNAs has only begun and presents a major bottleneck to understanding post-transcriptional regulation and the role it plays in disease development. In this work, Hfq-dependent sRNAs have been evaluated for phenotypic effects and molecular mechanisms using *E. amylovora* as a model for this study. In this undertaking, high-throughput phenotyping and sequencing approaches have been utilized. The findings of this work provide insights into roles of sRNAs in post-transcriptional regulation and how that regulation fits into virulence regulatory networks. Furthermore, these studies can serve as a model for similar studies in other phytopathogenic bacteria.

CHAPTER 2

Systematic study of the roles of Hfq-dependent sRNAs in regulation of virulence-associated traits in *Erwinia amylovora*

I. Abstract

Erwinia amylovora, the causative agent of fire blight disease of apple and pear trees, coordinates gene expression as it passes through several host environments, overcomes host defenses and emerges to disseminate to new hosts. *E. amylovora* has evolved to precisely regulate distinct virulence processes to be expressed during critical points in infection. Here we report a systematic study of the roles of Hfq-dependent small RNAs as post-transcriptional regulators of virulence-associated traits that play important roles in fine-tuning the regulation of critical virulence factors. In our study we systematically screened each identified sRNA by generating single-sRNA deletion mutants and overexpressing each sRNA singly in the wild-type genetic background. Several virulence-associated phenotypes were assessed in our library of sRNA mutants and overexpression strains, and we identified novel virulence functions for several sRNAs. Of note, we found that deletion of the sRNA Hrs1 led to a reduction in virulence, and we found that the sRNA Hrs21, previously associated with virulence by an unknown mechanism, is linked to multiple virulence-associated phenotypes. This work increases our understanding of the essential roles that sRNAs are playing during disease development in *E. amylovora* and highlights the importance of post-transcriptional regulation in the evolution of this pathogen.

II. Introduction

In recent years, research on plant-microbe interactions has seen great emphasis placed on riboregulation, in which RNA molecules play a major role in controlling cellular processes. In Eukaryotes, this emphasis has been observed in RNA mediated silencing and their role in mediating host defense processes (4, 97-99), as well as in genome editing, where small guide RNAs guide CRISPR complexes to target nucleic acids (100, 101). In Prokaryotes, technological advances, especially in high-throughput sequencing, have enabled discovery of

thousands of transcribed, yet non-coding small RNA (sRNA) molecules. Many of these prokaryotic sRNAs exert regulatory effects through base-pairing with target RNA molecules and can be classified as cis-coded antisense sRNAs (102, 103), trans-coded intergenic sRNAs (18), and extended 5' and 3' UTRs with regulatory functions (104). A major challenge following identification and initial classification of these sRNAs is the characterization of their biological functions. Prokaryotic sRNAs that are studied are those that are dependent on the chaperone protein Hfq (20, 21). As a chaperone, Hfq typically binds to AU rich RNAs and has stabilizing effects (20, 105). Hfq forms homohexamers, and each homohexameric complex can bind to an sRNA and its mRNA target to facilitate interactions (106, 107). Estimates in *Escherichia coli* suggest that in each cell there may be 5,000 to 10,000 hexameric Hfq complexes at once, allowing Hfq to interact with multiple different sRNAs and participate in their regulatory roles (107). Global studies of Hfq-RNA interactions indicate that Hfq interacts with dozens of sRNAs, each with its own set of cognate RNA targets (48, 49, 104).

Because Hfq-dependent sRNAs are dependent on Hfq for their stability and function, *hfq* deletion mutants presumably represent bacteria deficient in all Hfq-dependent sRNAs, suggesting that study of *hfq* deletion mutants is a potential method for identifying roles of Hfq-dependent sRNAs. Studies of the roles of Hfq-dependent sRNAs in plant pathogenic bacteria have found several virulence-associated phenotypes affected in *hfq* deletion mutants. Determinations of roles of Hfq through deletion of *hfq* have been conducted in *Agrobacterium tumefaciens* (63, 108), *Burkholderia glumae* (83), *Dickeya dadantii* (76), *Erwinia amylovora* (38, 39), *Pectobacterium carotovorum* (28), *Xanthomonas campestris* (84), and *Xanthomonas oryzae* (43). In all species and strains tested in these studies, deletion of *hfq* results in altered motility, exopolysaccharides, and biofilm formation. In some but not all species, Hfq also affects growth

(43, 83, 108), type III secretion (28, 39, 76), and stress response (83, 84). From this body of work, it is evident that in phytopathogenic bacteria, Hfq plays a critical role as a global regulator. However, it is unclear which Hfq-dependent sRNAs mediate these effects, which is a major limiting factor in the advancement of research in this area.

Erwinia amylovora, causative agent of fire blight disease of apple and pear trees, utilizes several virulence mechanisms to successfully colonize and infect susceptible hosts (109). For example, *E. amylovora* uses flagellar motility to swim through nectar and move to susceptible tissues (87, 88, 110). Catalases, exopolysaccharide production, and biofilm formation provide protection and favorable microenvironments to guard against host defense responses and build large cell densities (92, 93, 111). *E. amylovora* cells suppress host defenses through delivery of effector proteins via the type III secretion apparatus (94-96). Because *E. amylovora* systemically infects host flowers, leaves, shoots, and woody tissues, there is a high degree of complexity in the variety of cell types and structures with which the bacteria must successfully interact to infect and cause disease (112, 113). Critical to such success is effective control of expression of the virulence traits. Although transcriptional control plays a major role in this, post-transcriptional and post-translational regulations are required for maximal fitness.

E. amylovora is an effective model for the study of the roles of individual Hfq-dependent sRNAs because of its several virulence-associated phenotypes (109) and genetic tractability (114). Hfq-dependent sRNAs have been identified as well (39). Additionally, the roles of several transcription factors and associated regulatory networks are well characterized in control of virulence-associated traits. Examples of these transcriptional regulatory networks include: Rcs phosphorelay control of the amylovoran biosynthetic gene cluster (115), the HrpX/Y-HrpS-HrpL signaling cascade control of type III secretion system genes (116, 117), and the RlsA,

RlsB, RlsC proteins as transcriptional regulators of the levansucrase gene, *lsc* (118). The conservation of several transcription factor regulons among *Enterobacteriaceae* provides additional insight into the transcriptional regulatory modules (119). The current understanding of transcriptional control of several traits in *E. amylovora* enables sRNA research to place the effects of specific sRNAs within the context of specific regulatory modules with which they may interact.

Efforts to characterize the roles of Hfq-dependent sRNAs in control of virulence-associated phenotypes were partially completed in the deletion of 26 Hfq-dependent sRNAs (38, 39); however, this characterization was incomplete in that deletion mutants of an additional 16 Hfq-dependent sRNAs were not constructed, and only mutants were studied. In this work we generated a library of Hfq-dependent sRNA single mutants in *E. amylovora*, as well as a library of expression plasmids of Hfq-dependent sRNAs in *E. amylovora* wild-type strain Ea1189. We have tested these strains for a variety of phenotypes, including several virulence-associated phenotypes and have identified several novel relationships between *E. amylovora* Ea1189 Hfq-dependent sRNAs and virulence-associated traits, and we observed that deletion of the sRNA *hrs1* results in reduced virulence in an immature pear infection model.

III. Materials and methods

Culture conditions, media types, growth, and plasmids

Strains and plasmids generated and used in this study can be found in Table A.1 and Table A.2, respectively. *E. amylovora* strains were cultured in LB (10 g L^{-1} tryptone, 5 g L^{-1} yeast extract, 5 g L^{-1} sodium chloride) media at 28^{o}C, except where noted for specific assays. *Escherichia coli* strains were routinely cultured in LB media at 37^{o}C. When appropriate, the antibiotics ampicillin (100 µg mL^{-1}) and/or chloramphenicol (10 µg mL^{-1}) were added to culture

media. For induction of sRNA overexpression strains, isopropyl-β-D-1-thiogalactopyranoside (IPTG) was added to a final concentration of 1 mM.

Single sRNA deletion mutants were generated using a lambda-red recombinase approach as described (120). Expression plasmids were generated using traditional cloning methods into vector pHM-tac (121). Oligonucleotides used for generation of deletion mutants and overexpression constructs are found in Table A.3.

Swimming motility assay

For swimming motility assay, cells from overnight cultures were collected and adjusted to an OD_{600} of 0.2. Cell suspensions were stab inoculated into soft agar media (0.25% w/v agar; 10 g L^{-1} tryptone, 5 g L^{-1} sodium chloride) and incubated at 28^{o}C for 24 hours. Plates were imaged and the halo area covered by swimming cells was quantified using ImageJ (122).

Determinations of exopolysaccharides and biofilm assays

Assessment of production of the exopolysaccharide amylovoran was conducted as described (123), using reduced volumes to facilitate completion of the assay in a 96-well microtiter plate. Briefly, overnight cultures grown in LB were resuspended in MBMA (per liter, 3 g KH_2PO_4,7g K_2HPO_4, 1 g $(NH_4)_2SO_4$, 2 ml glycerol, 0.5 g citric acid, 0.03 g $MgSO_4$) with 1% (wt/vol) sorbitol to an OD_{600} of 0.2 and grown for 48 hr at 28^{o}C, as appropriate IPTG was added to a final concentration of 1mM. Culture supernatants were mixed in a 20:1 ratio with 50 mg mL^{-1} cetylpyridinium chloride and mixed well. Resulting turbidity measured as OD_{600} and values were normalized to the final OD_{600} of the cells grown in MBMA to account for any variation in growth in the MBMA media.

Determination of levansucrase activity secreted into culture supernatants was completed as described (124). Briefly, supernatants from overnight cultures grown in LB or LB with IPTG

were mixed in a 1:1 ratio with phosphate buffered sucrose (2 M sucrose, 0.5x PBS), and incubated for 24 hrs at 37ºC. The OD_{600} (turbidity) of the resulting solution was measured and normalized to the cell density of the culture from which the supernatants originated to account for any variation in growth.

Biofilm formation was assessed using a 96-well microtiter plate assay as described (125). Briefly, cells were adjusted to an OD_{600} of 0.2 and grown for 48 hrs at 28ºC in wells of a microtiter plate. Planktonic cells were removed by inverting and draining the plate. Adherent cells were heat fixed to the microtiter plate by drying at 85ºC and then staining with 1% crystal violet. Excess stain was rinsed away using excess distilled water. Once dry, the stain in each well was resolubilized using a 4:1 (vol/vol) mix of ethanol and acetone and the OD_{595} was measured.

Catalase assay

Catalase activity was assessed as described (126). Briefly, cells grown overnight were collected and suspended in phosphate buffered saline at an OD_{600} of 0.4. Cells were mixed in a 1:1:1 ratio with 1% (vol/vol) Triton X-100 and 8M hydrogen peroxide. Catalase activity resulted in evolution of gaseous bubbles, which were stabilized by the Triton X-100 detergent and subsequently measured and normalized relative to the catalase activity of wild-type cells. To qualitatively assess catalase activity in culture supernatants, supernatants from overnight cultures were mixed in a 1:1 ratio with 8M hydrogen peroxide and monitored for formation of bubbles.

Heat shock transformation and reporter fusion assay

Chemically competent cells were prepared using the TSS method as described (127). Briefly, cells grown to exponential phase were collected and resuspended in 0.1 volumes of ice-cold TSS buffer (5 g PEG8000, 1.5 mL 1M $MgCl_2$, 2.5 mL DMSO, adjust volume to 50 mL with

liquid LB). Cells (50 µL) were added to a chilled tube containing 2 µL of purified plasmid. Following incubation on ice for 30 minutes, cells were heat-shocked by transferring tubes containing cells to a heat block held at 42°C for 50 seconds and returning the cells to ice for 2 minutes. To recover the cells, 150 µL of liquid LB were added and cells were incubated at 28°C for 1.5 hrs with agitation. Successful transformants were selected on solid media containing appropriate antibiotics. Strains carrying reporter plasmids were grown overnight in LB, then induced in *hrp*-inducing minimal media (HIMM, 128) and induced with IPTG. Fluorescence of the green fluorescent protein reporter was measured using a Spark microplate reader (Tecan, Männedorf, Switzerland) with 488 nm excitation and 535 nm emission wavelengths.

Immature pear virulence assay

Twenty-six mutant strains were previously tested for virulence using an immature pear model (38, 39). In this work, the remaining mutants were assessed for virulence on immature pears using the same method as previously. Briefly, immature pears were wounded and inoculated with 1 x 10^4 cells from overnight cultures and incubated at 28°C with high relative humidity. Necrotic and water-soaking symptoms were measured 4 days post-inoculation. Overexpression strains were not tested for virulence due to concerns regarding ability to IPTG-induce and select for plasmid maintenance during infection, especially if the induction resulted in a severe fitness defect, which would create high pressure for plasmid loss or instability.

Computational and statistical analyses

Generation of virulence trait heatmap and principal component analysis were conducted using ClustVis software (129). For analyses, data were not scaled because observations were already normalized to the *E. amylovora* Ea1189 wild-type phenotypes. For each virulence trait, each strain was tested with at least four biological replicates. In assessment of statistical

differences in all traits, a conservative Bonferroni multiple hypothesis correction was applied (130) because of the high number of strains and traits being tested.

IV. Results

A library of sRNA deletion mutants was generated for all *E. amylovora* Ea1189 Hfq-dependent sRNAs previously identified, with the exceptions of *hrs3* and *hrs26*, for which we were unable to successfully obtain mutants after several attempts. Subsequent analysis indicated that *hrs3* has experienced a tandem duplication and two copies of the sRNA are present in the *E. amylovora* genome, which we hypothesize to be the reason we were unable to delete this sRNA. The sRNA *hrs26* is located between *pepT* and *EAM_1768*, encoding an uncharacterized hypothetical protein. Using the sRNA expression plasmid pHM-tac (121), we constructed an expression plasmid for each *E. amylovora* Hfq-dependent sRNA, and transformed each plasmid singly into wild-type *E. amylovora* strain Ea1189. We selected 9 sRNA expression strains and evaluated the sRNA overexpression upon treatment with IPTG by quantitative real-time PCR. We found that IPTG treatment increased expression of each of these sRNAs (Figure 2.1).

We assessed the *E. amylovora* Hfq-dependent sRNAs for simple parameters and found a wide length distribution and a pattern of low GC content. sRNAs ranged from 54 to 244 nucleotides, with a mean length of 115.5 nucleotides (Figure 2.2A). In GC content, Hfq-dependent sRNAs ranged from 33.3 % GC content to 60 % GC content, with an average of 43.9 % GC content (Figure 2.2B). Only one of the Hfq-dependent sRNAs in *E. amylovora*, *hrs4*, had GC content greater than the genome-wide average of 53.6 % GC content.

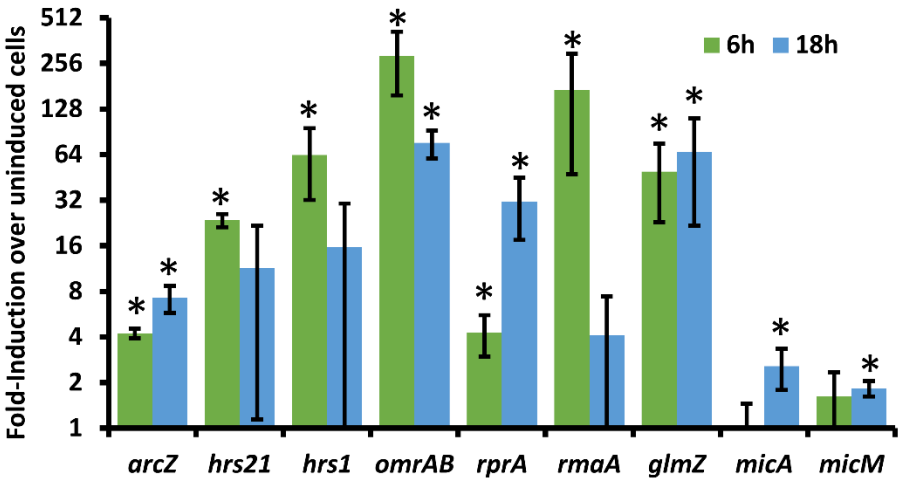

Figure 2.1: qPCR confirmation of sRNA overexpression plasmids. Total RNA was isolated from cells grown in LB for 6 or 18 hrs, with and without IPTG to induce sRNA expression. Quantitative real-time PCR was conducted with cDNA synthesized from total RNA as template with *recA* used as an endogenous control. Asterisks indicate significant increase ($P < 0.05$) relative to uninduced cells by student's t test.

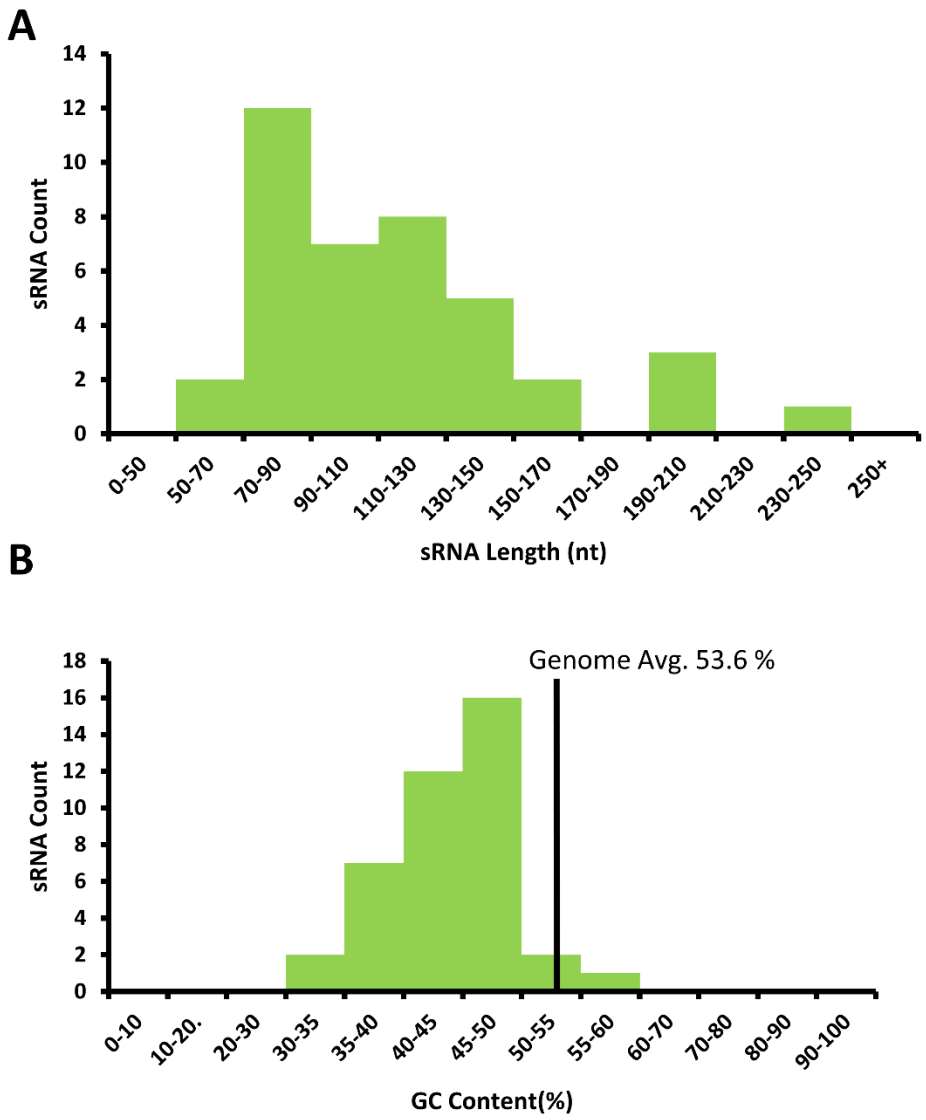

Figure 2.2: Hfq-dependent sRNAs have a broad size distribution and in general have low GC content. Histograms of sRNA lengths (A) and percent GC content (B). Vertical line in panel B indicates genome-wide average GC content.

In a general assessment of the strains in our mutant and overexpression libraries, we did not observe any differences in gross colony morphology when grown on LB solid media. Similarly, we stained cells for each strain in our sRNA mutant and expression libraries with crystal violet and observed cell morphology at 400X magnification and did not find any strains in our libraries that differed from wild-type morphology when grown in LB media (data not shown).

Flagellar motility

We observed six sRNA deletion mutants with altered swimming motility and nine sRNAs that affected swimming motility when overexpressed (Figure 2.3). Among the sRNAs that affected swimming motility were three sRNAs ArcZ, OmrAB, and RmaA, previously reported to affect swimming motility in *E. amylovora* (39, 131). In addition to these three mutants, deletion of *hrs25* or *hrs1* decreased swimming motility relative to wild-type *E. amylovora* Ea1189 cells. The sRNA *hrs7* was the only sRNA that increased swimming motility when deleted. Hrs7 is similar to the sRNA FnrS of *Escherichia coli* and other members of the *Enterobacteriaceae* (Figure 2.4). Overexpression of the sRNA Spot42 increased swimming motility, and induction of Hrs10, Hrs12, Hrs13, Hrs32, or Hrs33 reduced swimming motility relative to wild-type cells carrying empty vector.

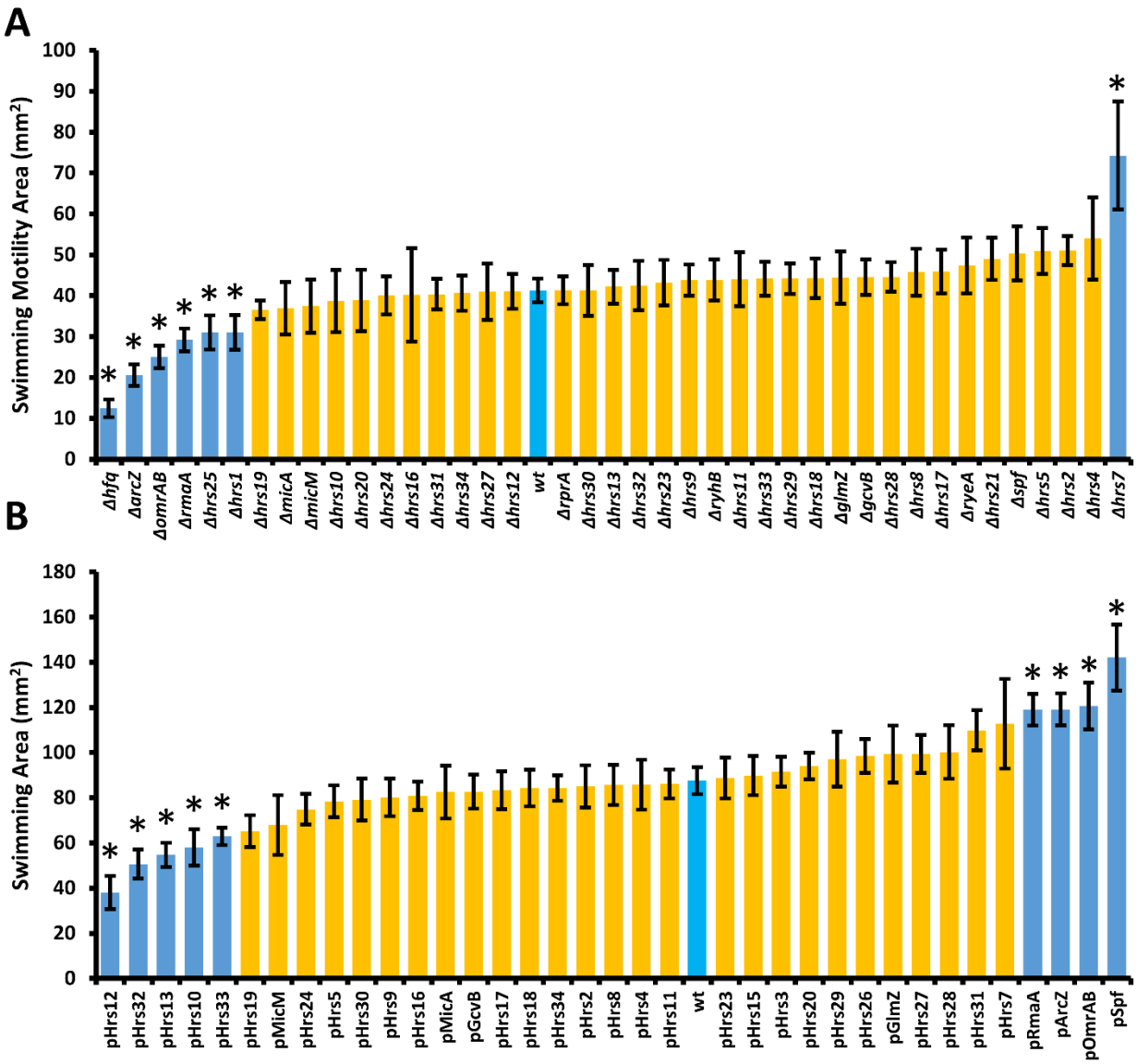

Figure 2.3: *E. amylovora* Ea1189 Hfq-dependent sRNAs modulate flagellar motility. Swimming motility was assessed following 24 hrs of incubation after strains were stab inoculated in soft-agar (0.25% w/v agar). sRNA deletion mutants, Δ*hfq* deletion mutant, and wild-type cells were compared (A). sRNA overexpression strains were compared to wild-type carrying empty pHM-tac under inducing conditions (B). Asterisks indicate significant differences ($P_{adj} < 0.05$) by student's t test with Bonferroni correction.

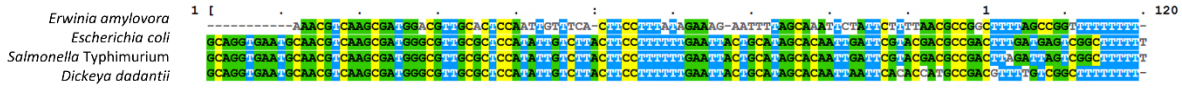

Figure 2.4: *E. amylovora hrs7* is similar to, yet distinct from *fnrS* of other *Enterobacteriaceae*. Multiple sequence alignment between *E. amylovora hrs7*, and *fnrS* of *Escherichia coli, Salmonella* Typhimurium, and *Dickeya dadantii*.

Amylovoran production

To assess production of exopolysaccharides, we grew strains on minimal medium with sorbitol as the sole carbon source and monitored growth and morphology. We observed that the Δ*hfq* mutant was non-mucoid compared to wild-type *E. amylovora* Ea1189 cells, and that the Δ*hrs21* mutant was unable to grow on this minimal medium (Figure 2.5). To verify if this was due to use of sorbitol as the carbon source, we tested glucose, fructose, and sucrose as carbon sources and observed that the Δ*hrs21* mutant is unable to grow on this minimal medium regardless of the carbon source (data not shown). When tested in liquid culture, eight sRNA deletion mutants exhibited altered amylovoran production, and 15 sRNAs affecting amylovoran production when overexpressed (Figure 2.6). Of the 15 sRNAs affecting amylovoran when overexpressed, 12 had negative effects on amylovoran and only 3 had positive effects, suggesting that amylovoran is subject to tight regulation and is closely tied to sRNA regulation. The sRNAs ArcZ and OmrAB, previously shown to affect amylovoran production, were confirmed for this activity.

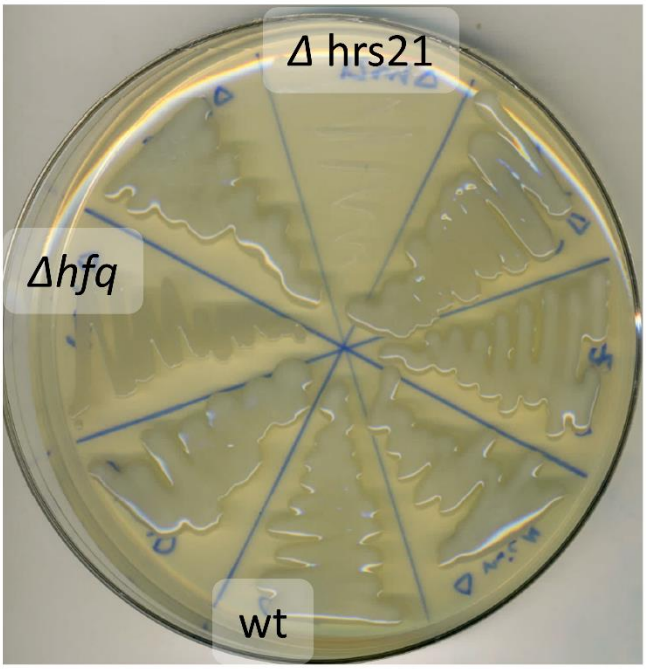

Figure 2.5: sRNAs regulate colony morphology when mutant strains are grown on minimal media. Wild-type *E. amylovora* Ea1189 forms mucoid colonies on minimal media with sorbitol as the carbon source, but the Δ*hfq* deletion mutant forms non-mucoid colonies, and the Δ*hrs21* mutant is unable to grow.

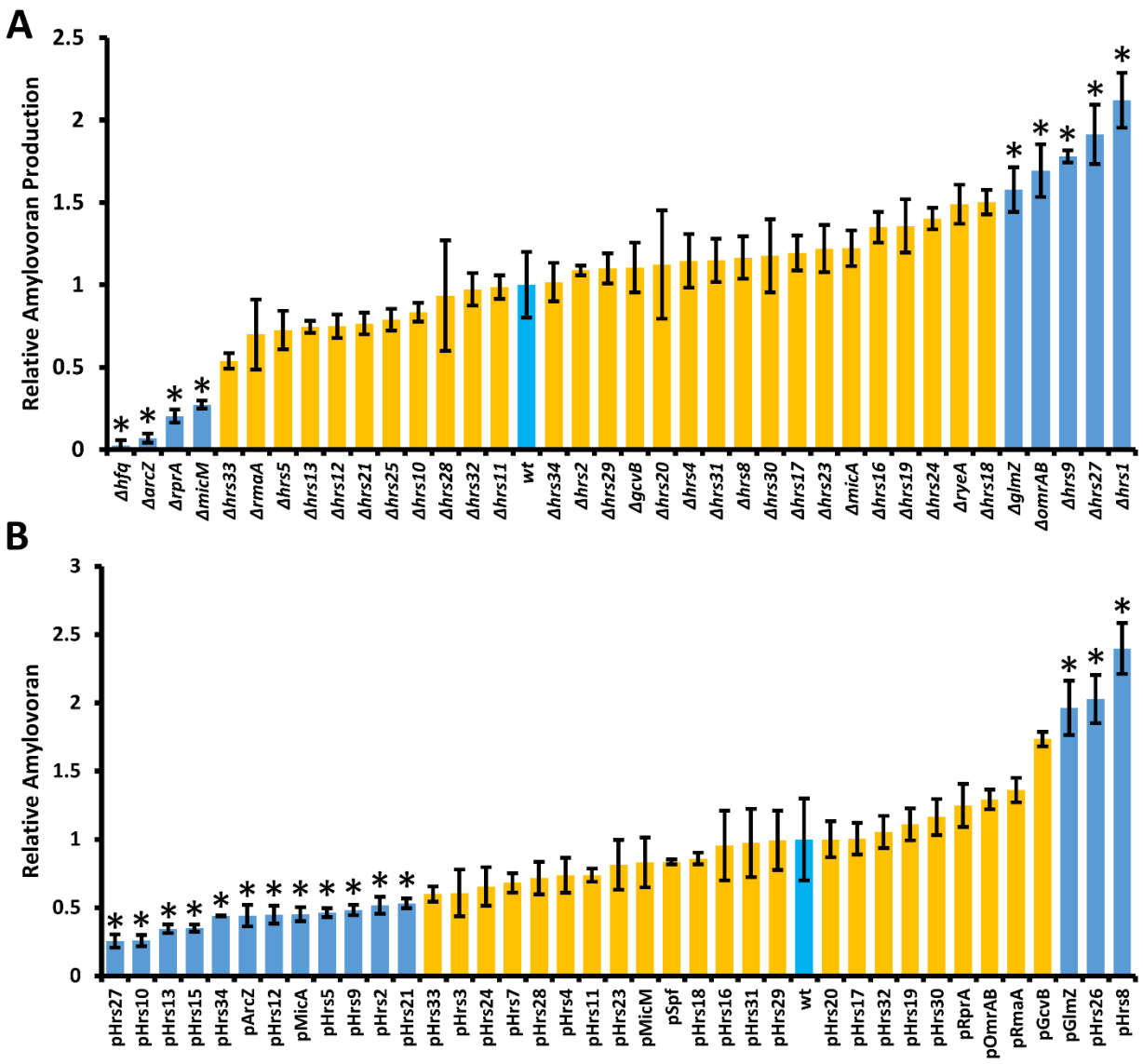

Figure 2.6: *E. amylovora* Ea1189 Hfq-dependent sRNAs affect amylovoran production. For assessment of amylovoran production, cells were grown in MBMA media for 48 hrs and acidic exopolysaccharides in culture supernatants were precipitated by addition of cetylpyridinium chloride. Resulting turbidity was measured via absorbance at 600 nm. sRNA deletion mutants, and the Δ*hfq* deletion mutant were compared (A) relative to wild-type strain Ea1189 amylovoran production. sRNA overexpression strains were compared (B) relative to amylovoran production by wild-type cells carrying empty pHM-tac under inducing conditions. Asterisks indicate significant differences ($P_{adj} < 0.05$) by student's t test with Bonferroni correction.

.

Levan production

To assess the roles of *E. amylovora* Ea1189 Hfq-dependent sRNAs in production of the exopolysaccharide levan through levansucrase activity, we first grew each strain in our library of mutant and overexpression strains on LB amended with 5% sucrose (wt/vol). Although several strains demonstrated subtle differences in colony morphology compared to the wild-type *E. amylovora* strain Ea1189, the MicA- and ArcZ-overexpressing strains exhibited quite dramatic phenotypes, with colonies displaying visually reduced viscosity and a spreading morphology, resulting in poorly defined colony boundaries (Figure 2.7).

For each strain, we determined the amount of levansucrase activity secreted into culture supernatants. We found five sRNA deletion mutants with increased levansucrase activity and five deletion mutants with reduced levansucrase activity (Figure 2.8A). Overexpression of seven sRNAs resulted in lower secreted levansucrase activity, whereas overexpression of two sRNAs led to increased secreted levansucrase activity (Figure 2.8B). Overexpression of MicA, which resulted in colonies with visually reduced viscosity when grown in the presence of sucrose, had the lowest levels of secreted levansucrase activity. In contrast, overexpression of ArcZ, which also resulted in spreading colonies on media containing sucrose, resulted in increased secreted levansucrase activity. Additionally, deletion of *omrAB*, a known regulator of amylovoran (39) and motility (39, 131) resulted in dramatically higher levels of secreted levansucrase relative to *E. amylovora* wild-type strain Ea1189.

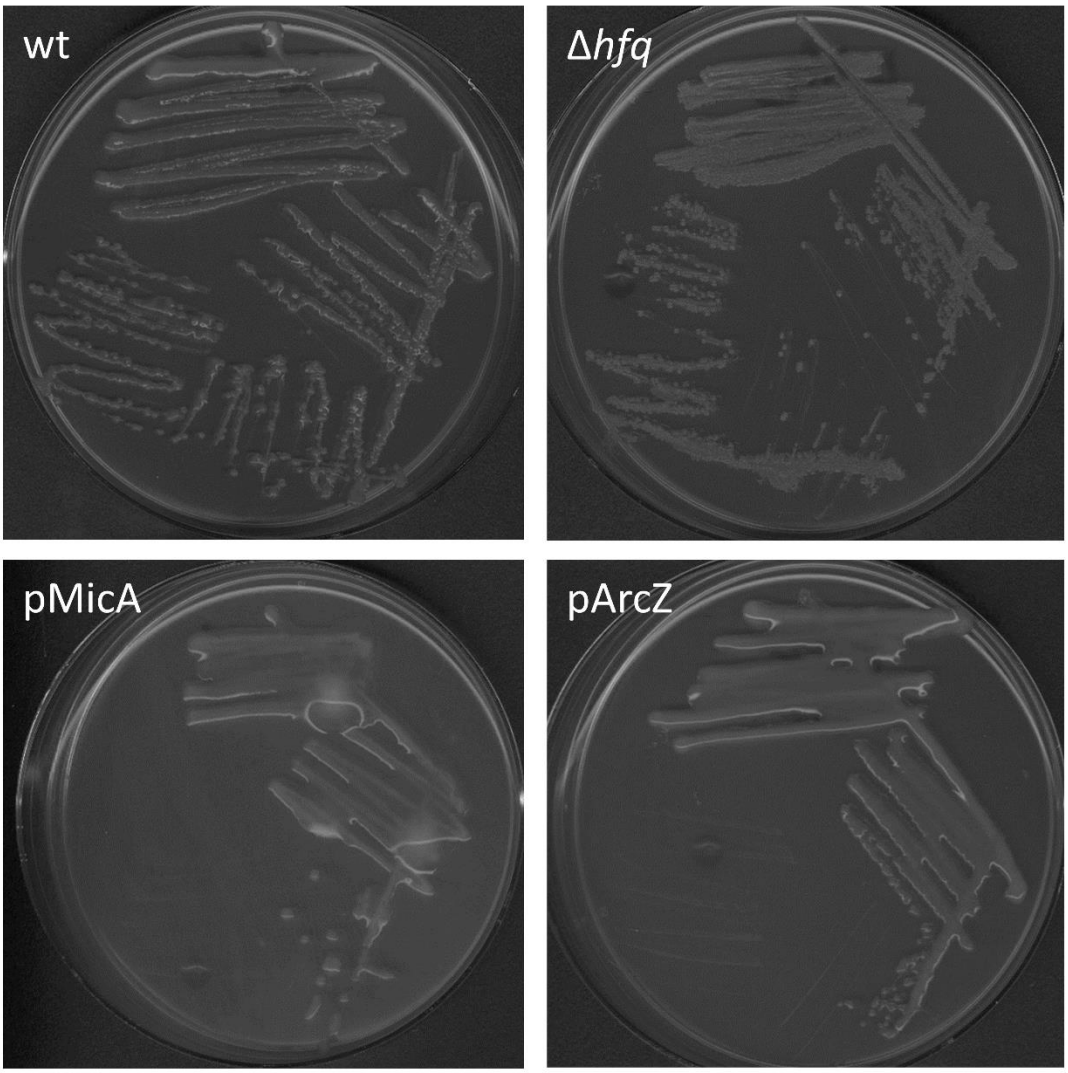

Figure 2.7: sRNAs regulate colony morphology when grown on sucrose. Wild-type *E. amylovora* Ea1189 forms domed colonies on LB media amended with 5% sucrose, but the Δ*hfq* deletion mutant forms low, non-spreading colonies. Overexpression of MicA or ArcZ results in reduced viscosity and a spreading colony morphology.

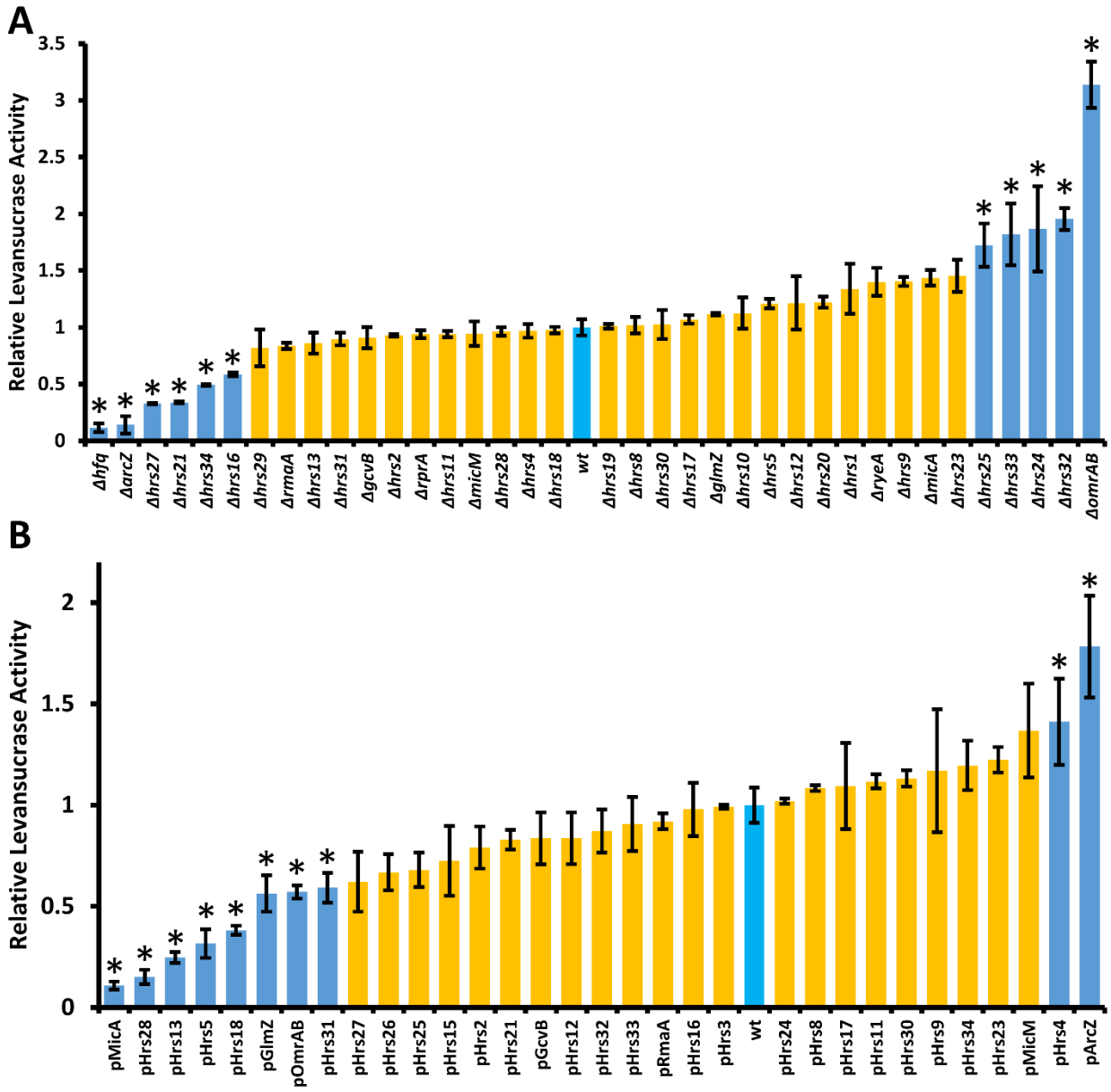

Figure 2.8: *E. amylovora* Ea1189 Hfq-dependent sRNAs affect levansucrase activity. Secreted levansucrase activity was assessed in culture supernatants following overnight growth in LB media. Culture supernatants were mixed in a 1:1 ratio with phosphate buffered sucrose (2 M) and incubated at 37°C for 48 hrs to allow the enzymatic reaction to proceed. Resulting turbidity was measured as absorbance at 600 nM. sRNA deletion mutants, and the Δ*hfq* deletion mutant were compared (A) relative to wild-type strain Ea1189 levansucrase activity. sRNA overexpression strains were compared (B) relative to levansucrase activity in wild-type cells carrying empty pHM-tac under inducing conditions. Asterisks indicate significant differences ($P_{adj} < 0.05$) by student's t test with Bonferroni correction.

Biofilm formation

Biofilm formation is a complex trait that is a product of several other traits such as exopolysaccharide formation, attachment, and motility (91-93). We assessed biofilm formation by the sRNA deletion and overexpression strains using a crystal violet staining approach. We found that six sRNA deletion mutants had higher crystal violet staining than wild-type *E. amylovora* Ea1189 cells, but only one sRNA deletion mutant, *gcvB*, had reduced crystal violet staining (Figure 2.9A). Overexpression of six sRNAs led to reduced crystal violet staining whereas overexpression of three sRNAs increased crystal violet staining (Figure 2.9B). Deletion of *gcvB* reduced crystal violet staining, and overexpression of GcvB increased crystal violet staining. In contrast, deletion of *hrs21* increased crystal violet staining, while overexpression of Hrs21 decreased crystal violet staining. Although our microscopy analysis of cells grown in agitated liquid culture did not reveal any differences between these strains, further microscopy work is needed to reveal whether these effects on crystal violet staining are due to differences in formation of mature biofilm or differences in other traits such as exopolysaccharide production or attachment, because the Δ*hfq* mutant exhibits high crystal violet staining without forming mature biofilms due to a hyper-attachment phenotype (39).

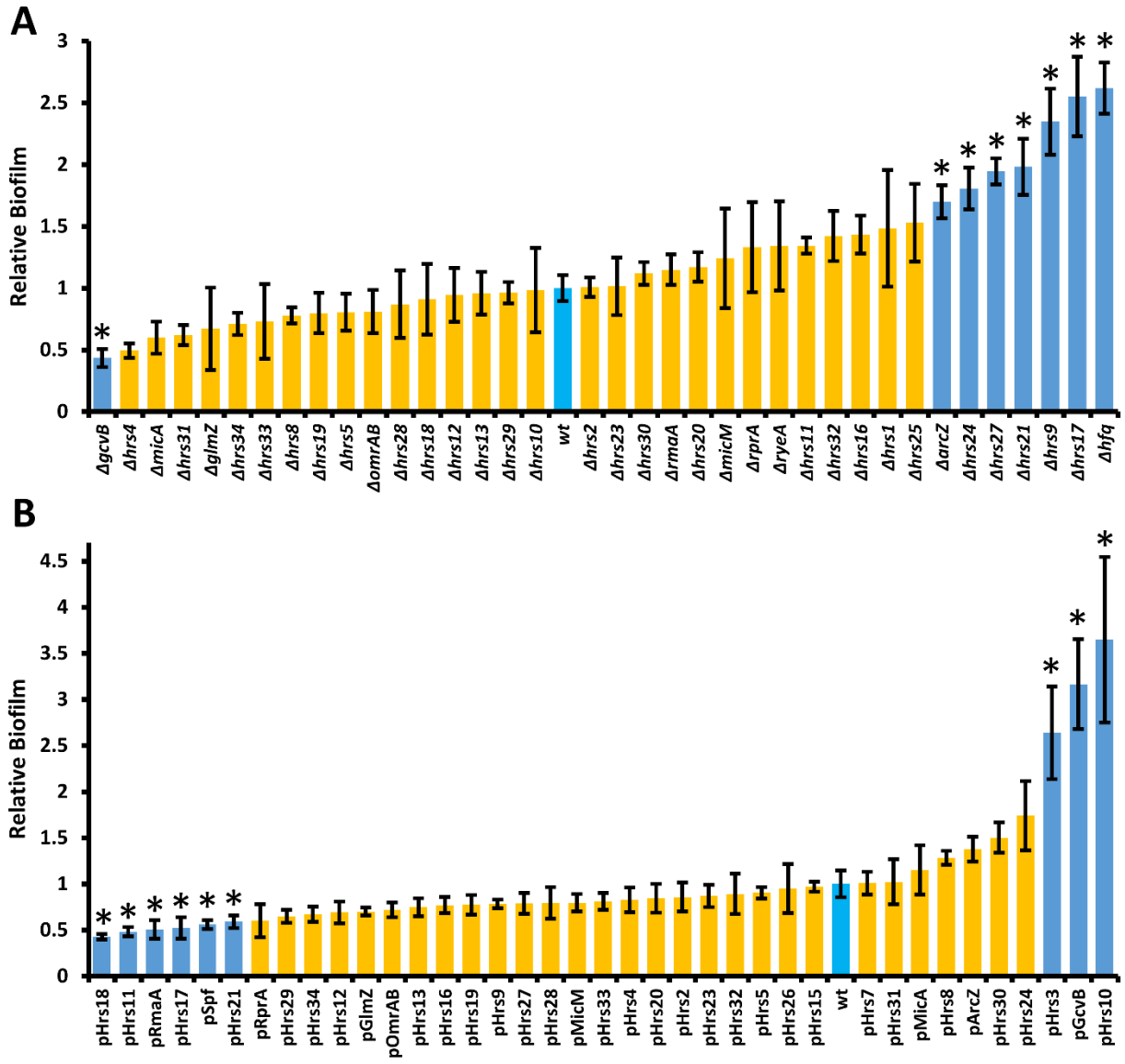

Figure 2.9: *E. amylovora* Ea1189 Hfq-dependent sRNAs contribute to regulation of biofilm formation. Crystal violet staining of adherent cells was used as a proxy for biofilm formation following 48 hs of growth in MBMA media in a 96-well microtiter plate. sRNA deletion mutants, and the Δ*hfq* deletion mutant were compared (A) relative to wild-type crystal violet staining. sRNA overexpression strains were compared (B) relative to crystal violet staining of wild-type cells carrying empty pHM-tac under inducing conditions. Asterisks indicate significant differences ($P_{adj} < 0.05$) by student's t test with Bonferroni correction.

Catalase activity

Because several sRNAs are involved in stress response pathways (77), we tested the effect of sRNAs on catalase activity, which is involved in the mitigation of oxidative stress from hydrogen peroxide. Determination of catalase activity in cell pellets showed that three sRNA deletion mutants had altered catalase activity relative to wild-type *E. amylovora* Ea1189 cells (Figure 2.10A). The Δ*arcZ* mutant had reduced catalase activity and the Δ*glmZ* and Δ*rmaA* deletion mutants had increased catalase activity relative to wild-type strain Ea1189. Upon overexpression, six sRNAs decreased catalase activity relative to wild-type Ea1189 cells carrying empty pHM-tac (Figure 2.10B). During our testing, we observed that some sRNA deletion and overexpression mutants released significant amounts of catalase activity to the culture supernatant, but the wild-type cells only released a small amount of catalase activity to culture supernatants (Figure 2.10). Deletion of *ryeA* or *hrs24* led to increased catalase activity in culture supernatants and overexpression of ArcZ, GlmZ, Hrs10, Hrs13, Hrs19, Hrs27, Hrs32, Hrs33, or MicA each resulted in increased catalase activity in culture supernatants. Because several of these strains exhibited lower catalase activity in cell pellets, but increased catalase activity in supernatants, it is possible that these sRNAs are regulating some type of secretion, rather than regulating production of catalase enzymes.

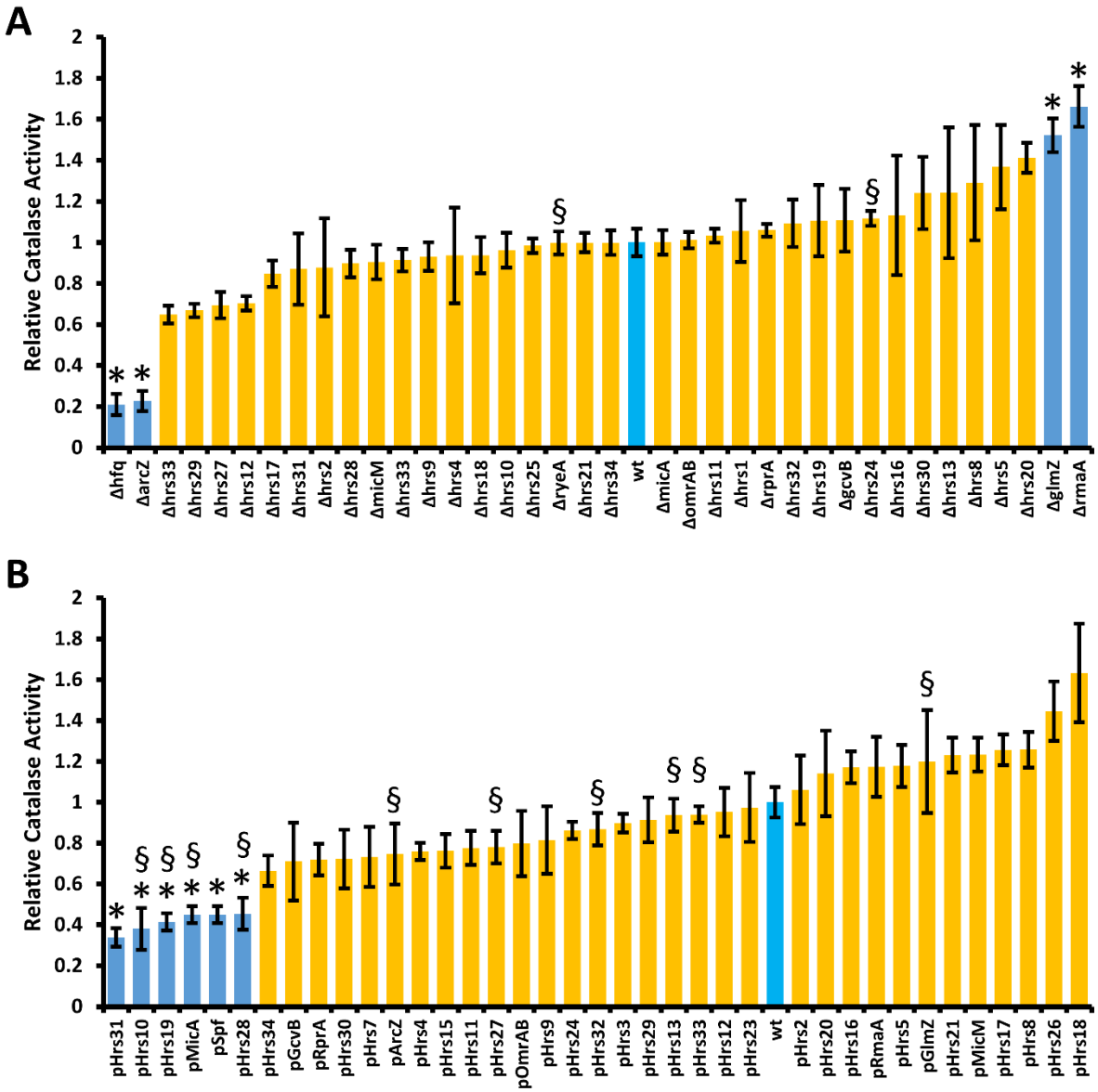

Figure 2.10: The effects of Hfq-dependent sRNAs on catalase activity in *E. amylovora* Ea1189. Catalase activity was assessed following overnight growth by mixing cell suspension with 1% Triton X-100 and 8 M H_2O_2 in a 1:1:1 ratio and monitoring formation of bubbles, demonstrating evolution of gas. sRNA deletion mutants, and the Δ*hfq* deletion mutant were compared (A) relative to wild-type catalase activity. sRNA overexpression strains were compared (B) relative to catalase activity of wild-type cells carrying empty pHM-tac under inducing conditions. Asterisks indicate significant differences ($P_{adj} < 0.05$) by student's t test with Bonferroni correction. § indicates strains with qualitatively increased amounts of catalase activity in culture supernatants relative to wild-type *E. amylovora* strain Ea1189.

hrpA promoter activity

In order to assess effects of regulators on type III secretion, cells are typically infiltrated into leaves of non-host *Nicotiana* species (tobacco) and then monitored for cell death indicative of a hypersensitive response (132). The elicitation of a hypersensitive response is dependent on translocation of type III effector proteins and thus is representative of a fully functional pathogen type III secretion system (133, 134). However, this system is also sensitive to cell density and typically only provides binary observations because testing is typically only carried out at a single cell density. Because of these limitations, we generated a promoter fusion for *hrpA*, the structural pilin of the type III secretion system, which includes a binding site for the alternative sigma factor HrpL and green fluorescent protein as a reporter. We transformed this reporter construct into each of the sRNA overexpressing strains to assess fluorescence as a proxy for transcriptional activation of type III secretion system genes. Although only assessing expression of the *hrpA* pilin gene rather than a fully functional type III secretion system, this approach provides a high-throughput method with high sensitivity to quantitatively assess subtle differences in promoter activity in response to manipulation of Hfq-dependent sRNAs. When assessed for *hrpA* promoter activity, we found that overexpression of five sRNAs, Hrs8, Hrs11, ArcZ, Hrs24, and OmrAB all resulted in increased fluorescence compared to wild-type Ea1189 cells carrying empty pHM-tac (Figure 2.11). Overexpression of only one sRNA, Hrs4, reduced *hrpA* promoter activity relative to wild-type *E. amylovora* Ea1189 cells carrying empty pHM-tac.

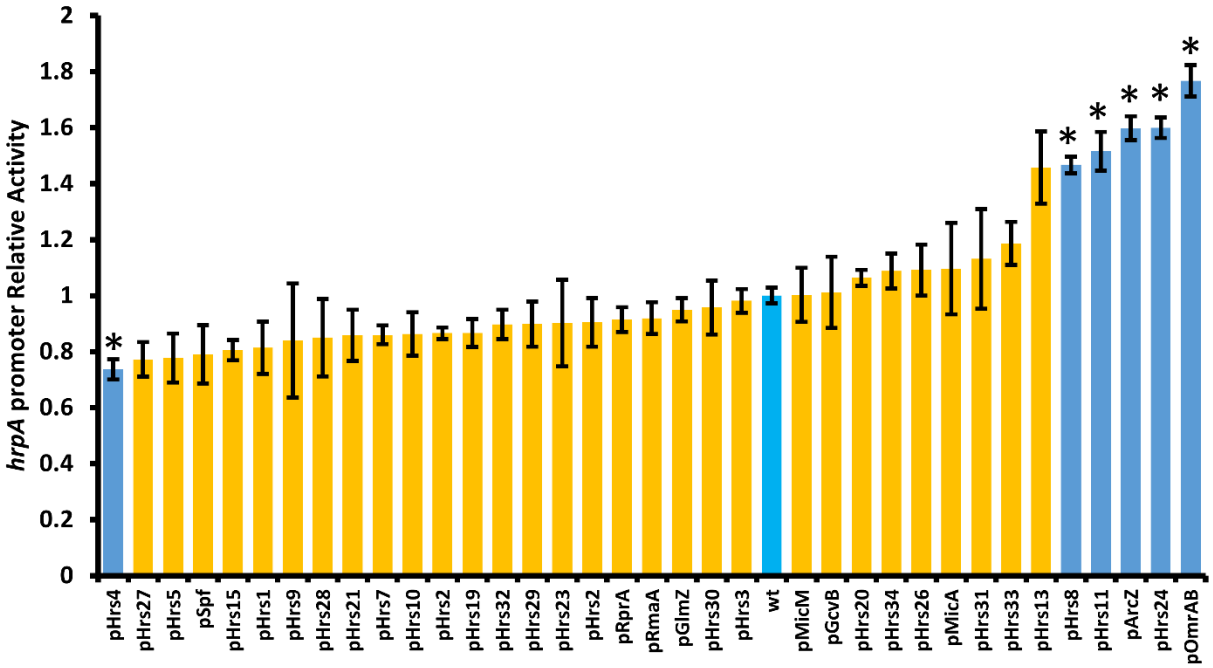

Figure 2.11: *E. amylovora* Ea1189 Hfq-dependent sRNAs affect expression of type III secretion pilin, *hrpA*. Cells grown overnight were induced in HIMM for 16 hrs, after which fluorescence was measured as a proxy for *hrpA* promoter activity. sRNA overexpression strains were compared relative to fluorescence of wild-type cells carrying empty pHM-tac with IPTG added at the time of transfer to HIMM. Asterisks indicate significant differences ($P_{adj} < 0.05$) by student's t test with Bonferroni correction.

Testing sRNA overexpression strains with a single reporter required transformation of several strains. Because of the large effort and materials required to transform over 40 strains by the electroporation methods routinely used in *E. amylovora* (135), we sought to utilize a method with higher throughput for the generation of these strains. As previously reported (136), we found that calcium/magnesium chloride competent cell preparation with heat shock approaches were highly variable and had unsuitably low transformation efficiency. However, we observed that TSS chemically competent cells (127) with heat shock at 42^{o}C produced satisfactory and useful transformation rates, albeit less efficiently than electroporation (data not shown).

Virulence

Because several *E. amylovora* Ea1189 sRNA deletion mutants were previously assessed for virulence on immature pears (38, 39), we assessed the remainder of the sRNA deletion mutants for effects on virulence using the same immature pear infection model. Overexpression strains were not assessed because of an inability to consistently induce and select for plasmid maintenance *in planta*. Virulence of select strains is shown in Figure 2.12. In addition to Δ*arcZ*, Δ*hrs21*, and Δ*rprA*, previously found to have reduced virulence in immature pears (38, 39), we found that the Δ*hrs1* deletion mutant had reduced virulence compared to wild-type *E. amylovora* strain Ea1189. Although several other Hfq-dependent sRNAs had significant effects on virulence-associated phenotypes, no other sRNA deletion mutants displayed reduced symptom development on immature pears. This is consistent with the observation that during infection of immature pears, some critical virulence traits are sufficient for full virulence even when expressed at low levels, as shown in Chapter 4.

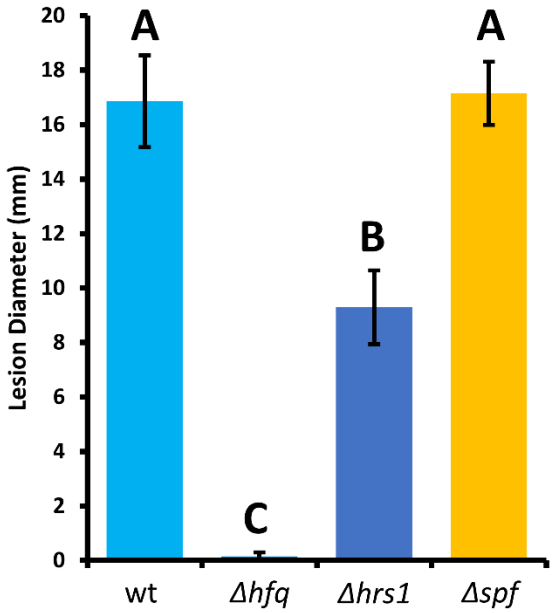

Figure 2.12: Screening of *E. amylovora* Ea1189 Hfq-dependent sRNAs reveals a novel sRNA deletion mutant with virulence defects. Immature pears were inoculated with indicated strains and monitored for water soaking or necrotic symptom development. Measurements shown were made 4 days post-inoculation. Groups with shared letter designation did not differ significantly ($P > 0.05$) from each other by Tukey's honest significant difference (HSD) test.

Multidimensional analysis

Because each sRNA was tested for impacts on several virulence-associated traits, we analyzed our dataset using a multidimensional analysis. A heatmap was generated, clustering phenotypes and sRNAs based on our data (Figure 2.13). This clustering resulted in 28 sRNAs that clustered with wild-type, and 13 sRNAs that did not cluster with wild-type. We further conducted principal component analysis of our multidimensional dataset (Figure 2.14). Similar to the clustering in the heatmap, principal component analysis revealed that a majority of the sRNAs cluster closely to the wild-type strain, which is indicated by a light blue dot in Figure 2.14. However, with principal component analysis several strains stand out that are not part of the cluster with wild-type strain Ea1189, indicating that these sRNAs are likely playing important roles in coordinating virulence-associated phenotypes. Some of the sRNAs that stand out are sRNAs with known effects on virulence using the immature pear model of infection and are indicated by dark blue dots in Figure 2.14. Other sRNAs suggested to have strong regulatory roles based on principal component analysis include OmrAB, GcvB, Hrs10, Hrs17, Hrs27, GlmZ, Hrs18, Hrs8, and MicA. A high degree of complexity in our data was demonstrated by the fact that principal components 1 and 2 together only explained 46% of the variance in the data. This observation further suggests that each virulence-associated trait assessed is primarily regulated independently of the other virulence traits. This is consistent with each virulence trait playing a unique role during distinct stages of fire blight disease development.

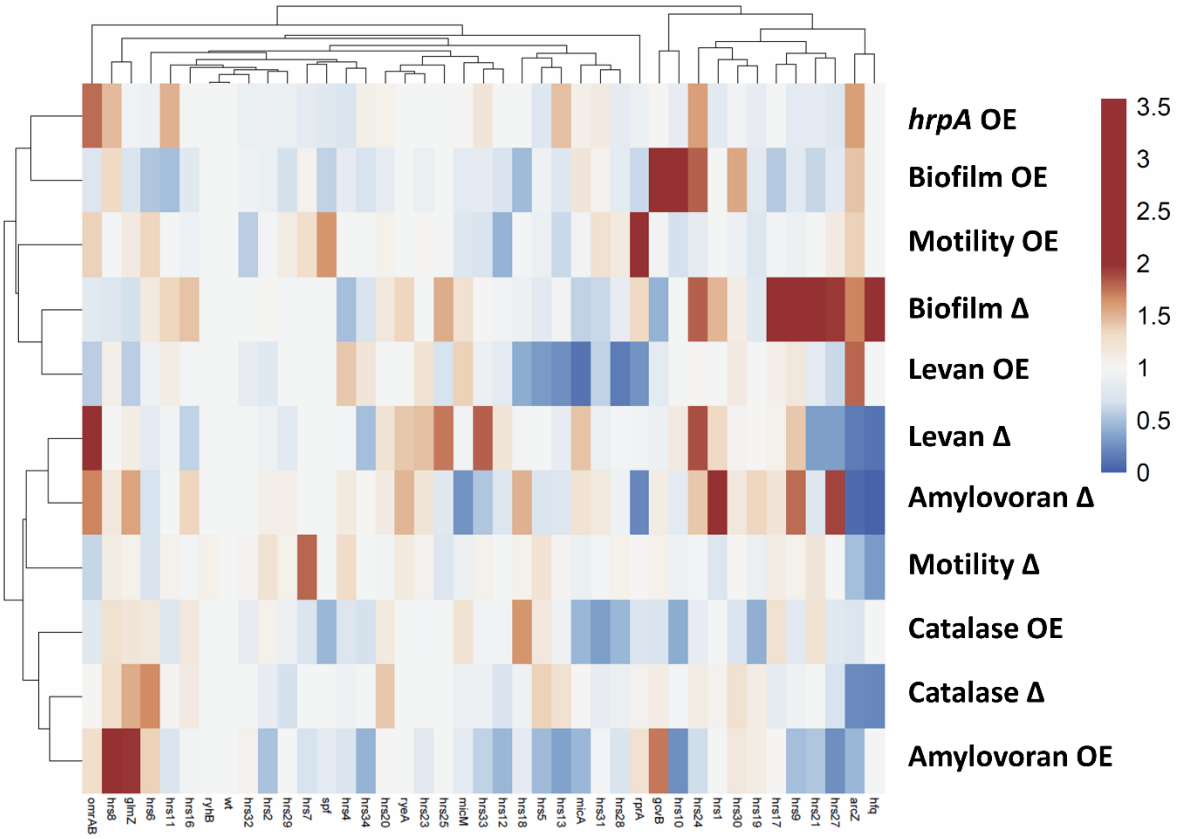

Figure 2.13: Multidimensional analysis of interactions between *E. amylovora* Ea1189 Hfq-regulated sRNAs and assessed virulence-associated traits. Aggregate data from virulence-trait assessments were utilized to generate this heatmap using ClustVis software. Rows designated with Δ represent data from deletion mutants, and rows designated OE represent data from overexpression strains. Rows and columns were unscaled and were clustered by Euclidean distance. Color scale from blue to white to red represents relative measurements. As data observations are relative to wild-type, blue represents values lower than wild-type, red represents values higher than wild-type, and white represents values similar to wild-type *E. amylovora* strain Ea1189.

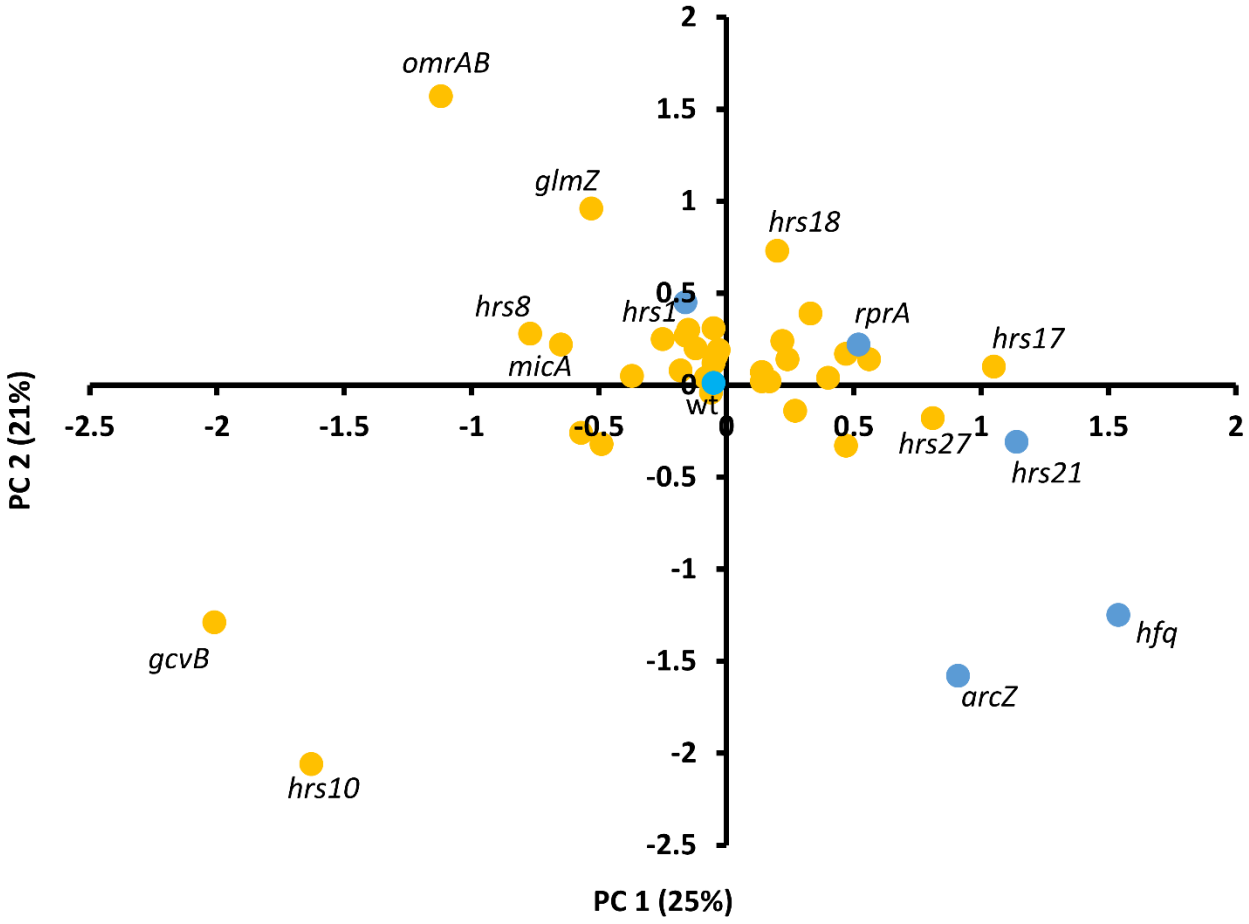

Figure 2.14: Principal component analysis of multidimensional virulence data reveals *E. amylovora* Ea1189 sRNAs with strongest effects on virulence-associated traits. Each dot represents an sRNA or strain tested in this study. The light blue dot (near the origin) represents the wild-type strain. Dark blue dots indicate *hfq* and sRNAs that have virulence defects when deleted from the genome. Additional labels indicate other outlying sRNAs of interest for deviation from wild-type phenotypes for the tested virulence-associated traits.

V. Discussion

In this work, we generated a library of single-deletion mutants and overexpression plasmids for the known Hfq-dependent sRNAs in *E. amylovora* Ea1189. We used this library to characterize the effects of Hfq-dependent sRNAs on critical virulence-associated traits. Most sRNAs assessed had only weak effects on phenotypes, and few sRNAs had strong effects under the conditions tested in our experiments. Although several Hfq-dependent sRNAs were observed to have only subtle effects on virulence-associated phenotypes, it is likely that these sRNAs play important roles in maximizing bacterial fitness through fine-tuning of other physiological processes or may play important roles under other environmental conditions. Our multidimensional analysis of these data supports the idea that most Hfq-dependent sRNAs do not dramatically affect virulence-associated phenotypes, but that some of them do play major roles in the expression of these traits. This is consistent with the findings of a similar sRNA library screen in *Escherichia coli* in which most sRNAs had only modest effects (121).

We identified Δ*hrs1* as a new *E. amylovora* sRNA deletion mutant with effects on virulence, as the deletion of *hrs1* resulted in strongly reduced symptom development during infection of immature pears. The sRNA *hrs1* is located in the genome between *cpxP* and *fieF* and is relatively abundant (39). In our work, we found *hrs1* affecting production of the exopolysaccharide amylovoran and conferring a small but significant effect on swimming motility, which provides potential mechanisms whereby this sRNA could be linked to virulence. Future work to determine the specific targets and mechanisms by which this sRNA is affecting virulence is needed to determine its specific regulatory roles. In *E. amylovora* Ea1189, deletion of *arcZ*, *hrs1*, *hrs21*, or *rprA* results in reduced virulence in immature pears. Of these, *arcZ* and *rprA* are well conserved in *Enterobacteriaceae*, whereas *hrs21* is unique to pathogenic members

of the genus *Erwinia* (39). The sRNA *hrs1* is unique to pathogenic *Erwinia*, but similar sequences also occur in *Pantoea agglomerans*, however it is not known whether it is expressed as an sRNA in other species.

The sRNA Hrs21 was previously found to play a role in virulence through an unknown mechanism (39). Through the characterization of our sRNA library, we have found multiple virulence traits affected by Hrs21. We found that the Δ*hrs21* mutant was unable to grow on minimal media independent of the carbon source. Despite this growth defect in minimal media, we did not observe any growth or morphological differences from wild-type strain Ea1189 when grown on LB media. One potential explanation of this observation is that the Δ*hrs21* mutant could be an auxotroph. Regardless, this growth defect indicates that nutrient availability plays a critical role for the Δ*hrs21* mutant, suggesting that the virulence defect in immature pears may be due to some nutrient that is lacking in the pears that the Δ*hrs21* mutant needs for growth. In addition to this growth defect, we found that Hrs21 affected production of the exopolysaccharide amylovoran, secreted levansucrase activity, and biofilm formation. Although we did not observe a growth defect in the media used for these assays, it is possible that the observed effects of Hrs21 on these virulence-associated traits is due to indirect effects through control of metabolic processes. Further work to characterize the nutritional requirements of the Δ*hrs21* mutant as well as its growth in pears is necessary to clarify the role of this sRNA in regulating physiological and virulence processes.

Several phenotypic roles for the sRNA ArcZ have previously been reported which have been confirmed in this work including effects on flagellar motility (131), amylovoran production (39), levansucrase activity (Chapter 4), and expression of the type III secretion system (39). The phenotypic similarities between the Δ*arcZ* mutant and the Δ*hfq* deletion mutant were also

confirmed by the clustering together of ArcZ and Hfq through both the multidimensional heatmap clustering as well as in the principal component analysis. Recent studies have linked ArcZ to transcriptional regulators and pathways that connect to flagellar motility, production of the exopolysaccharides amylovoran and levan, and biofilm formation, (131); Schachterle and Sundin 2019). However, further work is needed to uncover the mechanism connecting ArcZ to expression of the type III secretion system.

The sRNA OmrAB, which is well conserved in *Enterobacteriaceae* (131), has previously been characterized for its roles in regulating amylovoran production and flagellar motility (39). In our sRNA library screen, we confirmed those roles and expanded the characterization of OmrAB to include the findings that it affects secreted levansucrase activity as well as expression of the type III secretion pilin *hrpA*. These effects agree with the result that clustering and principal component analysis showed OmrAB as unique from other sRNAs in its effects on virulence-associated traits. Together our data suggest that OmrAB may be an important virulence regulator under specific environmental conditions. To date, no direct targets of OmrAB have been demonstrated in *E. amylovora*. Future studies are needed to identify direct targets and better understand the role OmrAB is playing in *E. amylovora* expression of virulence-associated traits.

The sRNA *hrs4* is located in the genome between *mtr*, encoding a tryptophan transporter, and *fur*, encoding ferric uptake regulator, the iron responsive transcription factor (39). In our study we observed that Hrs4 is the only *E. amylovora* Hfq-dependent sRNA with GC content greater than the genome-wide average. In our sRNA library screen of phenotypes, overexpression of Hrs4 increased secreted levansucrase activity and Hrs4 was the only sRNA to reduce promoter activity of the type III secretion pilin *hrpA* upon overexpression. Because of the

effects of Hrs4 on type III secretion, future work to determine the mechanisms underlying this effect may uncover regulatory functions that are important to disease development.

The MicA overexpression strain demonstrated reduced viscosity and a spreading colony morphology when grown on LB media amended with sucrose, but not when sucrose was absent. Although mucoid morphologies are typically associated with elevated exopolysaccharide production (137), overexpression of MicA resulted in a strong reduction in the production of the exopolysaccharides amylovoran and levan. We hypothesize that reduced exopolysaccharide production results in a lack of structure for colony formation but why this only occurs when grown on sucrose as opposed to on LB is unclear. Because we only assessed secreted levansucrase activity, this may represent an alteration of secretion by MicA rather than as a direct regulator of exopolysaccharides. This hypothesis is supported by the finding that overexpression of MicA reduced intracellular catalase activity but increased secreted catalase activity. However, additional experiments are needed to directly test this hypothesis.

The sRNA Hrs7 is homologous to *Escherichia coli* FnrS with 65.6 % identity. In our library screen, we observed that Hrs7 is a negative regulator of flagellar motility. *Escherichia coli* FnrS affects biofilm formation, but not motility (121), suggesting that although similar, and likely of shared evolutionary origin, these sRNAs have divergent roles and mRNA targets.

In all, our work in generating and screening a library of *E. amylovora* Hfq-dependent sRNAs has resulted in discovery of several sRNA-phenotype interactions. Furthermore, the amount of data that is now generated in increased-throughput phenotyping methods has also enabled multi-dimensional analysis of the data that has further facilitated determination of the sRNAs with the strongest and most important effects. Increased throughput and ability to generate and utilize such libraries will help to overcome the sRNA characterization bottleneck

that has developed in the wake of deep-sequencing studies to identify sRNAs. With developing technologies to determine sRNA targets in a high-throughput manner (48, 49, 138, 139), such sRNA libraries will help to bridge the gap between sRNA identification and target determination by characterizing the roles of the identified sRNAs in specific phenotypes. Continued work to characterize *E. amylovora* sRNAs and their regulatory mechanisms will improve understanding of how this pathogen rapidly adapts to and succeeds in the many environmental niches encountered during systemic infection.

CHAPTER 3

Three Hfq-dependent small RNAs regulate flagellar motility in the fire blight pathogen *Erwinia amylovora*

This chapter has been accepted for publication and is accessible in its entirety at:

Schachterle, J.K.; Zeng, Q.; Sundin, G.W. (2019). Three Hfq-dependent small RNAs regulate flagellar motility in the fire blight pathogen *Erwinia amylovora*. *Mol. Microbiol.*

doi:10.1111/mmi.14232

I. Abstract

Erwinia amylovora, the causative agent of fire blight disease of apple and pear trees, causes disease on flowers by invading natural openings at the base of the floral cup. To reach these openings, the bacteria use flagellar motility to swim from stigma tips to the hypanthium and through nectar. We have previously shown that the Hfq-dependent sRNAs ArcZ, OmrAB, and RmaA regulate swimming motility in *E. amylovora*. Here we tested these three sRNAs to determine at what regulatory level they exert their effects and to what extent they can complement each other. We found that ArcZ and OmrAB repress the flagellar master regulator *flhD* post-transcriptionally. We also found that ArcZ and RmaA positively regulate *flhD* at the transcriptional level. The role of ArcZ as an activator of flagellar motility appears to be unique to *E. amylovora* and may have recently evolved. Our results suggest that the Hfq-dependent sRNAs ArcZ, OmrAB, and RmaA play an integral role in regulation of flagellar motility by acting primarily on the master regulator, FlhD, but also through additional factors.

CHAPTER 4

The leucine-responsive regulatory protein Lrp participates in virulence regulation downstream of small RNA ArcZ in *Erwinia amylovora*

This chapter has been accepted for publication in an open-access format and is accessible in its entirety at:

Schachterle JK, Sundin GW. 2019. The leucine-responsive regulatory protein Lrp participates in virulence regulation downstream of small RNA ArcZ in Erwinia amylovora. mBio 10:e00757-19. https://doi.org/10.1128/mBio.00757-19.

I. Abstract

Erwinia amylovora causes the devastating fire blight disease of apple and pear trees. During systemic infection of host trees, pathogen cells must rapidly respond to changes in their environment as they move through different host tissues that present distinct challenges and sources of nutrition. Growing evidence indicates that small RNAs (sRNAs) play an important role in disease progression as post-transcriptional regulators. The sRNA ArcZ positively regulates the motility phenotype and transcription of flagellar genes in *E. amylovora* Ea1189 yet is a direct repressor of translation of the flagellar master regulator, FlhD. We utilized transposon mutagenesis to conduct a forward genetic screen and identified suppressor mutations that increase motility in the Ea1189Δ*arcZ* mutant background. This enabled us to determine that the mechanism of transcriptional activation of the *flhDC* mRNA by ArcZ is mediated by the leucine-responsive regulatory protein, Lrp. We show that Lrp contributes to expression of virulence and several virulence-associated traits including production of the exopolysaccharide amylovoran, levansucrase activity, and biofilm formation. We further show that Lrp is regulated post-transcriptionally by ArcZ through destabilization of *lrp* mRNA. Thus, ArcZ regulation of FlhDC directly and indirectly through Lrp forms an incoherent feed-forward loop that regulates levansucrase activity and motility as outputs. This work identifies Lrp as a novel participant in virulence regulation in *E. amylovora* and places it in the context of a virulence-associated regulatory network.

CHAPTER 5

Small RNA ArcZ regulates oxidative stress response genes and regulons in *Erwinia amylovora*

I. Abstract

Erwinia amylovora, causative agent of fire blight disease of apple and pear trees, has evolved to use small RNAs for post-transcriptional regulation of virulence traits important for disease development. The sRNA ArcZ regulates several virulence traits, and to better understand its roles, we conducted a transcriptomic comparison of wild-type and Δ*arcZ* mutant *E. amylovora*. We found that ArcZ regulates multiple cellular processes including expression of enzymes involved in mitigating the threat of reactive oxygen species, and that the Δ*arcZ* mutant has reduced catalase activity and is more susceptible to exogenous hydrogen peroxide. We quantified hydrogen peroxide production by apple leaves inoculated with *E. amylovora* and found that while the wild-type *E. amylovora* cells produce enough catalase to cope with defense peroxide, the Δ*arcZ* mutant is likely limited in virulence because of its inability to cope with peroxide levels in host leaves. We further found that the ArcZ regulon overlaps significantly with the regulons of transcription factors involved in oxidative state sensing including Fnr and ArcA. In addition, we show that ArcZ regulates *arcA* at the post-transcriptional level suggesting a role for this system in mediating adaptations to oxidative state, especially during disease development.

II. Introduction

When pathogenic microbes arrive on a host plant, the plant perceives the arrival of a threat through recognition of pathogen associated molecular patterns (PAMPs) (1). The recognized patterns include conserved molecules associated with pathogenic microbes, such as chitin (140), flagellin (141), and translation elongation factor Tu (142). The binding of these PAMPs to surface receptors triggers a complex signaling cascade that activates defense responses (1). Host plant defense responses are diverse and include actions such as stomatal

closure (143), hormone signaling (144), callose deposition (145), and production of reactive oxygen species (146). Plant pathogenic microbes have responded to these host defenses through the evolution of effector proteins that act to suppress and subvert host defense signaling and activity (147). In the case of bacterial pathogens, the effectors are often translocated directly into the host cytoplasm via the type III secretion system, a needle-like protein structure (148). In an ongoing biochemical arms race, hosts and pathogens alike have evolved numerous effector-target relationships that affect disease outcomes (1-3). For many bacterial pathogens, this has resulted in a number of effector proteins that are essential for full virulence (149, 150). In addition to effector proteins, bacterial pathogens have evolved additional virulence strategies that allow them to flourish in the environment of a host plant and avoid host defenses. For example, *Erwinia amylovora*, causative agent of fire blight disease of apple and pear trees, utilizes several virulence strategies to avoid, suppress, and cope with host defenses (92-94, 96, 151, 152). For pathogenesis, *E. amylovora* requires effective translocation of the type III effectors DspE and AvrRpt2$_{Ea}$ into host cells to suppress host defenses and induce necrosis (94, 153). Additional virulence traits that play a key role for *E. amylovora* include exopolysaccharide production and biofilm formation (89, 91, 92, 123), motility (87, 88), ability to mitigate the threat of reactive oxygen species (111), and ability to acquire and utilize essential nutrients (154, 155).

Production of the exopolysaccharides amylovoran (89, 123), levan (90, 92), and cellulose (91) along with proteinaceous attachment structures (93) contribute to biofilm formation. Biofilm formation provides protective layers that can serve to both prevent host defense molecules, like reactive oxygen species, from reaching the bacteria (156), and to conceal the bacteria from host detection, reducing the degree of host defense response (157). Motility enables bacteria to use flagella or pili to migrate and move to more favorable locations where

host defenses may be reduced or nutrient availability may be more favorable (87, 151). Although *E. amylovora* can be concealed through some virulence traits, move away from host defenses, and even directly reduce the host defense response through type III effectors, the bacteria will still have to cope with host defense compounds and responses as well as acquire sufficient nutrients to maintain growth during infection (158). Thus, the ability to face host defenses and mitigate the threat of reactive oxygen species is also critical for full virulence (111). To coordinately express each virulence-associated trait under the precise conditions, *E. amylovora* has evolved elaborate environmental sensing and signal transduction cascades (119). Efforts to characterize these regulatory pathways have successfully linked several regulatory systems with virulence associated traits.

Recent work has revealed the importance of small non-coding RNAs (sRNAs) in the regulation of virulence and virulence-associated traits in *E. amylovora* (38, 39). sRNAs are typically involved in post-transcriptional regulation. One class of sRNAs that affects virulence in *E. amylovora* includes those that are dependent on the chaperone protein Hfq (38). The Hfq chaperone stabilizes a family of trans-acting sRNAs that regulate targets by RNA-RNA base-pairing (19-21). In *E. amylovora*, 42 Hfq-dependent sRNAs have been identified, and the Hfq-dependent sRNA ArcZ in particular is critical for virulence and several virulence-associated traits including production of the exopolysaccharides levan and amylovoran, normal biofilm formation, flagellar motility and translocation of type III effectors to plant cells (39). We have recently shown that ArcZ regulates flagellar motility through a direct interaction with the flagellar master regulator FlhD in *E. amylovora* (131) and that ArcZ impacts exopolysaccharide production and biofilm formation through the leucine responsive regulator protein Lrp (Chapter

4). However, it is not known how ArcZ regulates type III secretion, nor is it known if there are further virulence-associated traits being regulated by ArcZ.

Because of the breadth of phenotypes ArcZ regulates, we conducted a transcriptomic comparison of the Δ*arcZ* mutant relative to wild-type to gain additional insights into the breadth and mechanisms of ArcZ regulation of virulence-associated traits. In addition to previously known interactions between ArcZ and Lrp, we found that ArcZ regulates several genes involved in mitigating the threat of reactive oxygen species, and present evidence that this regulation is critical for *in planta* survival. We also found a significant amount of overlap between the ArcZ regulon and regulons of global transcription factors associated with oxidative state signaling, including the ArcBA two-component system. We further present evidence that ArcZ regulates *arcA* post-transcriptionally, indicating that ArcZ plays a major role in the oxidative status responsive regulatory pathways.

III. Materials and methods

Strain growth and culture conditions

Bacterial strains were routinely grown using LB culture media. *E. amylovora* strains were cultured at 28ºC and *Escherichia coli* strains were cultured at 37ºC. When appropriate, antibiotics were used in the following final concentrations: ampicillin 100 µg mL^{-1}, kanamycin 30 µg mL^{-1}, chloramphenicol 20 µg mL^{-1}. Bacterial strains and oligonucleotides used in this study are found in Table A.4 and Table A.5, respectively.

RNA extraction and sequencing

RNA was isolated from cells induced in *hrp*-inducing minimal medium (HIMM, 128) using the approach of Rivas et al. (159), with modifications specified in Chapter 4. RNA was quantified using the Qubit fluorescence method (ThermoFisher Scientific, Waltham, MA, USA). RNA

quality was ensured by visualization of ribosomal RNA bands in agarose gel and by LabChipGX HS RNA analysis (Caliper Life Sciences, Waltham, MA, USA). Total RNA was depleted of ribosomal RNA using bacterial Ribo-Zero kits (Illumina, San Diego, CA, USA) and remaining RNA was used for library preparation with the Illumina TruSeq Stranded Total RNA Library Preparation Kit on a Perkin Elmer Sciclone G3 robot using manufacturer's recommendations (Perkin Elmer, Waltham, MA, USA). Completed libraries were quality checked and quantified using a combination of Qubit RNA HS (ThermoFisher Scientific, Waltham, MA, USA) and Caliper LabChipGX HS RNA assays. All libraries were combined in equimolar amounts and pools were quantified using the Kapa Biosystems Illumina Library Quantification qPCR kit. Sequencing was performed in a single-end 50bp read format using HiSeq 4000 SBS reagents and base calling was done by Illumina Real Time Analysis (RTA) v.2.7.6. Output of RTA was demultiplexed and converted to FastQ format with Illumina Bcl2fastq v2.19.0.

Differential gene expression analysis

Reads obtained from RNA sequencing were trimmed of adapter sequences and filtered to remove low-quality reads using Trimmomatic (160). Trimmed and filtered reads were mapped to the *E. amylovora* ATCC49946 genome (161) using bowtie2 (162). The resulting SAM file of mapped reads was sorted for downstream applications using SAMTools (163). The *E. amylovora* ATCC49946 genome annotation file was used in conjunction with HTSeq (164) to count the number of reads mapping to each annotated feature. Read counts by feature across all samples were analyzed using the R package DESeq (165) to determine statistically differentially expressed genes between wild-type and Δ*arcZ* mutant samples with a false-detection rate of 0.05.

Quantitative real-time PCR

For qRT-PCR validation of select differentially expressed genes, RNA samples were collected in the same manner as for RNA sequencing. 500 ng of total RNA was used as template for reverse transcriptase reactions using the High-Capacity Reverse Transcriptase kit (Applied Biosystems, Foster City, CA, USA) following prescribed protocols. Resulting cDNA was utilized as template in qRT-PCR reactions set up using SYBR green 2X master mix (Applied Biosystems, Foster City, CA, USA) according to manufacturer's protocols and run on an Applied Biosystems StepOnePlus instrument. The housekeeping gene *recA* was included as an endogenous control, and relative mRNA abundance was calculated using the 2^{-ddCt} method (166).

Catalase activity, zone of inhibition, and minimum inhibitory concentration assays

Catalase activity assays were conducted as described (126), using cells grown overnight in liquid LB. Zone of inhibition was assayed by spread-plating bacteria cultures with an OD_{600nm} of 0.2 onto agar plates and then placing a filter paper disk in the center of the plate. A total of 10 µL of 8M H_2O_2 was dripped onto the filter paper, and plates were incubated for 24 hrs at 28ºC, after which the plate was imaged and the area of the zone of clearing around the filter paper disk was quantified using ImageJ image analysis software (122). For determination of the minimum inhibitory concentration (MIC) of H_2O_2, LB or minimal media (4 g L^{-1} L-asparagine, 2 g L^{-1} K_2HPO_4, 0.2 g L^{-1} $MgSO_4 \cdot 7H_2O$, 3 g L^{-1} NaCl, 0.2 g L^{-1} nicotinic acid, 0.2 g L^{-1} thiamin hydrochloride, 10 g L^{-1} sorbitol) were prepared with varying concentrations of hydrogen peroxide. Cells were inoculated into this media at an initial density of $1x10^7$ cfu mL^{-1} and incubated with shaking at 28ºC overnight. The MIC was determined to be the lowest concentration of hydrogen peroxide at which bacterial growth was inhibited.

Survival in tobacco apoplast

The ability of bacterial cells to survive in the apoplast of *Nicotiana tabacum* leaves was assessed as described (111), with the modification that surviving bacterial populations were enumerated at 5 days post-inoculation by dilution plating, rather than across a time-course.

Quantitation of hydrogen peroxide in apple leaves

Hydrogen peroxide levels in apple leaves were determined using a potassium iodide method (167). For the assay, apple leaves were inoculated as described (92) with a cell suspension of wild-type *E. amylovora* cells at a density of 5×10^8 cfu mL^{-1}, or inoculated with phosphate buffered saline. Inoculated leaves were sampled at indicated time points and 1 cm diameter disks were punched from the leaves, homogenized in potassium iodide buffer, and supernatants from homogenates were incubated in the dark for 30 minutes. Following incubation, 345 nm absorbance was measured, and background color from leaf tissue was subtracted by using leaf disks homogenized in water without any potassium iodide. Absorbance values were converted to concentrations of hydrogen peroxide using a standard curve.

Reporter fusion generation and testing

For translational fusions, the 5' untranslated region (UTR) of each gene of interest was amplified from the transcriptional start site through 20 amino acids into the coding region and cloned in-frame with *gfp* in plasmid pXG20 (168) using an in-vivo assembly approach (169). For the *katA* promoter fusion, the 500 bases upstream from the *katA* start codon were amplified and cloned into plasmid pPROBE-NT (170). Strains harboring the reporter fusions were assessed for GFP fluorescent output using a Tecan Spark plate reader (Tecan, Männedorf, Switzerland) with excitation wavelength of 488 nm and emission wavelength of 535 nm. Relative fluorescence

was determined by normalizing arbitrary fluorescence units to cell density, and relative to the wild-type strain.

Regulon analysis

Known *Escherichia coli* transcription factor regulons were obtained from RegulonDB (171) and corresponding gene sequences were extracted from the *Escherichia coli* K-12 genome (172). *Escherichia coli* gene sequences were used as queries to search for presence in *E. amylovora* using tblastx from BLAST+ (173). If a BLAST hit had an e-value of less than 0.001, that gene from *Escherichia coli* was considered present in *E. amylovora.* Using the assumption that if a transcription factor and its regulated genes are conserved across *Escherichia coli* and *E. amylovora*, regulatory relationships are likely to be similar, we used this assessment to generate putative *E. amylovora* regulons for several transcription factors. Putative *E. amylovora* regulons were tested for significant overlap with the ArcZ regulon determined herein using Fisher's exact test with adjustment for multiple hypothesis testing.

IV. Results

Transcriptomic characterization of the *E. amylovora* Δ*arcZ* mutant relative to wild-type

We sequenced the *E. amylovora* Ea1189 transcriptome using RNA from wild-type and Δ*arcZ* mutant cells induced for six or eighteen hrs in HIMM (128). Our sequencing resulted in a total of 128.4 million reads generated, of which 96.9 percent had per-base quality scores greater than 30. Of these reads, 97.2 percent mapped to the *E. amylovora* ATCC49946 genome. Following normalization and statistical analysis, we found a total of 342 differentially expressed genes between wild-type and Δ*arcZ* mutant cells. Of these, 62 genes were differentially regulated after six hours of induction (27 up-regulated, 35 down-regulated) and 302 were differentially expressed after eighteen hours of induction (176 up-regulated, 126 down-regulated)

with 22 genes differentially expressed at both time points (19 down-regulated, 3 up-regulated). Principal component analysis, based on differentially expressed genes showed that samples clustered by strain and time point (Figure 5.1).

Visualization of differentially expressed genes across samples is provided as a heatmap in Figure 5.2. Genes clustered into four main groups by strain and time point differences, designated groups I, II, III, and IV. Group I genes are characterized by higher expression in the Δ*arcZ* mutant after 6 h of induction in HIMM, but no dramatic differences between wild-type and Δ*arcZ* at 18 h. Genes of interest in group I include the aerotaxis receptor, *aer*, and the leucine responsive regulatory protein, *lrp*, which, as demonstrated in Chapter 4, is destabilized post-transcriptionally by ArcZ. Group II genes are characterized by higher expression in wild-type samples at 6 hrs of induction relative to 18 h of induction in HIMM and reduced expression in general in the Δ*arcZ* mutant at both time points. This is the largest cluster of differentially expressed genes and includes genes involved in several metabolic and virulence processes. Examples of virulence associated genes include flagellar motility genes (*flhC*, *motB*, and *flgE*) and type III secretion genes (*hrpA*, *hrpW*, and *hrpJ*). Examples of metabolic genes include *crp* encoding the global regulator catabolite repressor protein, and other genes involved in metabolism such as *argD*, *cysD*, *gcvP*, *livM*, and *metB*. Group III genes are characterized by higher expression in wild-type at 18 hrs in HIMM compared to wild-type after 6 hrs of induction in HIMM, but not elevated in the Δ*arcZ* samples after 18 h of induction in HIMM. Many of these genes are also general metabolism genes and include *tktA* and *rpsS*. Group IV genes have elevated expression in the Δ*arcZ* mutant cells after 18 h of induction in HIMM. Most of these genes are uncharacterized, but multiple genes in this group are likely involved in reactions with phospho-sugars, such as *pgsA* and EAM_1622.

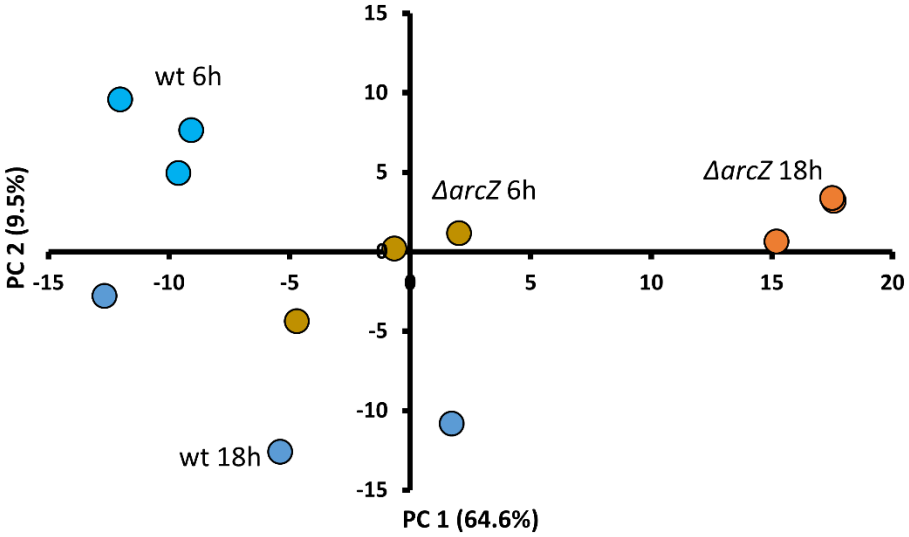

Figure 5.1: Principal component analysis across all genes of wt and Δ*arcZ* RNAseq samples shows clustering by strain/timepoint.

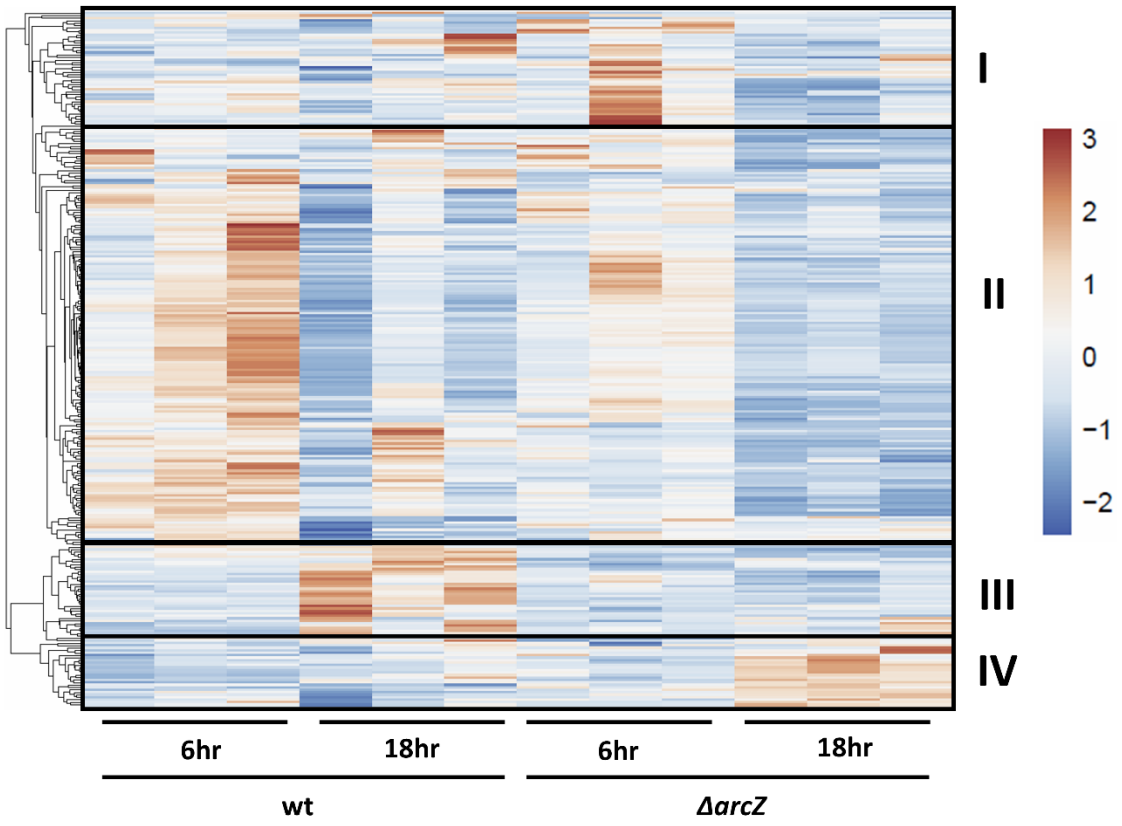

Figure 5.2: RNAseq heatmap comparing expression of differentially-expressed genes across all samples all samples. Rows are centered and unit variance scaling is applied to rows. Rows are clustered using correlation distance and average linkage. Four main clusters of differentially expressed genes have been designated as groups I, II, III, and IV.

Pathway enrichment in ArcZ regulon

We tested for enrichment of specific cell pathways as annotated by the Kyoto Encyclopedia of Genes and Genomes (KEGG) (174). We found no pathways significantly enriched in the set of genes differentially expressed in the six hour time point, however at the eighteen hour time point we found several pathways that were significantly enriched in differentially expressed genes (Figure 5.3). Several pathways that were enriched were involved in carbon metabolism and amino acid biosynthesis and metabolism. Because we observed that *crp* mRNA was affected by deletion of *arcZ*, it is possible that the carbon metabolism related pathway effects are due to this regulation, but it remains unknown if these are direct or indirect effects. The several genes and pathways involved in amino acid biosynthesis and metabolism are likely targets of the transcription factor Lrp, which is regulated by ArcZ and which we found to be differentially regulated in the Δ*arcZ* mutant in our transcriptomic analysis. The type III secretion system was also significantly enriched for differentially expressed genes, the function of which is known to be affected by deletion of *arcZ* (39). Other affected KEGG pathways included sulfur metabolism, selenocompound metabolism, monobactam biosynthesis, RNA polymerase, and quorum sensing. Some of these pathways, although annotated in the KEGG database, may not be functional in *E. amylovora* as experimental evidence is lacking.

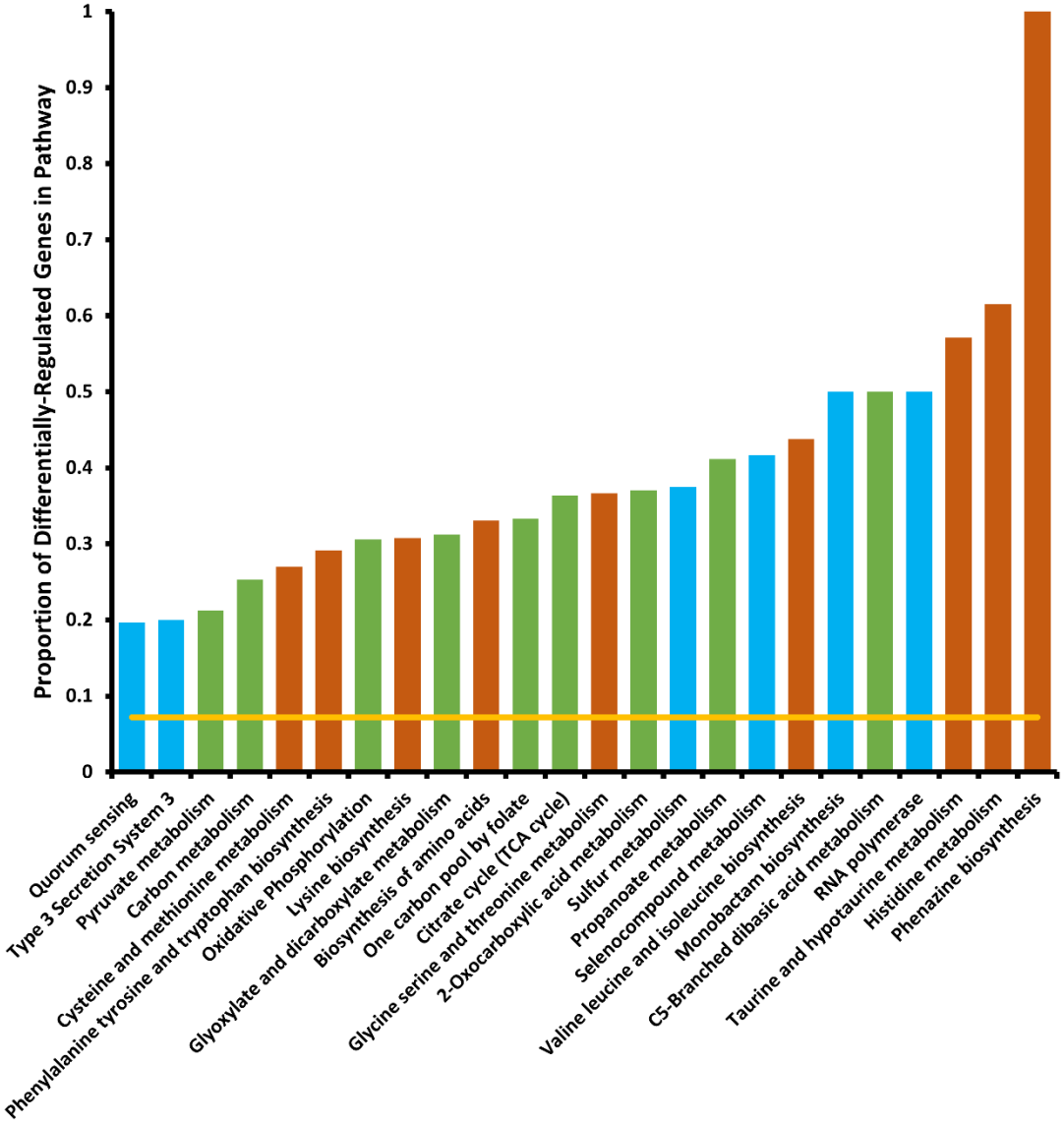

Figure 5.3: KEGG pathways significantly enriched in differentially-expressed genes. Yellow line indicates expected proportion of differentially-expressed genes if randomly distributed. Bars correspond to observed proportions of differentially-expressed genes in KEGG pathways. Green bars indicate KEGG pathways related to carbon and central metabolism, burnt-orange bars indicate KEGG pathways relating to amino acid biosynthesis and metabolism and blue bars indicate other KEGG pathways. All bars shown are significantly enriched ($P_{adj} < 0.05$) by Fisher's exact test.

When analyzing the KEGG pathway for glycolate/glyoxylate metabolism, we found that *E. amylovora* has neither genes coding for enzymes that generate glycolate nor glyoxylate. In other organisms, glycolate oxidase, which converts glycolate to glyoxylate, generates hydrogen peroxide as a byproduct of this enzymatic reaction (175), and catalase is considered to be a part of this pathway for the detoxification of the peroxide. Although *E. amylovora* does not code for a glycolate oxidase enzyme, plants do, and have been shown to use this enzyme for generating hydrogen peroxide as a pathogen defense mechanism (176, 177). This led us to search for other genes differentially regulated by ArcZ that may play a role in coping with oxidative stress.

ArcZ regulates oxidative stress response genes

In our search of differentially expressed genes that have links to the oxidative stress response, we found *katA*, encoding a catalase, *tpx*, encoding a thiol-peroxidase, and *osmC*, encoding an osmotically inducible peroxiredoxin. *katA* and *osmC* were both down-regulated in the Δ*arcZ* mutant, and *tpx* mRNA was more abundant (Figure 5.4A). Although recent work has indicated that another catalase, KatG, plays a role in *E. amylovora* mitigation of oxidative stress (111), *katG* was not differentially expressed in the Δ*arcZ* mutant relative to wild-type. Nonetheless, as an additional oxidative stress mitigation enzyme, we have included *katG* in several of our experiments to better understand its role with the other ArcZ-regulated oxidative stress mitigation enzymes. We independently verified by quantitative real-time PCR that *katA* and *osmC* are down-regulated in the Δ*arcZ* mutant, and that *tpx* is up-regulated (Figure 5.4B). Consistent with our RNAseq data, there was no difference in relative abundance of *katG* mRNA between wild-type and the Δ*arcZ* mutant.

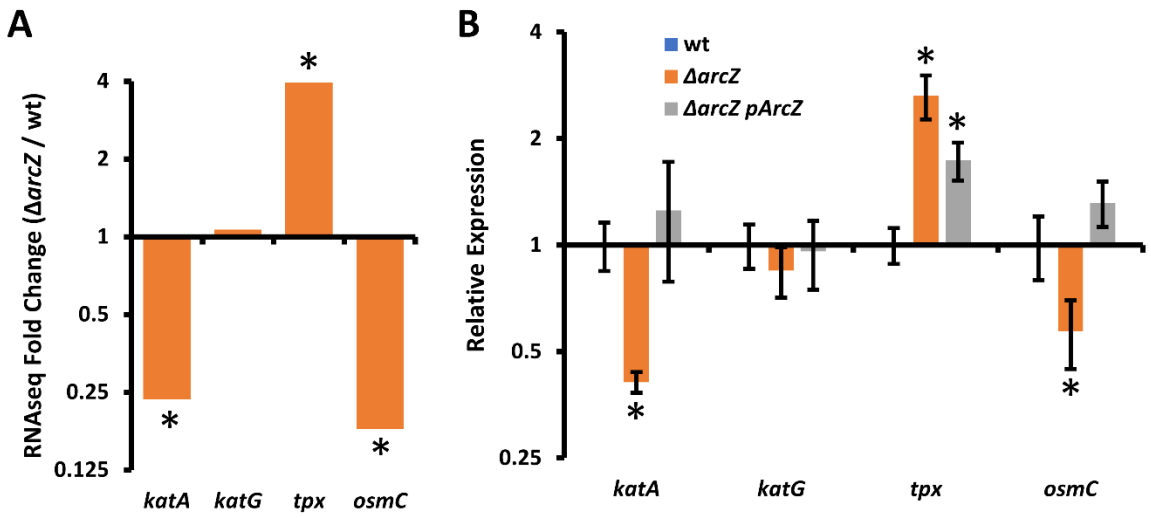

Figure 5.4: Oxidative stress mitigation enzymes are differentially expressed in *E. amylovora* Ea1189 Δ*arcZ* mutant relative to wild-type. Relative expression of *katA*, *katG*, *tpx*, and *osmC* based on (**A**) RNAseq (Δ*arcZ*/wt) or (**B**) quantitative real-time PCR Asterisks indicate significant difference ($P < 0.05$) from wild-type by negative binomial distribution (RNAseq; through DESeq) or Student's t-test (qPCR data).

ArcZ regulated oxidative stress response genes are critical for survival of exogenous hydrogen peroxide

Because KatA and KatG have been shown to play a role in *E. amylovora* response to exogenous hydrogen peroxide, we tested the Δ*arcZ* mutant, along with the Δ*katA*, Δ*katG*, Δ*tpx*, and Δ*osmC* mutants for their catalase activity and survival after treatment with excess hydrogen peroxide. We found that the Δ*katA* mutant had no detectable catalase activity (Figure 5.5A) and exhibited increased susceptibility to hydrogen peroxide in a disk diffusion assay (Figure 5.5B). The catalase activity of the Δ*arcZ* mutant was reduced nearly 10-fold relative to wild-type and the mutant also showed an increase in sensitivity to hydrogen peroxide in a disk-diffusion assay. The Δ*tpx* mutant had a reduction in catalase activity of about 3-fold and increased sensitivity to hydrogen peroxide in the disk diffusion assay. The Δ*katG* and Δ*osmC* mutants had only a slight decrease in overall catalase activity, and the Δ*katG* mutant had increased susceptibility in the disk diffusion assay. It is likely that the Δ*katG* mutant did not show decreased catalase activity in the catalase activity assay but does have increased susceptibility in the disk-diffusion assay because of the differences in growth in liquid culture for the catalase activity assay and growth on solid media for the disk-diffusion assay, as it is known that *katG* expression is growth phase dependent (111). The sensitivity of the Δ*osmC* mutant was not different from wild-type in the disk-diffusion assay.

During our determination of catalase activity in *E. amylovora*, we observed that a small amount of catalase activity is secreted into the culture medium. To determine whether the secreted catalase is KatA or KatG, we concentrated culture supernatants from overnight cultures of the Δ*katA* and Δ*katG* mutants. Concentrated supernatants were mixed with hydrogen peroxide and monitored for evolution of gas through formation of bubbles. Catalase activity was observed

in the Δ*katG* culture supernatants, but not in the Δ*katA* culture supernatants, indicating that KatA is responsible for the secreted catalase activity (data not shown). Because secreted catalase activity has not been reported in other *Enterobacteriaceae*, we conducted a multiple sequence alignment of KatA and KatE protein sequences from phylogenetically diverse bacteria. This analysis revealed that *E. amylovora* KatA is more similar to KatA from *Bacillus subtilis* and *Pseudomonas aeruginosa* than to KatE from *Escherichia coli* (Figure 5.6). Protein BLAST (173) further showed that the most similar hits for a search with *E. amylovora* KatA as query came from the genera *Erwinia, Pantoea*, and *Pseudomonas*.

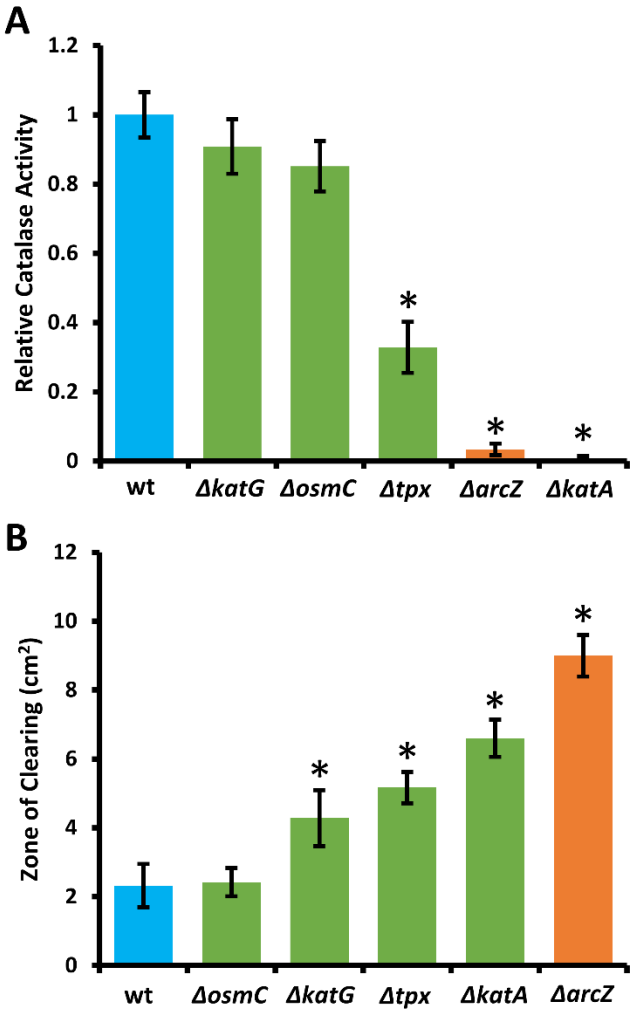

Figure 5.5: *E. amylovora* Ea1189 Δ*arcZ* mutant has reduced catalase activity and increased susceptibility to exogenous hydrogen peroxide. Relative catalase activity (**A**), determined from cells grown overnight in LB broth. Zone of clearing (**B**) around a filter paper disk treated with 10 µL of 8M hydrogen peroxide on LB solid media. Assays were repeated at least 4 times. Asterisks indicate significant ($P < 0.05$) difference from wild-type by Student's t-test.

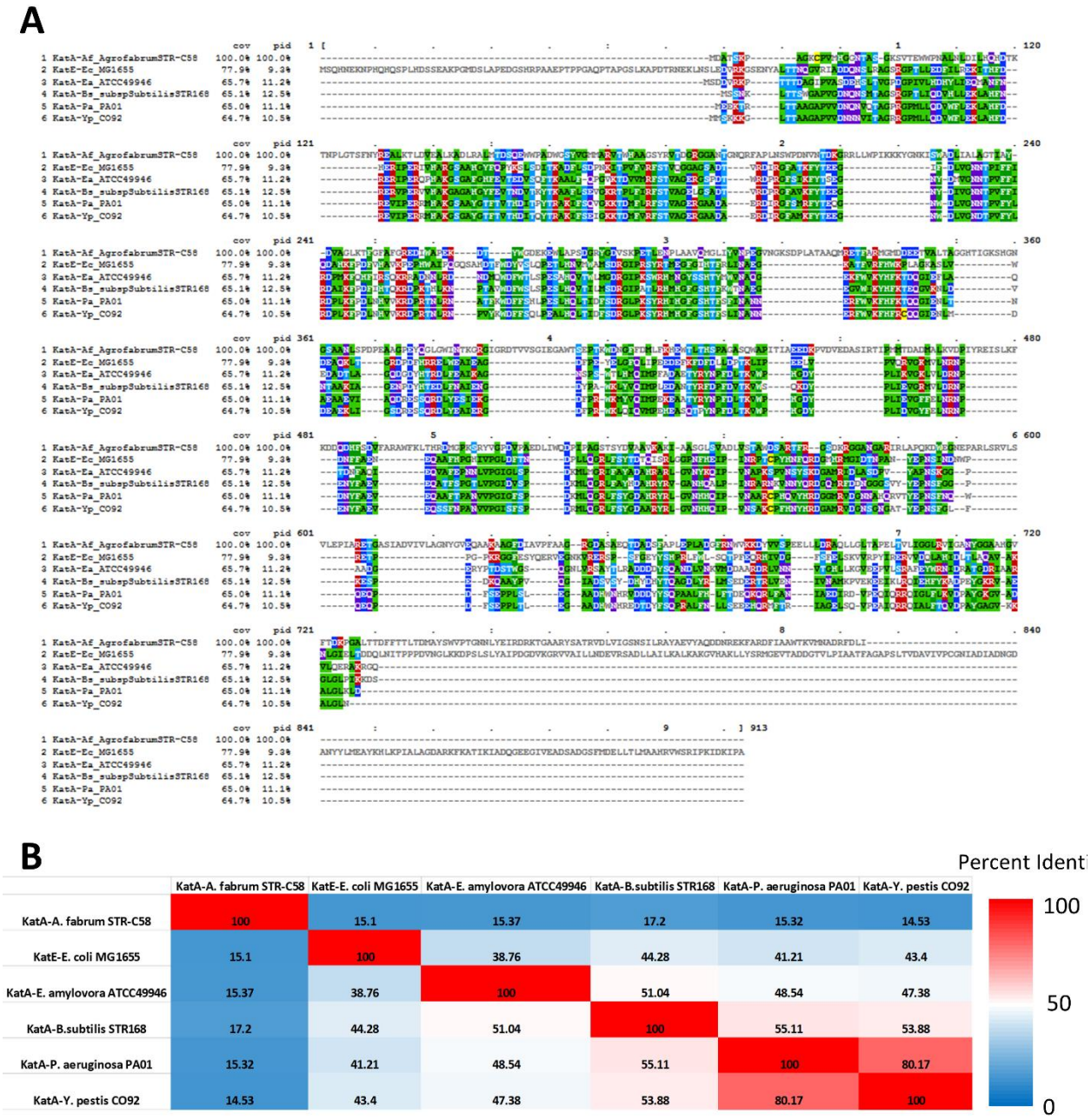

Figure 5.6: KatA from *E. amylovora* is more similar to KatA from *Bacillus subtilis* and *Pseudomonas aeruginosa* than KatE from *Escherichia coli.* (A) Multiple sequence alignment of KatA and KatE protein sequences generated using MUSCLE and visualized using MVIEW. (B) Percent identity matrix based on multiple sequence alignment in (A).

Mutation of *arcZ* can be complemented by *katA*

Because Δ*arcZ* has reduced catalase activity relative to wild-type and is more susceptible than wild-type to exogenous hydrogen peroxide both on solid media and in liquid media, we wanted to determine if any of the oxidative stress mitigation enzymes would be able to restore wild-type phenotypes in these tests. To test this, we complemented the Δ*arcZ* mutant with *katA*, *katG*, *tpx*, or *osmC*, each on a plasmid with the respective native promoter. When tested for catalase activity, we found that introduction of any of these genes on a plasmid led to increased catalase activity relative to the Δ*arcZ* mutant (Figure 5.7A). However, providing *katG*, *tpx*, or *osmC* in the Δ*arcZ* mutant still resulted in catalase activity well below that of wild-type cells. Only providing *katA* on a plasmid restored catalase activity to greater than wild-type levels. When we tested the Δ*arcZ* mutant complemented with *katA* in the disk-diffusion assay for susceptibility to exogenous hydrogen peroxide, we found that *katA* restored wild-type levels of growth in the Δ*arcZ* mutant (Figure 5.7B).

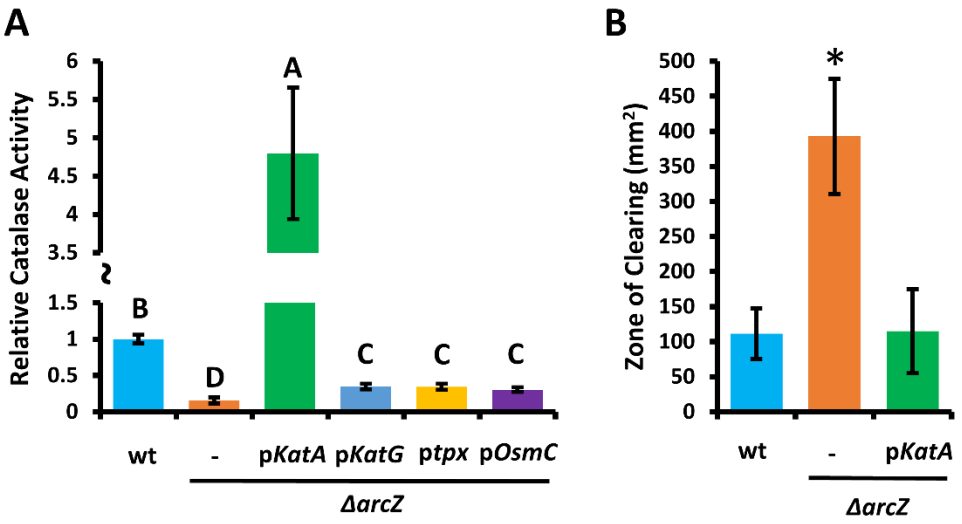

Figure 5.7: Providing *katA* on a plasmid restores catalase activity and resistance to exogenous hydrogen peroxide in the *E. amylovora* Ea1189 Δ*arcZ* mutant. Relative catalase activity (**A**) of wild-type or Δ*arcZ* mutant carrying empty plasmid (-) or the indicated gene with its corresponding native promoter. Groups with shared letter designation do not differ from each other significantly ($P < 0.05$) by Tukey's HSD test. Zone of clearing (**B**) around a filter paper disk treated with 10 µL of 1M hydrogen peroxide on LB solid media. Tests were conducted at least 4 times and asterisks denote significant differences ($P < 0.05$) from wild-type by Student's t-test.

Hydrogen peroxide produced by inoculated apple shoots

In order to relate the difference in hydrogen peroxide susceptibility of our various strains to the interactions between *E. amylovora* and host apple shoots, we quantified hydrogen peroxide levels in apple leaves over the course of infection with wild-type *E. amylovora* cells. We detected a baseline of approximately 1 mM hydrogen peroxide in uninfected apple leaves (Figure 5.8A). One day post-inoculation, before visual disease symptoms developed, hydrogen peroxide levels doubled to nearly 2 mM. After two days post-inoculation, when visual symptoms had developed in the main vein of the leaf, hydrogen peroxide levels had doubled again, to over 4 mM. After three and four days post-inoculation, as visual fire blight symptoms spread from the main vein to the rest of the leaf, hydrogen peroxide levels decreased again to below 2 mM (Figure 5.8A).

In order to determine the hydrogen peroxide concentration to which *E. amylovora* wild-type and Δ*arcZ* mutant cells are susceptible, we tested for the minimum inhibitory concentration (MIC) of hydrogen peroxide. We found that the MIC of hydrogen peroxide for wild-type cells is 5 mM whether tested in minimal medium or rich LB medium (Figure 5.8B). The MIC of hydrogen peroxide for Δ*arcZ* mutant cells was found to be 1 mM in minimal medium and 2 mM when tested in LB medium. This is consistent with the finding that metabolism of specific amino acids available in rich media can help to mitigate oxidative threats (178) The MIC of hydrogen peroxide to the Δ*arcZ* mutant was complemented back to wild-type levels by providing *arcZ* on a plasmid under control of its native promoter. The Δ*arcZ* mutant with *katA* on a plasmid grew uninhibited at concentrations of hydrogen peroxide up to 10 mM. It is noteworthy that the hydrogen peroxide MIC for wild-type cells was determined to be 5 mM, but *in planta* hydrogen peroxide levels peaked at just over 4 mM.

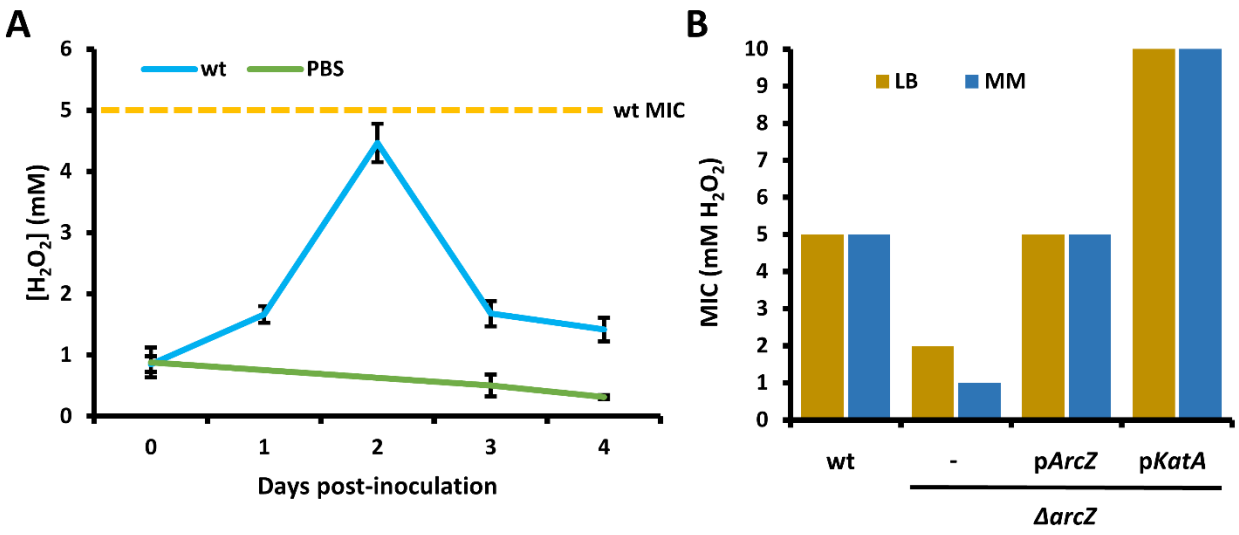

Figure 5.8: *Erwinia amylovora* Ea1189 elicits hydrogen peroxide production response from apple leaves and has evolved to cope with high levels of exogenous hydrogen peroxide. (**A**) Levels of hydrogen peroxide in apple leaves inoculated with wild-type *E. amylovora* or mock-inoculated with phosphate buffered saline (PBS), across time following inoculation. Dotted line indicates the H_2O_2 minimum inhibitory concentration (MIC) of wild-type *E. amylovora* Ea1189. (**B**) The MIC of hydrogen peroxide for wild-type or Δ*arcZ* mutant carrying empty plasmid (-) or the indicated gene with its native promoter. MIC was tested in LB and minimal media with sucrose as the carbon source (MM).

ArcZ and KatA are critical for survival of *E. amylovora* during the hypersenstitive response in tobacco

Because the hydrogen peroxide MIC for wild-type and Δ*arcZ* mutant cells and our quantification of hydrogen peroxide levels in apple leaves suggested that the inability of the Δ*arcZ* mutant to cope with oxidative stress may play an important role in ability of the bacteria to survive and successfully infect host plants, we wanted to test the impact of catalase activity on bacterial survival *in planta*. Because loss of *arcZ* leads to decreases in several virulence-associated traits, we also wanted to uncouple survival during the *in planta* oxidative burst from other virulence defects. To accomplish this, we assessed survival in non-host *Nicotiana tabacum* (tobacco) which will undergo a hypersensitive response, including an oxidative burst (179), in response to type III effector translocation when *E. amylovora* cells are infiltrated into the tobacco apoplast (134). We infiltrated tobacco leaves with *E. amylovora* Ea1189 wild-type and Δ*arcZ* mutant cells at a density of 10^9 CFU mL^{-1} and assessed survival five days post-infiltration by sampling a 1 cm^2 leaf disk. We found that on average 10^7 CFU/cm^2 wild-type cells survived but only 10^5 CFU/cm^2 of Δ*arcZ* mutant cells survived (Figure 5.9). The survival defect in the Δ*arcZ* mutant could be rescued by providing *katA* on a plasmid, suggesting that the survival defect in the Δ*arcZ* mutant is due to increased susceptibility to reactive oxygen species, and not just to other pleiotropic effects of ArcZ. To verify whether provision of *katA* on a plasmid in the Δ*arcZ* mutant would be sufficient to complement the Δ*arcZ* virulence defect, we inoculated immature pears and monitored symptom development. We found that providing *katA* on a plasmid did not increase virulence of the Δ*arcZ* mutant on immature pears (data not shown).

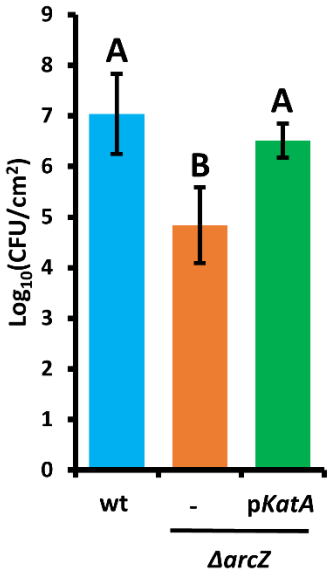

Figure 5.9: Survival of *E. amylovora* Ea1189 cells in tobacco leaves following elicitation of the hypersensitive response. Leaf disks were sampled 5 days post-infiltration. Each strain was tested at least 6 times. Error bars represent standard deviation and groups with shared letter designation do not differ significantly from each other ($P > 0.05$) by Tukey's HSD test.

ArcZ regulates *katA* transcriptionally and *tpx* post-transcriptionally

Because ArcZ is a post-transcriptional regulator and modulates *katA* transcript abundance, we assessed whether ArcZ regulates *katA* at the transcriptional or post-transcriptional level. To do so, we constructed a promoter fusion with the *katA* promoter upstream of a promoter-less *gfp* in plasmid pPROBE-NT (170), and a translational fusion with the 5' UTR of *katA* and first 18 amino acids in-frame with *gfp* in plasmid pXG20 (168). We observed reduced *katA* promoter activity in the Δ*arcZ* mutant relative to wild-type but no difference on the *katA* translational fusion between wild-type and Δ*arcZ* (Figure 5.10).

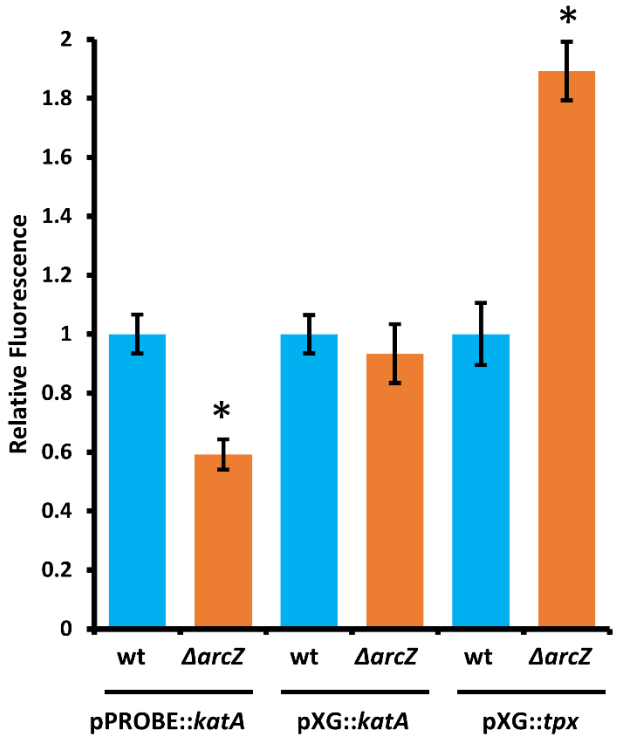

Figure 5.10: ArcZ of *E. amylovora* Ea1189 regulates *katA* promoter activity and regulates *tpx* post-transcriptionally. Relative fluorescence of indicated reporter fusions tested in Δ*arcZ* mutant cells and relative to fluorescence of wild-type cells carrying the same construct. Asterisks indicate significant difference ($P < 0.05$) by Student's t-test between Δ*arcZ* and wild-type carrying the same construct.

Because ArcZ is known to post-transcriptionally repress *tpx* mRNA in *Salmonella* Typhimurium through a direct interaction (75), we tested whether ArcZ repression of *tpx* also occurs through post-transcriptional regulation in *E. amylovora*. We generated a translational fusion with the 5' UTR of *tpx* and first amino acids in-frame with *gfp* in plasmid pXG20 (168), and compared relative fluorescence between wild-type and Δ*arcZ* mutant cells. We found increased GFP fluorescence in the Δ*arcZ* mutant relative to wild-type (Figure 5.10), suggesting that the ArcZ-*tpx* interaction is likely conserved between *Salmonella* Typhimurium and *E. amylovora*. To determine if this interaction is likely to occur between the same bases in these two organisms, we predicted the interaction between ArcZ and *tpx* using RNAhybrid (180), and found that the same region is predicted to interact in *E. amylovora* as in *Salmonella* Typhimurium (Figure 5.11). Because the same interaction is predicted, and the fact that ArcZ has a high degree of conservation in the interacting region (131), it is likely that the post-transcriptional repression of *tpx* mRNA in *E. amylovora* occurs through the same interaction as in *Salmonella* Typhimurium.

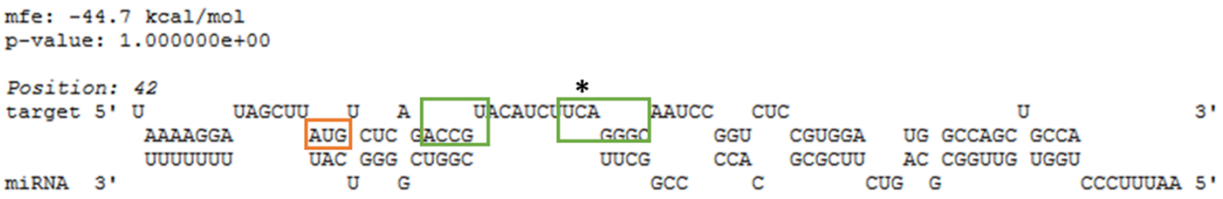

Figure 5.11: ArcZ predicted interaction with *tpx* as predicted by RNAhybrid. Orange box indicates *tpx* start codon, green boxes indicate bases predicted to be involved in base-pairing in *Salmonella* Typhimurium, and asterisk indicates a base that reduced ArcZ-*tpx* interaction when mutated in *S.* Typhimurium.

ArcZ regulon overlaps with known transcription factor regulons

Because ArcZ regulates *katA* at the transcriptional level, we utilized our RNAseq data to search for candidate regulators that could explain the ArcZ regulation of *katA*. We analyzed the ArcZ regulon for overlap with known transcription factors with known regulons. We inferred *E. amylovora* transcription factor regulons on the assumption that if a transcription factor and its target gene are conserved between *Escherichia coli* and *E. amylovora* then the target is also a part of the regulon in *E. amylovora*. We acquired *Escherichia coli* regulon information from regulondb.com and utilized BLAST+ to search for transcription factor and target homologs in *E. amylovora*. Using this approach, we found 38 conserved regulators with conserved targets in those regulons, with an average of 48.5% of targets conserved in each regulon. When we tested these putative regulons for overlap with our determined *E. amylovora* ArcZ regulon, we found six regulons with a significant ($P_{adj} < 0.05$; Fisher's exact test) amount of overlap (Figure 5.12). The six transcription factors with overlapping regulons are ArcA, Fnr, IHF, Lrp, NarL, and PurR. We note also that the overlap between the ArcZ and Fur regulons was nearly significant ($P_{adj} = 0.069$). Of these regulons, ArcA, Fnr and Fur all form a network of interactions and are known to have impacts on oxidative sensing and response (including catalase) in *Escherichia coli* (181-184). Furthermore, this core set ArcA, Fnr, and Fur also has known interactions with IHF (185), NarL (186), and PurR (187), three of the remaining regulators with ArcZ regulon overlap. Additionally, Chapter 4 reported that Lrp is regulated post-transcriptionally by ArcZ.

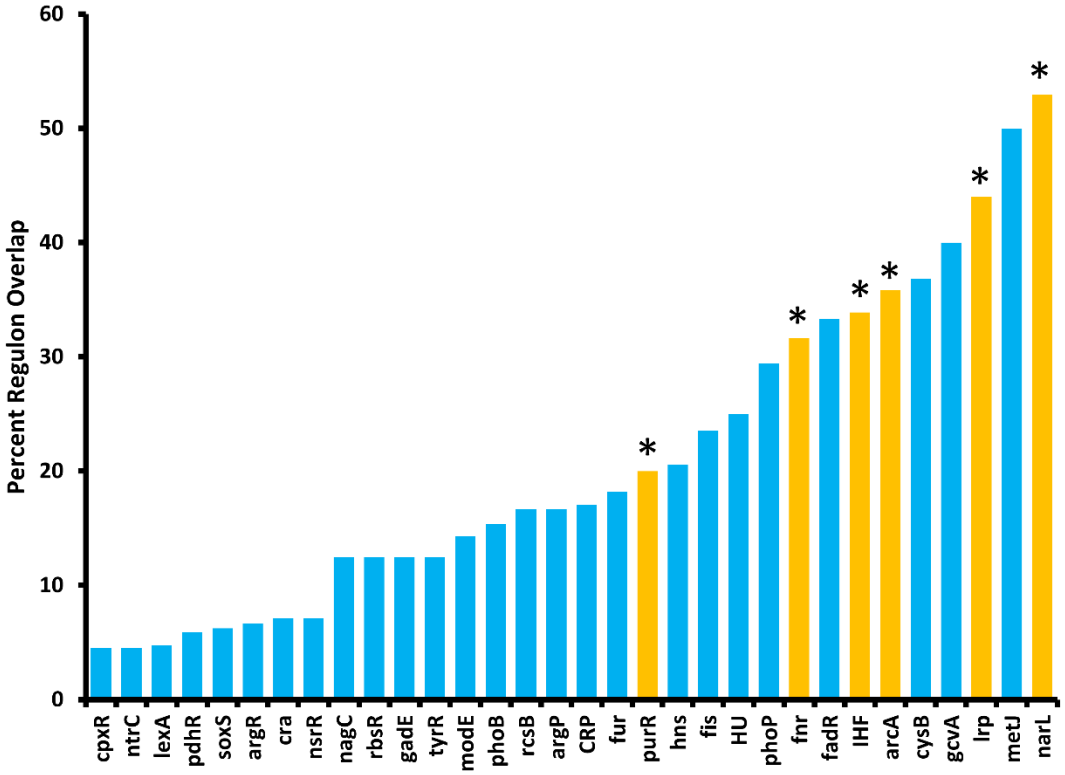

Figure 5.12: The *E. amylovora* Ea1189 ArcZ regulon overlaps with several putative transcription factor regulons. Transcription factor regulons were inferred in *E. amylovora* based on documented regulons in *Escherichia coli* and tested for significant ($P_{adj} < 0.05$; indicated by asterisks above bars) overlap with the ArcZ regulon by Fisher's exact test. Transcription factor regulons with no overlap with the ArcZ regulon are not shown.

ArcZ regulation is recapitulated by *arcA* and *arcB* mutants

To determine the regulatory roles that the ArcBA two-component system, along with Fnr and Fur may share with ArcZ, we generated single-gene deletion mutants for each of the genes encoding these transcriptional regulators. We determined the effect of these mutations on swimming motility and susceptibility to exogenous hydrogen peroxide, two phenotypic traits affected by deletion of *arcZ*. We found that the Δ*arcA* mutant had reduced swimming motility compared to wild-type, but that deletion of *arcB*, *fnr*, or *fur* had no effect (Figure 5.13A). Similarly, we found increased susceptibility to exogenous hydrogen peroxide in the Δ*arcA* and Δ*arcB* mutants compared to wild-type, but no difference in susceptibility to hydrogen peroxide in the Δ*fnr* and Δ*fur* mutants (Figure 5.13B).

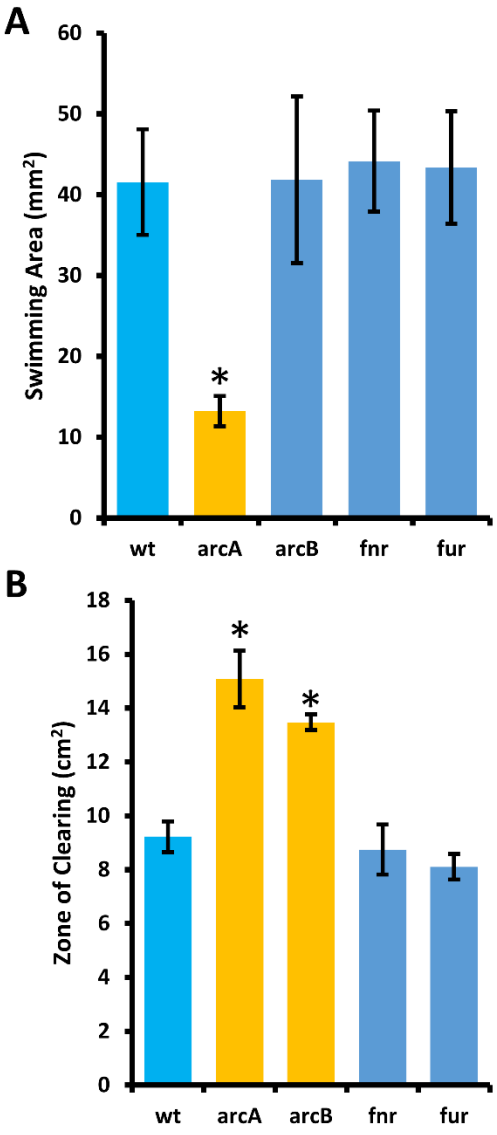

Figure 5.13: The *E. amylovora* Ea1189 ArcBA two-component system affects swimming motility and hydrogen peroxide susceptibility. (**A**) Swimming motility area of indicated strains 24 hours after stab inoculation into soft agar (0.25% w/v) plates. (**B**) Zone of clearing around a filter paper disk treated with 8 M hydrogen peroxide on LB solid media. Asterisks indicate significant difference ($P < 0.05$) from wild-type strain.

ArcZ regulates ArcA post-transcriptionally

Because deletions in *arcA* or *arcB* of the ArcBA two-component system had similar effects to Δ*arcZ* on the motility and susceptibility to hydrogen peroxide phenotypes, we generated translational fusions for *arcA* and *arcB* to test whether ArcZ regulates these genes post-transcriptionally. We additionally generated a *fur* translational fusion to determine if ArcZ regulates *fur* post-transcriptionally because Fur is a transcriptional regulator of the catalase *katE* in *Escherichia coli* (184). The *arcA*, *arcB*, and *fur* translational fusions with *gfp* reporter were tested in an *Escherichia coli* strain carrying *arcZ* under control of an IPTG-inducible *tac* promoter. Upon induction of *arcZ* expression, we found no difference in the strain carrying the *arcB* or *fur* translational fusion constructs but did find increased fluorescence in the strain carrying the *arcA* construct (Figure 5.14A). To confirm this result, we tested the *arcA* translational fusion in *E. amylovora* wild-type and Δ*arcZ* mutant cells and found a 20 percent reduction in fluorescence in the Δ*arcZ* mutant compared to wild-type (Figure 5.14B). Together these results indicate that ArcZ regulates *arcA* post-transcriptionally in *E. amylovora*. We predicted candidate interactions between ArcZ and *arcA* mRNA using RNAHybrid (180) and found a strong candidate interaction 50 bases upstream of the ArcA start codon (Figure 5.15). Consistent with the idea that ArcZ is affecting *katA* at the transcriptional level through post-transcriptional regulation of *arcA*, we found three direct repeats of the ArcA binding motif upstream of *katA* in the *E. amylovora* genome (Figure 5.16). These three direct repeats of the ArcA binding motif represent a common arrangement of binding motifs in ArcA regulated genes (188).

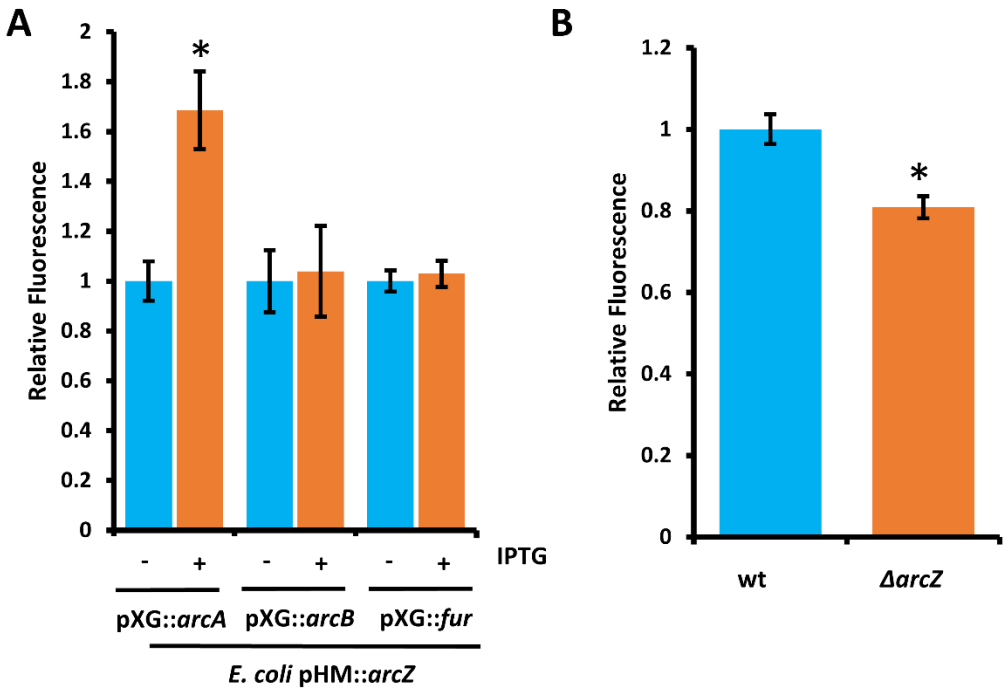

Figure 5.14: ArcZ of *E. amylovora* Ea1189 regulates *arcA* post-transcriptionally. (**A**) *Escherichia coli* carrying *E. amylovora arcZ* on a plasmid under control of the IPTG-inducible *tac* promoter, with the indicated translational fusions comparing relative fluorescence between un-induced and induced cells. (**B**) Relative fluorescence of *E. amylovora* wild-type or Δ*arcZ* mutant cells carrying the *arcA* translational fusion. Asterisks indicate significant difference ($P < 0.05$) from wild-type or un-induced cells carrying the same reporter plasmid by Student's t-test.

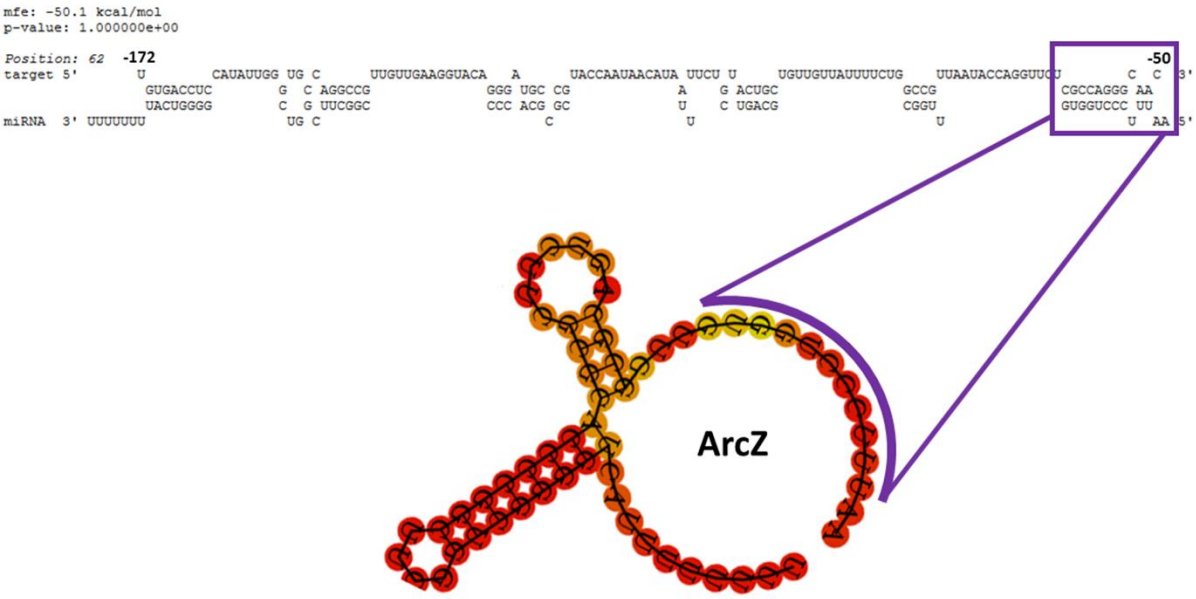

Figure 5.15: ArcZ predicted interaction with *arcA* as predicted by RNAhybrid, with indication of accessible ArcZ bases typically involved in target interaction.

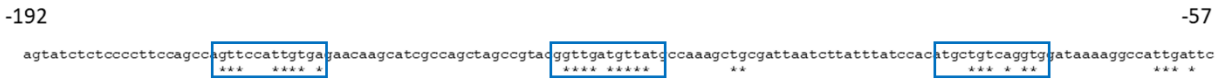

Figure 5.16: ArcA predicted binding motifs upstream of *katA* in *E. amylovora* genome. The *katA* promoter has 3 ArcA motif direct repeats with good agreement with consensus motif at 21-22 bp intervals. Asterisks indicate bases that match the ArcA binding motif.

V. Discussion

Here we present transcriptomic analysis of the sRNA ArcZ regulon, providing evidence that in *E. amylovora*, ArcZ is a global regulator with a regulon of at least 342 genes, or 9.8% of the genome, based on the culture conditions used in our study. Furthermore, analysis of the ArcZ regulon identified an important role for ArcZ in regulation of genes involved in coping with oxidative stress. We found that ArcZ regulates *katA* at the transcriptional level and while it affects *tpx* transcript abundance, ArcZ represses *tpx* post-transcriptionally.

In addition to transcriptional regulation of *katA* and post-transcriptional regulation of *tpx*, we found that ArcZ regulates *arcA* post-transcriptionally. In *Escherichia coli*, ArcA is the response regulator of the ArcBA (anoxic redox control) two-component system, which is responsive to oxidative status of the cell (189). This two-component system is activated in a sigmoidal response pattern in response to oxidative state of quinones (190). The sRNA ArcZ has received this Arc acronym for its position adjacent to *arcB* in the genome as an arc-associated sRNA (75). Although *arcB* and *arcZ* are distal to *arcA* in the genome, it has been found in *Escherichia coli* that *arcZ* is transcriptionally regulated in response to oxygen levels in an ArcA dependent manner (74). Because we are reporting that ArcZ regulates *arcA* post-transcriptionally in *E. amylovora*, this suggests that if these regulatory relationships are conserved between *E. amylovora* and *Escherichia coli*, ArcZ and ArcA may form a feedback loop to reinforce cellular responses in response to oxygen availability and oxidative status.

Given our findings that ArcZ regulates *katA* at the transcriptional level and *arcA* and *tpx* post-transcriptionally, we propose a regulatory model in which the ArcBA two-component system acts as an oxygen sensor to transcriptionally regulate *arcZ* and *katA*, and that ArcZ in turn activates *arcA* post-transcriptionally, providing positive feedback on catalase activity

(Figure 5.17). ArcA regulates transcription of *arcZ* in *Escherichia coli* in an oxygen dependent manner (74), but further work is necessary to confirm that this same regulation occurs in *E. amylovora*. We hypothesize that this proposed regulatory loop is significant during infection of host tissue, because of variations in oxygen accessibility across tissues. For example, in tissues with high oxygen availability such as leaves and flowers, *E. amylovora* cells are interacting with living host cells that are the most prone to mount defense responses including production of reactive oxygen species. It has been shown previously that *E. amylovora* cells trigger defense mechanisms including generation of an oxidative burst during compatible interactions (i.e. successful infection) (191-193). Indeed, we demonstrate here that concentrations of hydrogen peroxide in infected apple leaves peak at levels of 4 to 5 mM at two days post-inoculation (Figure 5.8A). In contrast, host cells are dead in mature xylem vessels, and host-produced reactive oxygen species are likely to be scarce. Furthermore, in woody xylem, it has been shown that oxygen levels are typically reduced to half of atmospheric oxygen with ample water flow, but that when xylem flow is restricted, oxygen levels can drop to anaerobic levels (194). The oxygen-responsive nature of the proposed ArcZ-ArcA-KatA feedback loop suggests that oxygen and oxidative state may play an essential role in proper expression of genes for coping with reactive oxygen species during disease progression. Future work to determine the specific roles of oxygen availability as an environmental signal modulating virulence gene expression shows great promise to provide novel insights into how *E. amylovora* integrates environmental signals to determine virulence behaviors. Such insights are of great importance in understanding the basic biology of this pathogen to guide development of strategies that can limit its devastating effects.

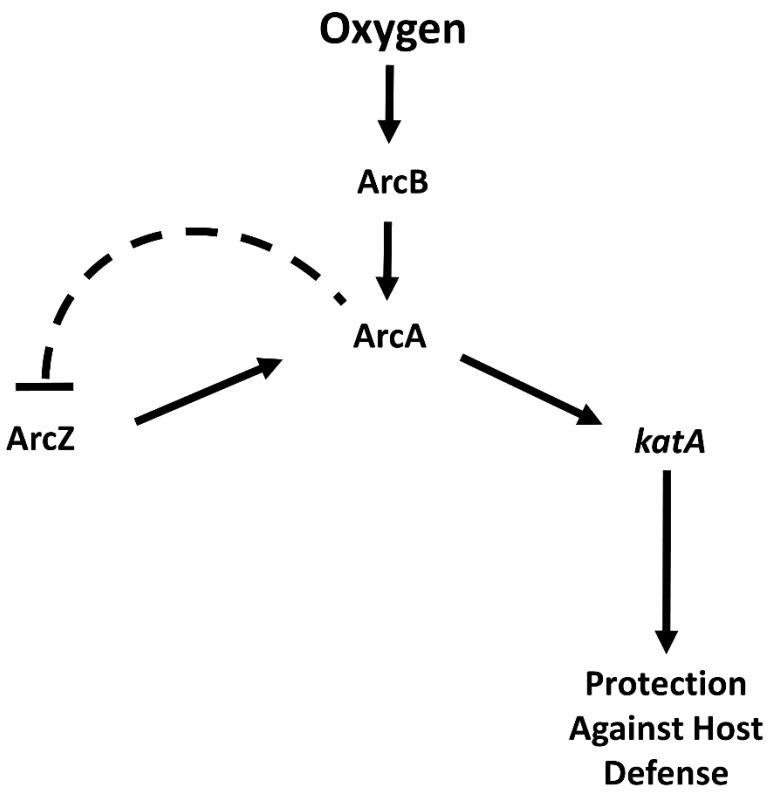

Figure 5.17: Proposed model of ArcZ regulation of *katA*. In this proposed model, ArcZ positively regulates ArcA post-transcriptionally through a predicted direct interaction, and ArcA regulates *katA* by binding directly to predicted sites in the *katA* promoter.

In support of the importance of ability to cope with reactive oxygen species during infection, we found that provision of *katA* on a plasmid in the Δ*arcZ* mutant background not only restored catalase activity and wild-type susceptibility to exogenous hydrogen peroxide in *in vitro* tests, but also restored survival in non-host tobacco during hypersensitive response. This suggests that although Δ*arcZ* mutant cells are deficient in several virulence factors (39), coping with reactive oxygen species is a major limiting factor for this mutant *in planta* independent of other virulence-associated traits.

We found that ArcZ regulation of *katA* occurs at the transcriptional level and not at the post-transcriptional level. However, we did find that ArcZ regulates *arcA* and *tpx* post-transcriptionally. Interaction predictions between ArcZ and the *arcA* 5'UTR indicate a likely interaction that could explain the effect of ArcZ on the *arcA* 5' UTR, but further work is needed to provide experimental confirmation that these bases participate in direct interactions. The presence of three sequential ArcA binding sites upstream of *katA* suggests that the ArcZ regulation of *katA* is through the observed post-transcriptional effects on *arcA*. Again, future experimentation is necessary to confirm that ArcA directly regulates *katA* transcription.

The determined ArcZ regulon had significant overlap with the inferred regulons of ArcA, Fnr, PurR, Lrp, IHF, and NarL. Work in Chapter 4 indicated that ArcZ regulates *lrp*, and that finding was confirmed in this work in the significant amount of overlap between the ArcZ and Lrp regulons. In *Escherichia coli*, the remaining transcription factors with regulon overlap with ArcZ form a complex web of inter-regulation, which is also involved in transcriptional regulation of catalases and thiol peroxidase (181-184, 195). The finding that ArcZ regulates *arcA* post-transcriptionally provides a connection between this sRNA and this transcription factor network, although additional links may exist. Although ArcZ affected abundance of *osmC* transcripts,

deletion of *osmC* had little effect on the oxidative stress phenotypes we tested. Because *osmC* is a part of the *lrp* regulon (196), it seems possible that ArcZ is regulating *osmC* through its post-transcriptional regulation of *lrp*. Because we found weak effects in the Δ*osmC* mutant when testing with hydrogen peroxide, it is possible that in *E. amylovora* a peroxiredoxin OsmC functions to reduce the threat of organic peroxides but has little activity against inorganic hydrogen peroxide. Future work to understand the role of *osmC* and additional interactions between ArcZ and the transcription factors with overlapping regulons will help to uncover the contributions of these regulatory networks to *E. amylovora* physiology and virulence.

In this study, we observed catalase activity present in culture supernatants, and determined that *katA* is responsible for this activity. This suggests that during infection *E. amylovora* may be secreting catalase preemptively to reduce damage done to cellular structures when peroxide production is elicited as a part of host-defense responses. Additionally, because the protein sequence of *E. amylovora* KatA is more similar to catalases from gram-positive *Bacillus subtilis* than it is to KatE from *Escherichia coli*, *E. amylovora* may have acquired this gene during its evolution as a plant pathogen. Indeed, KatA from *E. amylovora* is most similar to catalases from *Pantoea* and *Pseudomonas* species, suggesting it may have been horizontally acquired from one of these species during evolution as bacteria from these genera all colonize apple flowers (197). Because *katA* does not encode a secretion signal peptide, further work will be needed to determine how KatA is being secreted, as well as further elucidation of the role that secretion plays during disease development.

In *E. amylovora*, ArcZ has been shown to directly interact with *flhDC* mRNA (131) and to post-transcriptionally regulate *lrp*. In *Salmonella* Typhimurium, ArcZ is known to regulate and interact with *sdaCB*, *tpx*, and a gene encoding a horizontally acquired methyl-accepting

chemotaxis protein (75). In *Escherichia coli*, ArcZ is also known to interact with and post-transcriptionally regulate *rpoS* (74). Herein we provide additional evidence that in *E. amylovora* ArcZ post-transcriptionally represses *tpx* similar to *S.* Typhimurium, and also acts as a post-transcriptional regulator of *arcA*. These interactions explain several of the phenotypes observed in the *E. amylovora* Δ*arcZ* mutant, however additional phenotypes remain unexplained, such as the effects of *arcZ* on type III secretion. This transcriptomic and molecular analysis of the ArcZ regulon will serve to guide and inform future studies to more fully understand the mechanisms and specific roles that ArcZ plays as a global regulator in coordinating virulence-associated traits in *E. amylovora*.

CHAPTER 6

Conclusions

I. Summary of Work

A growing body of evidence indicates that Hfq-dependent sRNAs are playing critical roles in the regulation of virulence traits in phytopathogenic bacteria. However, in most cases, it remains unknown through which sRNAs these effects are mediated. In this work, I have utilized *Erwinia amylovora* as a model for the study of Hfq-dependent sRNAs and their roles in regulation of virulence and virulence-associated traits.

Through generation of a library that includes single sRNA deletion mutants and single sRNA overexpression strains for each identified Hfq-dependent sRNA in *E. amylovora*, this work has demonstrated that several Hfq-dependent sRNAs are playing important roles in the regulation of all virulence-associated traits tested. These traits include flagellar motility, exopolysaccharide production, biofilm formation, catalase activity, type III secretion, and overall virulence. Although several sRNAs affect various virulence-associated traits, I observed virulence defects in only four deletion mutants, *arcZ*, *hrs1*, *hrs21*, and *rprA*, of which Hrs1 was not previously known to affect virulence.

Three sRNAs previously known to affect flagellar motility, ArcZ, OmrAB, and RmaA, were further investigated to better understand the mechanisms by which they exert control over motility. Experimentation demonstrated that all three of these sRNAs regulate flagellar motility by regulating the master regulator, *flhD* at the transcriptional and/or post-transcriptional levels. I observed that ArcZ and RmaA affect *flhD* promoter activity, whereas ArcZ and OmrAB affect *flhD* post-transcriptionally. Neither ArcZ nor OmrAB affected stability of *flhD* mRNA, suggesting that their post-transcriptional effects are due to altered mRNA accessibility to ribosomes.

The sRNA ArcZ, which regulates *flhD* transcriptionally and post-transcriptionally, poses a contradiction as the transcriptional control is positive, but the post-transcriptional control is negative. Through a forward genetic screen, the leucine responsive regulatory protein Lrp was determined to act as an intermediate between ArcZ and *flhD*. ArcZ regulates *lrp* post-transcriptionally by destabilizing *lrp* mRNA, and in addition to transcriptional control of *flhD*, Lrp regulates additional virulence-associated traits. In addition to its strong effects on motility, deletion of *lrp* has effects on production of the exopolysaccharides amylovoran and levan, biofilm formation, and overall virulence.

Transcriptional analysis of the *arcZ* mutant uncovered a further role for the sRNA ArcZ as a regulator of enzymes involved in coping with oxidative stress. Experimental evidence suggests that this role is linked to the ArcBA two-component system suggesting that the ArcZ sRNA plays critical roles in mediating response to oxidative state, supporting the model proposed in Figure 6.1. This proposed model places the sRNA ArcZ at the intersection between a feedback loop with ArcA and a feed-forward loop involving Lrp and FlhDC. Through this role as a hub between global regulatory systems provides a potential explanation for how ArcZ is behaving as a global regulator affecting gene expression of more than 300 genes in *Erwinia amylovora*.

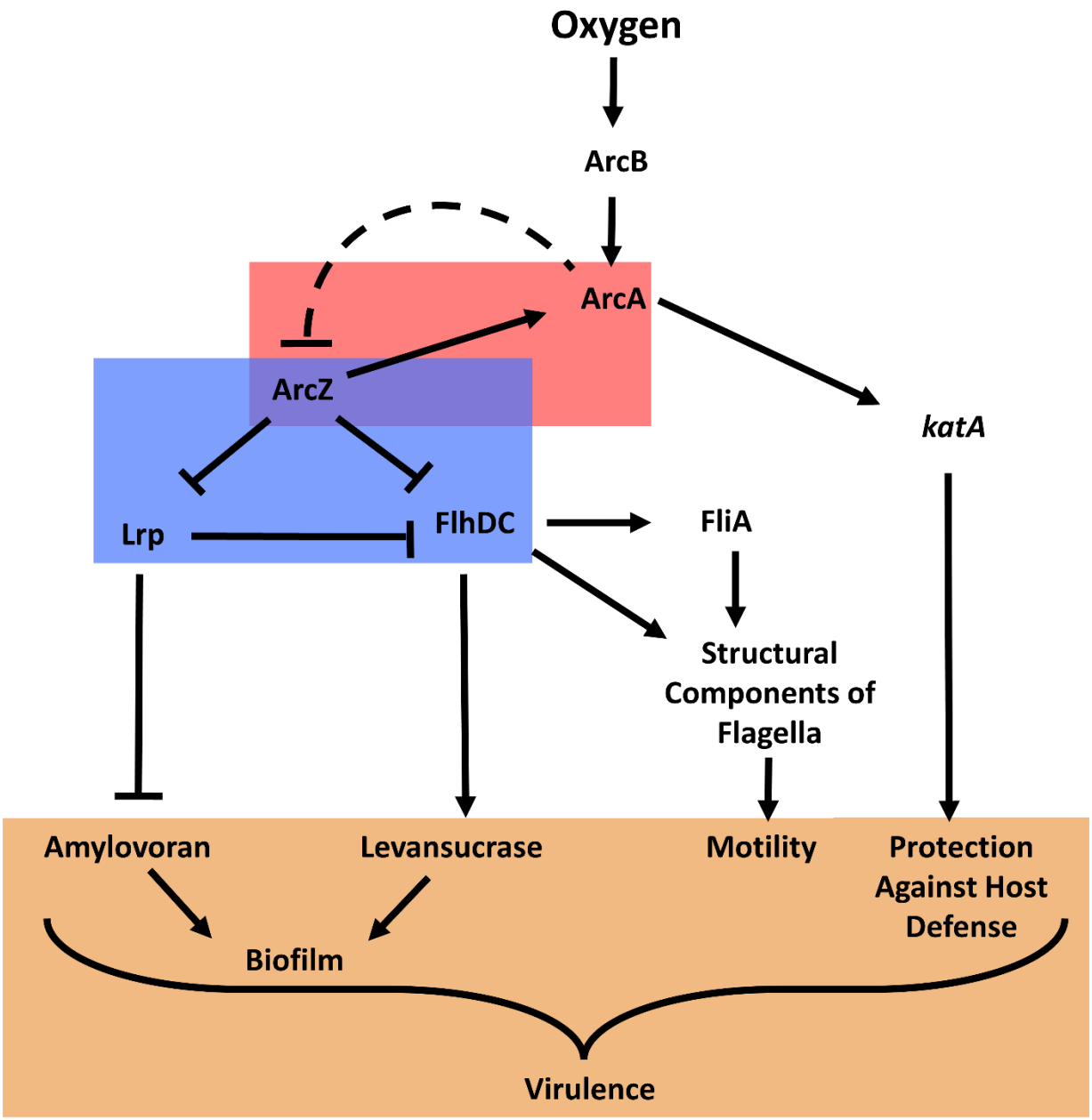

Figure 6.1: Proposed model of ArcZ virulence regulation. *Erwinia amylovora* sRNA ArcZ acts in the intersection between a proposed feedback loop with ArcA, and a feed-forward loop involving Lrp and FlhDC. Together these loops integrate ArcZ with regulation of biofilm formation, production of the exopolyaccharides amylovoran and levan, flagellar motility, and protection against host defense derived hydrogen peroxide.

II. Future Directions

Altogether this work provides evidence that several sRNAs are playing important roles in the virulence regulation of *E. amylovora*. The *arcZ* deletion mutant exhibits similar phenotypes to the *hfq* deletion mutant and ArcZ modulates several traits through multiple mRNA targets. In this work, *flhD* mRNA is shown to be a direct target of ArcZ, and evidence is provided that *lrp* and *arcA* are post-transcriptionally regulated by ArcZ, although further work is needed to confirm these as direct targets. Furthermore additional work is needed to clarify the link between the sRNA ArcZ and expression of the type III secretion system.

Because the screen of sRNA deletion mutants and overexpression strains indicated that several sRNAs are playing important roles in virulence regulation, future efforts to apply methods to *in vivo* determine global sRNA-target interactions are warranted. While such methods are continuing to be developed to allow for consistent and repeatable results, follow-up work on OmrAB and Hrs4 is of great importance as data herein indicate that overexpression of these sRNAs affects expression of the type III secretion system pilin *hrpA*. Although no virulence defect was observed upon deletion of either *omrAB* or *hrs4*, the affected phenotype upon overexpression suggests that these sRNAs may have low background expression, but increased expression under specific environmental stimuli could result in important virulence regulation.

In addition to in-depth studies of the downstream effects of Hfq-dependent sRNAs, future work is needed to characterize how sRNAs are being regulated. The studied sRNAs were identified for dependence on Hfq for their abundance, presumably primarily through direct interactions to stabilize the sRNAs post-transcriptionally. However, no specific transcriptional regulators are known in *E. amylovora* for any of these sRNAs. To better understand the

physiological and virulence roles that these sRNAs are playing, transcriptional studies utilizing small RNA sequencing during distinct stages of growth or during disease progression are needed. These studies can aid to guide further studies to specifically link sRNAs to known regulatory networks, as well as their roles and mechanisms during fire blight disease development. Coupled with such transcriptomic approaches, computational prediction of sigma factor and transcription factor binding sites can leverage the power of discovery to accelerate increased understanding of the roles Hfq-dependent sRNAs are playing in virulence.

APPENDIX

Table A.1 List of strains generated and used in CHAPTER 2

Strains	Relevant Characteristics	Source or Reference
Erwinia amylovora		
Ea1189	wild-type	GSPB[a]
Ea1189 Δ*hfq*	*hfq* deletion mutant	(38)
Ea1189 Δ*arcZ*	*arcZ* deletion mutant	(38)
Ea1189 Δ*rprA*	*rprA* deletion mutant	(38)
Ea1189 Δ*spf*	*spf* deletion mutant	(38)
Ea1189 Δ*micA*	*micA* deletion mutant	(38)
Ea1189 Δ*omrAB*	*omrAB* deletion mutant	(38)
Ea1189 Δ*ryhB*	*ryhB* deletion mutant	(38)
Ea1189 Δ*micM*	*micM* deletion mutant	(38)
Ea1189 Δ*ryeA*	*ryeA* deletion mutant	(38)
Ea1189 Δ*glmZ*	*glmZ* deletion mutant	(38)
Ea1189 Δ*hrs31*	*hrs31* deletion mutant	(39)
Ea1189 Δ*rmaA*	*rmaA* deletion mutant	(39)
Ea1189 Δ*hrs20*	*hrs20* deletion mutant	(39)
Ea1189 Δ*hrs5*	*hrs5* deletion mutant	(39)
Ea1189 Δ*hrs15*	*hrs15* deletion mutant	(39)
Ea1189 Δ*hrs29*	*hrs29* deletion mutant	(39)
Ea1189 Δ*hrs27*	*hrs27* deletion mutant	(39)
Ea1189 Δ*hrs34*	*hrs34* deletion mutant	(39)
Ea1189 Δ*hrs21*	*hrs21* deletion mutant	(39)
Ea1189 Δ*hrs8*	*hrs8* deletion mutant	(39)
Ea1189 Δ*hrs10*	*hrs10* deletion mutant	(39)
Ea1189 Δ*hrs11*	*hrs11* deletion mutant	(39)
Ea1189 Δ*hrs13*	*hrs13* deletion mutant	(39)
Ea1189 Δ*hrs12*	*hrs12* deletion mutant	(39)
Ea1189 Δ*gcvB*	*gcvB* deletion mutant	This work
Ea1189 Δ*hrs1*	*hrs1* deletion mutant	This work
Ea1189 Δ*hrs13*	*hrs13* deletion mutant	This work
Ea1189 Δ*hrs16*	*hrs16* deletion mutant	This work
Ea1189 Δ*hrs17*	*hrs17* deletion mutant	This work
Ea1189 Δ*hrs18*	*hrs18* deletion mutant	This work
Ea1189 Δ*hrs19*	*hrs19* deletion mutant	This work
Ea1189 Δ*hrs2*	*hrs2* deletion mutant	This work
Ea1189 Δ*hrs23*	*hrs23* deletion mutant	This work
Ea1189 Δ*hrs24*	*hrs24* deletion mutant	This work

Table A.1 (cont'd)

Ea1189 Δ*hrs25*	*hrs25* deletion mutant	This work
Ea1189 Δ*hrs28*	*hrs28* deletion mutant	This work
Ea1189 Δ*hrs30*	*hrs30* deletion mutant	This work
Ea1189 Δ*hrs32*	*hrs32* deletion mutant	This work
Ea1189 Δ*hrs33*	*hrs33* deletion mutant	This work
Ea1189 Δ*hrs4*	*hrs4* deletion mutant	This work
Ea1189 Δ*hrs7*	*hrs7* deletion mutant	This work
Ea1189 Δ*hrs9*	*hrs9* deletion mutant	This work
Escherichia coli		
DH5α		Invitrogen

[a]GSPB, Göttinger Sammlung phytopathogener Bakterien, Göttingen, Germany.

Table A.2 List of plasmids generated and used in CHAPTER 2

Plasmids	Notes	Source
pHM-tac	sRNA overexpression, IPTG inducible *tac* promoter	(121)
pPROBE-*hrpA*	*hrpA* promoter fusion	This work
pHM-tac::arcZ	*arcZ* overexpression	(131)
pHM-tac::rmaA	*rmaA* overexpression	(131)
pHM-tac::omrAB	*omrAB* overexpression	(131)
pHM-tac::gcvB	*gcvB* overexpression	This work
pHM-tac::glmZ	*glmZ* overexpression	This work
pHM-tac::hrs1	*hrs1* overexpression	This work
pHM-tac::hrs10	*hrs10* overexpression	This work
pHM-tac::hrs11	*hrs11* overexpression	This work
pHM-tac::hrs12	*hrs12* overexpression	This work
pHM-tac::hrs13	*hrs13* overexpression	This work
pHM-tac::hrs15	*hrs15* overexpression	This work
pHM-tac::hrs16	*hrs16* overexpression	This work
pHM-tac::hrs17	*hrs17* overexpression	This work
pHM-tac::hrs18	*hrs18* overexpression	This work
pHM-tac::hrs19	*hrs19* overexpression	This work
pHM-tac::hrs2	*hrs2* overexpression	This work
pHM-tac::hrs20	*hrs20* overexpression	This work
pHM-tac::hrs21	*hrs21* overexpression	This work
pHM-tac::hrs23	*hrs23* overexpression	This work
pHM-tac::hrs24	*hrs24* overexpression	This work
pHM-tac::hrs25	*hrs25* overexpression	This work
pHM-tac::hrs26	*hrs26* overexpression	This work
pHM-tac::hrs27	*hrs27* overexpression	This work
pHM-tac::hrs28	*hrs28* overexpression	This work
pHM-tac::hrs29	*hrs29* overexpression	This work
pHM-tac::hrs3	*hrs3* overexpression	This work
pHM-tac::hrs30	*hrs30* overexpression	This work
pHM-tac::hrs31	*hrs31* overexpression	This work
pHM-tac::hrs32	*hrs32* overexpression	This work
pHM-tac::hrs33	*hrs33* overexpression	This work
pHM-tac::hrs34	*hrs34* overexpression	This work
pHM-tac::hrs4	*hrs4* overexpression	This work
pHM-tac::hrs5	*hrs5* overexpression	This work
pHM-tac::hrs7	*hrs7* overexpression	This work
pHM-tac::hrs8	*hrs8* overexpression	This work
pHM-tac::hrs9	*hrs9* overexpression	This work
pHM-tac::micA	*micA* overexpression	This work
pHM-tac::micM	*micM* overexpression	This work

Table A.2 (cont'd)

pHM-tac::rprA	*rprA* overexpression	This work
pHM-tac::spf	*spf* overexpression	This work

Table A.3 Oligonucleotides used in CHAPTER 2

Oligonucleotide	Sequence
Ea1189 gcvB KO F	ATTATAAATTGTCCGTTGAGGAACTGCCAGCAAATACCTATAGTTGCGCCGTGTAGGCTGGAGCTGCTTC
Ea1189 gcvB KO R	GTTCTGATGTGAAAGAGATGGTCGAAATGGATCAATAGTAAAATTCAGGCCATATGAATATCCTCCCTTA
Ea1189 hrs1 KO F	AGCAAGCAGCACCGATAGCACCCCTTAGTCACCAGTAACACGGTCAGCAGGTGTAGGCTGGAGCTGCTTC
Ea1189 hrs1 KO R	TCATAGCGCTGCTCACCTGATTTAGTTGATCAAGTATACTGGATCTCCGGCATATGAATATCCTCCTTA
Ea1189 hrs13 KO F	CCTGGTGATTCCAGTATGTGGTTCGGCAACGCCGAGATCTTCCGCTAAGTGTGTAGGCTGGAGCTGCTTC
Ea1189 hrs13 KO R	AATCCACGCCTGAAATCGTTAAGTTATGTAATTTTTGTCGAAGGGGGCATCATATGAATATCCTCCTTA
Ea1189 hrs16 KO F	TGCTGATATACAAGAACGTTCCCAGCAGGATTGATTTTAAGTATATCGAGGTGTAGGCTGGAGCTGCTTC
Ea1189 hrs16 KO R	AACACCTCAACAGGTGTTTTTTTCGTTTACAGAGCCGGAGATGACGCCCGCATATGAATATCCTCCTTA
Ea1189 hrs17 KO F	ATTGTAAAATTTTTCTTTAAGATTAATCTGCTTTCTGGTAAAAAAATAGCGTGTAGGCTGGAGCTGCTTC
Ea1189 hrs17 KO R	GAATAGGCGTAAACGTTTCTTTGAATGAGAATGAACTAGCCATATAATCCCATATGAATATCCTCCTTA
Ea1189 hrs18 KO F	CCAGATAGATAGCGGCAAAGACGACAAGAAGTTCTGGTACTAACATATTGGTGTAGGCTGGAGCTGCTTC
Ea1189 hrs18 KO R	AGTACGCAGAGCCAACGCATCTGCCGCTTAAGCATAAAGGAGTATTTAAGCATATGAATATCCTCCCTTA
Ea1189 hrs19 KO F	AGATACATTTCATCGTTTATCCTGCCAACGTGCCTGGGTTATTTTATTGTGTGTAGGCTGGAGCTGCTTC
Ea1189 hrs19 KO R	TCGTACCAACCAACTTATTGTTAGCAAAATAATGACCCTGTGATGCAAGGCATATGAATATCCTCCTTA
Ea1189 hrs2 KO F	ACATGGTTAAAGCGGCGCAAAACTTGCGAAATGCACAAAAAGCTTAAATATGTGTAGGCTGGAGCTGCTTC
Ea1189 hrs2 KO R	TTTTTATGCTGCCGGCGTCACGCCATACTGCCTGAACCATGCCAGCATTCCATATGAATATCCTCCTTA
Ea1189 hrs23 KO F	GGTATTGTGCTTTAAGTTCCAGGAAGCGTTGATAGCGTGCAATCATTTTTGGTGTAGGCTGGAGCTGCTTC
Ea1189 hrs23 KO F	CAGCAGCGGGCCGCTGCCGTTGATAGCCGTTTTTAATTGACCGGACTGCCCATATGAATATCCTCCTTA
Ea1189 *hrs24* KO F	TGCGATCTGGCGCTGAATTTTTTCTACAGTACTCATAAATGCCTTCCTCAGTGTAGGCTGGAGCTGCTTC
Ea1189 *hrs24* KO R	GCTCATGAGAAAATGTTATTTTGTTATCATCTTCTGACCGCAAAGCGGGTCATATGAATATCCTCCTTA
Ea1189 *hrs25* KO F	AATCAAGCATGATGAGTTCCTTGCTTTTTTCTGTTCATTTAAGATCAAACGTGTAGGCTGGAGCTGCTTC
Ea1189 *hrs25* KO R	TATAAACTGCGGAAAATCATCAAGATAGCTTTAACAGCCCGTATCGCTTACATATGAATATCCTCCTTA
Ea1189 *hrs28* KO F	GAAACACCCCAAATGCAGAATAAAATGCCAGTCAATATGATTGGTTCAGGGTGTAGGCTGGAGCTGCTTC
Ea1189 *hrs28* KO R	AATGCCGTGTTGCGGGGTGGCAACTTCTCACCCCGCTTTATGAATAATTGCATATGAATATCCTCCTTA
Ea1189 *hrs30* KO F	TTTTATGAAATGGCCTCTTTTTCTTCATGCCTGTCACCCGCATAATCTGGGTGTAGGCTGGAGCTGCTTC
Ea1189 *hrs30* KO R	ACATTCCGAGCCAGCGCTAAGGTTCTCTTCAGCGCTGGCAATGCACCCCTCATATGAATATCCTCCTTA
Ea1189 *hrs32* KO F	GTAAAAAGGAGTTACGAACGACGTGTAATGCTGTAATACATTACGGTTAAGTGTAGGCTGGAGCTGCTTC
Ea1189 *hrs32* KO R	AGCATCACGTTTCGCCTGCCTGAGTAGGTCTCTGCGGCTGGCAACTTTCACATATGAATATCCTCCTTA
Ea1189 *hrs33* KO F	AAATGGTGATGTCAGCCAATAAAAGTGCCCGCAAGGGTTGTCGGGGGACAGTGTAGGCTGGAGCTGCTTC

Table A.3 (cont'd)

Ea1189 *hrs33* KO R	CATGACGCGAGTTTGACATCGCCTGTTTCCATCACAATGATGCAAAAGGGCATATGAATATCCTCCTTA
Ea1189 *hrs4* KO F	TGCCGAGAAAATGAGACGCTCCACGACAAATAATCTGCACTTGATAACCGGTGTAGGCTGGAGCTGCTTC
Ea1189 *hrs4* KO R	TCAATCATTTCTTACGGTGGCTGGCTGCCGGTTTATGCTCAGTAGCAGGGCATATGAATATCCTCCTTA
Ea1189 *hrs7* KO F	TCAATACGGATAAAAGCCTGTGCAGATAAACTTCTTTTCGCAGGTGAATGGTGTAGGCTGGAGCTGCTTC
Ea1189 *hrs7* KO R	TTCTGGCCTCCGGCACATACTCACAGGCTATACTCTCACTTGATAATGAGCATATGAATATCCTCCTTA
Ea1189 *hrs9* KO F	ATGTACCATTTTCATTAGTTTTCATAAAATGCGAATGATATAATTCATACGTGTAGGCTGGAGCTGCTTC
Ea1189 *hrs9* KO R	TCTTTAATTGAGGTTAAGATGGGAAGCGGAGAAGGTAAGGTCATTCTCATCATATGAATATCCTCCTTA
pHM-tac::gcvB F	GACGAATTCACTTCCCGAGCCGGAACGAAAA
pHM-tac::gcvB R	GACTCTAGAACCGTTCTGATGTGAAAGAGATGG
pHM-tac::glmZ F	GACGAATTCTAGATGCTCATTCCATCTCTTAT
pHM-tac::glmZ R	GACTCTAGATATGCTGCTATAAACCGACG
pHM-tac::hrs1 F	GACGAATTCAAACACATTATCCCTGTTTACCTT
pHM-tac::hrs1 R	GACTCTAGACAAGTATACTGGATCTCCGG
pHM-tac::hrs10 F	GACGAATTCTTTCCTGCCAGAATTCACAGG
pHM-tac::hrs10 R	GACTCTAGAATCGGCGGTAAAGGGAGGTTCG
pHM-tac::hrs11 F	GACGAATTCTGTTACGCCTGAGCATTGTAAGC
pHM-tac::hrs11 R	GACTCTAGACCCTTGAACTCTGCGAAATCGAG
pHM-tac::hrs12 F	GACGAATTCCATTTTTATTTCATAATTACC
pHM-tac::hrs12 R	GACTCTAGAGAAATATCTGACTCAGTCATTG
pHM-tac::hrs13 F	GACGAATTCCACGCCCCTCTTTGACTGC
pHM-tac::hrs13 R	GACTCTAGAGTAATTTTTGTCGAAGGGGGCAT
pHM-tac::hrs16 F	GACGAATTCGTTAACGGCTACGATCCCTTTAT
pHM-tac::hrs16 R	GACTCTAGACGTTTACAGAGCCGGAGATGA
pHM-tac::hrs17 F	GACGAATTCGTGGGATGAACAACTCACTT
pHM-tac::hrs17 R	GACTCTAGAGAGAATGAACTAGCCATATAATCC
pHM-tac::hrs18 F	GACGAATTCCTTTCCTTTATATATTGCTAAC
pHM-tac::hrs18 R	GACTCTAGAAAGCATAAAGGAGTATTTAAG
pHM-tac::hrs19 F	GACGAATTCTATATTATAACGCCTTTCAAAGG
pHM-tac::hrs19 R	GACTCTAGAAACCAACTTATTGTTAGCAAAAT
pHM-tac::hrs2 F	GACGAATTCCTTAAATATCTGTGTTGTTGTGTTTTGAT

Table A.3 (cont'd)

pHM-tac::hrs2 R	GACTCTAGATAAAAAAAGGGGCGCTAAGC
pHM-tac::hrs20 F	GACGAATTCGCTATCTTTTGGTCGAACAGGA
pHM-tac::hrs20 R	GACTCTAGACAGATACCCGTTGCAACACC
pHM-tac::hrs21 F	GACGAATTCAGATTATCCAAACTCTCAGGTATT
pHM-tac::hrs21 R	GACTCTAGAGTAATCAACTCTGTGGCATCTT
pHM-tac::hrs23 F	GACGAATTCTTTTTGTAGTCCTTACAAAGAGGT
pHM-tac::hrs23 R	GACTCTAGATTTTTAATTGACCGGACTGC
pHM-tac::hrs24 F	GACGAATTCATACGATACTTCGTGTATAGCTGTA
pHM-tac::hrs24 R	GACTCTAGATTATCATCTTCTGACCGCAAA
pHM-tac::hrs25 F	GACGAATTCGTTAAGATAAAAGCATTGAAAATCA
pHM-tac::hrs25 R	GACTCTAGATTTAACAGCCCGTATCGCTTA
pHM-tac::hrs27 F	GACGAATTCCGATTAAAAATGTTAATACCGC
pHM-tac::hrs27 R	GACTCTAGAAGTTACAAAAGGGAATATCCC
pHM-tac::hrs28 F	GACGAATTCTTTAACCTTGTCATCATGAGGAT
pHM-tac::hrs28 R	GACTCTAGAACCCCGCTTTATGAATAATTG
pHM-tac::hrs29 F	GACGAATTCTTTTCCCTTTATAAAGAGCAGG
pHM-tac::hrs29 R	GACTCTAGACTAAAGGGTCAATGCTCAG
pHM-tac::hrs30 F	GACGAATTCCGACAGGCCAGGTTTTACCTGT
pHM-tac::hrs30 R	GACTCTAGATCTCTTCAGCGCTGGCAATG
pHM-tac::hrs31 F	GACGAATTCCCAAAGCGGATCATAATCTCAAG
pHM-tac::hrs31 R	GACTCTAGAGCGAGAGGCATTTTATTTTTGGT
pHM-tac::hrs32 F	GACGAATTCCTCATTACGGCAGAGATATCAGGGCAAC
pHM-tac::hrs32 R	GACTCTAGATCTCTGCGGCTGGCAACTTTCA
pHM-tac::hrs33 F	GACGAATTCTTTTCAATGGCATGTTTGACAG
pHM-tac::hrs33 R	GACTCTAGACATCACAATGATGCAAAAGGG
pHM-tac::hrs34 F	GACGAATTCGTCAGGAACTATTTTTAAAGATATCG
pHM-tac::hrs34 R	GACTCTAGACTGTAATCGACCGCTTATCA
pHM-tac::hrs4 F	GACGAATTCAATATGGCGCGCTGCGGGAA
pHM-tac::hrs4 R	GACTCTAGATGCCGGTTTATGCTCAGTAGCAGGG
pHM-tac::hrs5 F	GACGAATTCAATTTAAGCCTGCGCCGAACTT

Table A.3 (cont'd)

pHM-tac::hrs5 R	GACTCTAGACAGGGGGGGAACTGTATGTG
pHM-tac::hrs7 F	GACGAATTCAAACGTCAAGCGATGGACGTT
pHM-tac::hrs7 R	GACTCTAGAGCCTCCGGCACATACTCACAGGC
pHM-tac::hrs8 F	GACGAATTCTCTTTGTATGCCTTGCTGTTT
pHM-tac::hrs8 R	GACTCTAGATTTTGTCAGTTATCGCCTGTTCG
pHM-tac::hrs9 F	GACGAATTCTTGGCTTACCAGTAAGTGGCTGTT
pHM-tac::hrs9 R	GACTCTAGAGAGGTTAAGATGGGAAGCGGA
pHM-tac::micA F	GACGAATTCCTTTCTCGATCGCCAGACGT
pHM-tac::micA R	GACTCTAGATTACAAAGCAAAAGCTAGCGCC
pHM-tac::micM F	GACGAATTCACCCGTTTCAGCTTAATGCTT
pHM-tac::micM R	GACTCTAGATATGGTGAGGGTAACCTTCCCG
pHM-tac::rprA F	GACGAATTCAGGATTTGAAATCTTCCCACTGA
pHM-tac::rprA R	GACTCTAGACCGATCGTCCTTTTTTAAGGGC
pHM-tac::spf F	GCGCGAATTCAATTAACTATAAAAAACCCTTTTGAGCACC
pHM-tac::spf R	GCGCTCTAGACGGCACGACAGAAACCA
qPCR arcZ F	ACCCAATACCAAACCTGTGC
qPCR arcZ R	CCAGGGAAATTGGTAACCTG
qPCR hrs21 F	GCCATATTCATACCGGATCG
qPCR hrs21 R	GTGCAGGGTACAGAGTGACG
qPCR hrs1 F	CACATTATCCCTGTTTACCTTGC
qPCR hrs1 R	GCCATAAGGGCAGGGGTAG
qPCR omrAB F	CCAGAGGTATTGATGGGTGAA
qPCR omrAB R	GCGCAGGTTGGTGAAATAAA
qPCR rprA F	TGAAATCTTCCCACTGATTTTG
qPCR rprA R	AGGGGATGGGCAAAGACTAC
qPCR rmaA F	GGCGTGTTTACATGGGTTTT
qPCR rmaA R	CTGGAACCAACCTCTTCCTG
qPCR glmZ F	ATCTCTTATGTGGGCGCAAG
qPCR glmZ R	AACCATATTGGCTGGTTGGA
qPCR micA F	GATCGCCAGACGTCTCAGTA
qPCR micA R	GAAAAAGGCCACGTCACTGT
qPCR micM F	CAGCTTAATGCTTAAACGATAACTAAA
qPCR micM R	CAATATCGCTATCGGCCATT
pHM-tac::hrs3 F	GACGAATTCGATTTATCGCCGGGGGAGAAAA

Table A.3 (cont'd)

pHM-tac::hrs3 R	GACTCTAGAGTCAGCACAGTCATGATGCTTTTG
pHM-tac::hrs15 F	GACGAATTCGCTTTACAACTGCGAATGATAATGA
pHM-tac::hrs15 R	GACTCTAGAGTTCAAATTATTCGACGTAACGGG
pHM-tac::hrs26 F	GACGAATTCATCTTTAATCTATCTGCCCGGT
pHM-tac::hrs26 R	GACTCTAGAGATATTAGTTTGAAAGTTACCCTGG

Table A.4 List of strains and plasmids used in CHAPTER 5

Strains and Plasmids	Relevant Characteristics	Source or Reference
Escherichia coli		
DH5α		Invitrogen
Erwinia amylovora		
Ea1189	wild-type	GSPB[a]
Ea1189 Δ*arcZ*	*arcZ* deletion mutant	(38)
Ea1189 Δ*katA*	*katA*deletion mutant	This work
Ea1189 Δ*katG*	*katG*deletion mutant	This work
Ea1189 Δ*tpx*	*tpx*deletion mutant	This work
Ea1189 Δ*osmC*	*osmC*deletion mutant	This work
Ea1189 Δ*arcA*	*arcA*deletion mutant	This work
Ea1189 Δ*arcB*	*arcB* deletion mutant	This work
Ea1189 Δ*fnr*	*fnr*deletion mutant	This work
Ea1189 Δ*fur*	*fur*deletion mutant	This work
Plasmids		
pML-ArcZ	*arcZ* complementation	(38)
pHM-tac::ArcZ	*arcZ* Over-expression, IPTG inducible *tac* promoter	(131)
pBBR1::katA	*katA* complementation	This work
pBBR1::katG	*katG* complementation	This work
pBBR1::tpx	*tpx*complementation	This work
pBBR1::osmC	*osmC* complementation	This work
pXG20-KatA	*katA*translational fusion	This work
pPROBE-KatA	*katA* promoter fusion	This work
pXG20-Tpx	*tpx* translational fusion	This work
pXG20-ArcA	*arcA* translational fusion	This work
pXG20-ArcB	*arcB* translational fusion	This work
pXG20-Fur	*fur* translational fusion	This work

[a]GSPB, Göttinger Sammlung phytopathogener Bakterien, Göttingen, Germany.

Table A.5 List of oligonucleotides used in CHAPTER 5

Identifier	Sequence
katA qPCR F	TGGACGCTTCACATGCAGAT
katA qPCR R	TGCGGCCAGACTTTAGTGAG
katG qPCR F	AACGTGGCGCTGGAAAATTC
katG qPCR R	CGTCAGCCACTCTTTCTCGT
tpx qPCR F	AAAGACTATGGCGTGGCGAT
tpx qPCR R	GCTGGCTATGAATGACCCGA
osmC qPCR F	TAAGCAGGGTAAAGGCACGG
osmC qPCR R	CAGCGCCGATCAACTCTTCC
katA Knockout F	GTACTACACTTATCGTCGAAAATAACCATTTTAACATGGAGAGTATAG CGGTGTAGGCTGGAGCTGCTTC
katA Knockout R	GGGTGCCGCATGCTCAAAAAAAAGCGCCTTGCAGGCGCTTTATTCTGA GGCATATGAATATCCTCCTTA
katG Knockout F	ATTGGCGACAGTTAAGCTGGCTTTGTCAATATGAGTGATGGAGTCCGA AAGTGTAGGCTGGAGCTGCTTC
katG Knockout R	CAGCCTTTAGCCAAATAAAAACCCGGTAAGTTATCCTTACCGGGTTTA GCCATATGAATATCCTCCTTA
tpx Knockout F	CGACCGACACTGAAAACGATAAATCATCATAAACAATAAAAGGATAG CTTGTGTAGGCTGGAGCTGCTTC
tpx Knockout R	CGGCCAGCCAGCTAAGGCGCGCTCCAGACAAGGAGCGCACCACAGAA GAGCATATGAATATCCTCCTTA
*osmC*Knockout F	CAATACAGCGGCTATAATGGTAGCTGATGTTAAACAACCGGAGAACAA CAGTGTAGGCTGGAGCTGCTTC
osmC Knockout R	TCCTTAACAGTTTCCTGACTTAACCAGAACATCATCATCTTCAACCGGA GCATATGAATATCCTCCTTA
pBBR1 MCS F	CACTGCCCGCTTTCCAGTCGGG
pBBR1 MCS R	CCATGCACCGCGACGCAAC
katA complement F	CCCGACTGGAAAGCGGGCAGTG TGACCATCGCCTTCAGTTAC
katA complement R	GTTGCGTCGCGGTGCATGG ATTCAGCACTCAACAAAGGC
katG complement F	CCCGACTGGAAAGCGGGCAGTG GGGACTTGTTGCGGTTGACC
katG complement R	GTTGCGTCGCGGTGCATGG GAGAGCTTTATGGATTCGCCG
tpx complement F	CCCGACTGGAAAGCGGGCAGTG CTCAATTCCTTAACGGGTTCG
tpx complement R	GTTGCGTCGCGGTGCATGG CTGCGTGAGTATGGCATCAG
osmC complement F	CCCGACTGGAAAGCGGGCAGTG GTCTCTCAAACCTTACGCCTG
osmC complement R	GTTGCGTCGCGGTGCATGG CCTAAAGCAGAAGGATTAGTGCG
pXG20 F	TGTGCTCAGTATCTCTATCACTGATAGGGATGTCAATCTC
pXG20 R	GGTTCTGGCGAATTCATGAGCAAAGGAGAAGAACT
pPROBE F	GAGGATCCCCGGGTACCGAGCTC
pPROBE R	GCCGGCTTCCATTCAGGTCG
katA promoter F	GAGCTCGGTACCCGGGGATCCTCCGCTATACTCTCCATGTTAAAATG
katA promoter R	GAGCTCGGTACCCGGGGATCCTCCGGACTCCATCACTCATATTGAC
katA UTR F	GAGATTGACATCCCTATCAGTGATAGAGATACTGAGCACAGTCGAAAA TAACCATTTTAACATGG
katA UTR R	AGTTCTTCTCCTTTGCTCATGAATTCGCCAGAACCGACCGTTAAGGAAT GCTCATC

Table A.5 (cont'd)

tpx UTR F	GAGATTGACATCCCTATCAGTGATAGAGATACTGAGCACACGATAAATCATCATAAACAATAAAAGG
tpx UTR R	AGTTCTTCTCCTTTGCTCATGAATTCGCCAGAACCTTTGGCTACCAGAGTAAACGG
*arcA*Knockout F	AGCCGTATGTCCTGTTTCGATTTTTGTTGGCAATTTTAGGTAGCGATCACGTGTAGGCTGGAGCTGCTTC
*arcA*Knockout R	GAGGTAAGCCGTGGGACGGGCAGCTCAACAGCGCCCGTCCCGCCGAGACATATGAATATCCTCCTTA
arcB Knockout F	TTTAAACAAATCCGGTATGATTGCGGCTATCAGGCTGAAAGGGACATTATGTGTAGGCTGGAGCTGCTTC
arcB Knockout R	TCATTTTTTTTCAGCGTCTGTTACCCATTGCCGTAAAACTTCCATATCATCATATGAATATCCTCCTTA
fur Knockout F	GAGATTGACATCCCTATCAGTGATAGAGATACTGAGCACACATTGCGCTTTAGCGTCGAC
fur Knockout R	AGTTCTTCTCCTTTGCTCATGAATTCGCCAGAACCATGGCCTTCGGGTTCCTGAAG
*fnr*Knockout F	TAACTAAAATATGTAAATTAATGCGAGTCATTTATCATCGAGCGTAGATTGTGTAGGCTGGAGCTGCTTC
fnr Knockout R	AAAAAGTGGTAAACGAATCAATCAACTAAAAATATCGATCCGGCCCGGTTCATATGAATATCCTCCTTA
arcA UTR F	GAGATTGACATCCCTATCAGTGATAGAGATACTGAGCACAGCATCATCTGGCACTAACCCAG
arcA UTR R	AGTTCTTCTCCTTTGCTCATGAATTCGCCAGAACCAACCATGTAGCCTTCGGCTTC
arcB UTR F	GAGATTGACATCCCTATCAGTGATAGAGATACTGAGCACACCGGTATGATTGCGGCTATCA
arcB UTR R	AGTTCTTCTCCTTTGCTCATGAATTCGCCAGAACCCGCTGAAGCCAGCAGCAACGA
fur UTR F	GAGATTGACATCCCTATCAGTGATAGAGATACTGAGCACACATTGCGCTTTAGCGTCGAC
fur UTR R	AGTTCTTCTCCTTTGCTCATGAATTCGCCAGAACCATGGCCTTCGGGTTCCTGAAG

REFERENCES

REFERENCES

1. Jones JD, Dangl JL. 2006. The plant immune system. Nature 444:323.

2. Asai S, Shirasu K. 2015. Plant cells under siege: plant immune system versus pathogen effectors. Current opinion in plant biology 28:1-8.

3. Khan M, Subramaniam R, Desveaux D. 2016. Of guards, decoys, baits and traps: pathogen perception in plants by type III effector sensors. Current opinion in microbiology 29:49-55.

4. Westermann AJ, Förstner KU, Amman F, Barquist L, Chao Y, Schulte LN, Müller L, Reinhardt R, Stadler PF, Vogel J. 2016. Dual RNA-seq unveils noncoding RNA functions in host–pathogen interactions. Nature 529:496.

5. Weiberg A, Jin H. 2015. Small RNAs—the secret agents in the plant–pathogen interactions. Current opinion in plant biology 26:87-94.

6. Romeo T. 1998. Global regulation by the small RNA-binding protein CsrA and the non-coding RNA molecule CsrB. Molecular microbiology 29:1321-1330.

7. Steege DA. 2000. Emerging features of mRNA decay in bacteria. Rna 6:1079-1090.

8. Vercruysse M, Köhrer C, Davies BW, Arnold MF, Mekalanos JJ, RajBhandary UL, Walker GC. 2014. The highly conserved bacterial RNase YbeY is essential in Vibrio cholerae, playing a critical role in virulence, stress regulation, and RNA processing. PLoS pathogens 10:e1004175.

9. Chao Y, Li L, Girodat D, Förstner KU, Said N, Corcoran C, Śmiga M, Papenfort K, Reinhardt R, Wieden H-J. 2017. In vivo cleavage map illuminates the central role of RNase E in coding and non-coding RNA pathways. Molecular cell 65:39-51.

10. Grundy FJ, Henkin TM. 2006. From ribosome to riboswitch: control of gene expression in bacteria by RNA structural rearrangements. Critical reviews in biochemistry and molecular biology 41:329-338.

11. Oxender DL, Zurawski G, Yanofsky C. 1979. Attenuation in the Escherichia coli tryptophan operon: role of RNA secondary structure involving the tryptophan codon region. Proceedings of the National Academy of Sciences 76:5524-5528.

12. Gouy M, Gautier C. 1982. Codon usage in bacteria: correlation with gene expressivity. Nucleic acids research 10:7055-7074.

13. Dambach M, Sandoval M, Updegrove TB, Anantharaman V, Aravind L, Waters LS, Storz G. 2015. The ubiquitous yybP-ykoY riboswitch is a manganese-responsive regulatory element. Molecular cell 57:1099-1109.

14. Tripp HJ, Schwalbach MS, Meyer MM, Kitner JB, Breaker RR, Giovannoni SJ. 2009. Unique glycine-activated riboswitch linked to glycine–serine auxotrophy in SAR11. Environmental microbiology 11:230-238.

15. Smith KD, Lipchock SV, Ames TD, Wang J, Breaker RR, Strobel SA. 2009. Structural basis of ligand binding by a c-di-GMP riboswitch. Nature structural & molecular biology 16:1218.

16. Bevilacqua PC, Ritchey LE, Su Z, Assmann SM. 2016. Genome-wide analysis of RNA secondary structure. Annual review of genetics 50:235-266.

17. Chowdhury S, Maris C, Allain FHT, Narberhaus F. 2006. Molecular basis for temperature sensing by an RNA thermometer. The EMBO journal 25:2487-2497.

18. Majdalani N, Cunning C, Sledjeski D, Elliott T, Gottesman S. 1998. DsrA RNA regulates translation of RpoS message by an anti-antisense mechanism, independent of its action as an antisilencer of transcription. Proceedings of the National Academy of Sciences 95:12462-12467.

19. Sauer E, Schmidt S, Weichenrieder O. 2012. Small RNA binding to the lateral surface of Hfq hexamers and structural rearrangements upon mRNA target recognition. Proceedings of the National Academy of Sciences 109:9396-9401.

20. Sun X, Zhulin I, Wartell RM. 2002. Predicted structure and phyletic distribution of the RNA-binding protein Hfq. Nucleic acids research 30:3662-3671.

21. Vogel J, Luisi BF. 2011. Hfq and its constellation of RNA. Nature Reviews Microbiology 9:578.

22. Glover JM, Chaulk SG, Edwards RA, Arthur D, Lu J, Frost LS. 2015. The FinO family of bacterial RNA chaperones. Plasmid 78:79-87.

23. Heeb S, Haas D. 2001. Regulatory roles of the GacS/GacA two-component system in plant-associated and other gram-negative bacteria. Molecular plant-microbe interactions 14:1351-1363.

24. Weiberg A, Wang M, Bellinger M, Jin H. 2014. Small RNAs: a new paradigm in plant-microbe interactions. Annual Review of Phytopathology 52:495-516.

25. Coenye T, Drevinek P, Mahenthiralingam E, Shah SA, Gill RT, Vandamme P, Ussery DW. 2007. Identification of putative noncoding RNA genes in the Burkholderia cenocepacia J2315 genome. FEMS microbiology letters 276:83-92.

26. Ghosh S, Dureja C, Khatri I, Subramanian S, Raychaudhuri S, Ghosh S. 2017. Identification of novel small RNAs in Burkholderia cenocepacia KC-01 expressed under iron limitation and oxidative stress conditions. Microbiology 163:1924-1936.

27. Huang Y, Liu C, Wang H, Guan T, Liu L, Yu S. 2019. Bioinformatic analysis of the complete genome sequence of Pectobacterium carotovorum subsp. brasiliense BZA12 and candidate effector screening. Journal of Plant Pathology 101:39-49.

28. Wang C, Pu T, Lou W, Wang Y, Gao Z, Hu B, Fan J. 2018. Hfq, a RNA Chaperone, Contributes to Virulence by Regulating Plant Cell Wall–Degrading Enzyme Production, Type VI Secretion System Expression, Bacterial Competition, and Suppressing Host Defense Response in Pectobacterium carotovorum. Molecular Plant-Microbe Interactions 31:1166-1178.

29. Alkhateeb RS, Rückert C, Rupp O, Pucker B, Hublik G, Wibberg D, Niehaus K, Pühler A, Vorhölter F-J. 2017. Refined annotation of the complete genome of the phytopathogenic and xanthan producing Xanthomonas campestris pv. campestris strain B100 based on RNA sequence data. Journal of biotechnology 253:55-61.

30. Coenye T, Van Acker H, Peeters E, Sass A, Buroni S, Riccardi G, Mahenthiralingam E. 2011. Molecular mechanisms of chlorhexidine tolerance in Burkholderia cenocepacia biofilms. Antimicrobial agents and chemotherapy 55:1912-1919.

31. Jiang R-P, Tang D-J, Chen X-L, He Y-Q, Feng J-X, Jiang B-L, Lu G-T, Lin M, Tang J-L. 2010. Identification of four novel small non-coding RNAs from Xanthomonas campestris pathovar campestris. BMC genomics 11:316.

32. Dequivre M, Diel B, Villard C, Sismeiro O, Durot M, Coppée J-Y, Nesme X, Vial L, Hommais F. 2015. Small RNA deep-sequencing analyses reveal a new regulator of virulence in Agrobacterium fabrum C58. Molecular Plant-Microbe Interactions 28:580-589.

33. Sass A, Kiekens S, Coenye T. 2017. Identification of small RNAs abundant in Burkholderia cenocepacia biofilms reveal putative regulators with a potential role in carbon and iron metabolism. Scientific reports 7:15665.

34. Kwenda S, Gorshkov V, Ramesh AM, Naidoo S, Rubagotti E, Birch PR, Moleleki LN. 2016. Discovery and profiling of small RNAs responsive to stress conditions in the plant pathogen Pectobacterium atrosepticum. BMC genomics 17:47.

35. An SQ, Febrer M, McCarthy Y, Tang DJ, Clissold L, Kaithakottil G, Swarbreck D, Tang JL, Rogers J, Dow JM. 2013. High-resolution transcriptional analysis of the regulatory influence of cell-to-cell signalling reveals novel genes that contribute to X anthomonas phytopathogenesis. Molecular microbiology 88:1058-1069.

36. Zhao T, Zhang R, Wang M. 2010. Prediction of candidate small non-coding RNAs in by Agrobacterium by computational analysis. Journal of biomedical research 24:33-42.

37. Li B, Ibrahim M, Ge M, Cui Z, Sun G, Xu F, Kube M. 2014. Transcriptome analysis of Acidovorax avenae subsp. avenae cultivated in vivo and co-culture with Burkholderia seminalis. Scientific reports 4:5698.

38. Zeng Q, McNally RR, Sundin GW. 2013. Global small RNA chaperone Hfq and regulatory small RNAs control virulence in the fire blight pathogen Erwinia amylovora. Journal of bacteriology:JB. 02056-12.

39. Zeng Q, Sundin GW. 2014. Genome-wide identification of Hfq-regulated small RNAs in the fire blight pathogen Erwinia amylovora discovered small RNAs with virulence regulatory function. BMC genomics 15:414.

40. Lee K, Huang X, Yang C, Lee D, Ho V, Nobuta K, Fan J-B, Wang K. 2013. A genome-wide survey of highly expressed non-coding RNAs and biological validation of selected candidates in Agrobacterium tumefaciens. PLoS One 8:e70720.

41. Wilms I, Overlöper A, Nowrousian M, Sharma CM, Narberhaus F. 2012. Deep sequencing uncovers numerous small RNAs on all four replicons of the plant pathogen Agrobacterium tumefaciens. RNA biology 9:446-457.

42. Alkhateeb RS, Vorhölter F-J, Rückert C, Mentz A, Wibberg D, Hublik G, Niehaus K, Pühler A. 2016. Genome wide transcription start sites analysis of Xanthomonas campestris pv. campestris B100 with insights into the gum gene cluster directing the biosynthesis of the exopolysaccharide xanthan. Journal of biotechnology 225:18-28.

43. Liang H, Zhao Y-T, Zhang J-Q, Wang X-J, Fang R-X, Jia Y-T. 2011. Identification and functional characterization of small non-coding RNAs in Xanthomonas oryzae pathovar oryzae. BMC genomics 12:87.

44. Hu Y, Zhang L, Wang X, Sun F, Kong X, Dong H, Xu H. 2018. Two virulent sRNAs identified by genomic sequencing target the type III secretion system in rice bacterial blight pathogen. BMC plant biology 18:237.

45. Chen J, Huang H. Searching for small RNA genes in Xylella fastidiosa genomes, p. *In* (ed),

46. Khoo J-S, Chai S-F, Mohamed R, Nathan S, Firdaus-Raih M. Computational discovery and RT-PCR validation of novel Burkholderia conserved and Burkholderia pseudomallei unique sRNAs, p S13. *In* (ed), BioMed Central,

47. Bronstein PA, Filiatrault MJ, Myers CR, Rutzke M, Schneider DJ, Cartinhour SW. 2008. Global transcriptional responses of Pseudomonas syringae DC3000 to changes in iron bioavailability in vitro. BMC microbiology 8:209.

48. Melamed S, Peer A, Faigenbaum-Romm R, Gatt YE, Reiss N, Bar A, Altuvia Y, Argaman L, Margalit H. 2016. Global mapping of small RNA-target interactions in bacteria. Molecular cell 63:884-897.

49. Smirnov A, Förstner KU, Holmqvist E, Otto A, Günster R, Becher D, Reinhardt R, Vogel J. 2016. Grad-seq guides the discovery of ProQ as a major small RNA-binding protein. Proceedings of the National Academy of Sciences 113:11591-11596.

50. Griffiths-Jones S, Moxon S, Marshall M, Khanna A, Eddy SR, Bateman A. 2005. Rfam: annotating non-coding RNAs in complete genomes. Nucleic acids research 33:D121-D124.

51. Moreno R, Hernández-Arranz S, La Rosa R, Yuste L, Madhushani A, Shingler V, Rojo F. 2015. The Crc and Hfq proteins of P seudomonas putida cooperate in catabolite repression and formation of ribonucleic acid complexes with specific target motifs. Environmental microbiology 17:105-118.

52. Moreno R, Fonseca P, Rojo F. 2012. Two small RNAs, CrcY and CrcZ, act in concert to sequester the Crc global regulator in Pseudomonas putida, modulating catabolite repression. Molecular microbiology 83:24-40.

53. Filiatrault MJ, Stodghill PV, Wilson J, Butcher BG, Chen H, Myers CR, Cartinhour SW. 2013. CrcZ and CrcX regulate carbon source utilization in Pseudomonas syringae pathovar tomato strain DC3000. RNA biology 10:245-255.

54. Fineran PC, Blower TR, Foulds IJ, Humphreys DP, Lilley KS, Salmond GP. 2009. The phage abortive infection system, ToxIN, functions as a protein–RNA toxin–antitoxin pair. Proceedings of the National Academy of Sciences 106:894-899.

55. Yamaguchi Y, Park J-H, Inouye M. 2011. Toxin-antitoxin systems in bacteria and archaea. Annual review of genetics 45:61-79.

56. Kery MB, Feldman M, Livny J, Tjaden B. 2014. TargetRNA2: identifying targets of small regulatory RNAs in bacteria. Nucleic acids research 42:W124-W129.

57. Busch A, Richter AS, Backofen R. 2008. IntaRNA: efficient prediction of bacterial sRNA targets incorporating target site accessibility and seed regions. Bioinformatics 24:2849-2856.

58. Wright PR, Georg J, Mann M, Sorescu DA, Richter AS, Lott S, Kleinkauf R, Hess WR, Backofen R. 2014. CopraRNA and IntaRNA: predicting small RNA targets, networks and interaction domains. Nucleic acids research 42:W119-W123.

59. Eggenhofer F, Tafer H, Stadler PF, Hofacker IL. 2011. RNApredator: fast accessibility-based prediction of sRNA targets. Nucleic acids research 39:W149-W154.

60. Pain A, Ott A, Amine H, Rochat T, Bouloc P, Gautheret D. 2015. An assessment of bacterial small RNA target prediction programs. RNA biology 12:509-513.

61. Borgmann J, Schäkermann S, Bandow JE, Narberhaus F. 2018. A Small Regulatory RNA Controls Cell Wall Biosynthesis and Antibiotic Resistance. mBio 9:e02100-18.

62. Ulvé VM, Sevin EW, Chéron A, Barloy-Hubler F. 2007. Identification of chromosomal alpha-proteobacterial small RNAs by comparative genome analysis and detection in Sinorhizobium meliloti strain 1021. BMC genomics 8:467.

63. Wilms I, Möller P, Stock A-M, Gurski R, Lai E-M, Narberhaus F. 2012. Hfq influences multiple transport systems and virulence in the plant pathogen Agrobacterium tumefaciens. Journal of bacteriology 194:5209-5217.

64. Overlöper A, Kraus A, Gurski R, Wright PR, Georg J, Hess WR, Narberhaus F. 2014. Two separate modules of the conserved regulatory RNA AbcR1 address multiple target mRNAs in and outside of the translation initiation region. RNA biology 11:624-640.

65. Wilms I, Voss B, Hess WR, Leichert LI, Narberhaus F. 2011. Small RNA-mediated control of the Agrobacterium tumefaciens GABA binding protein. Molecular microbiology 80:492-506.

66. Jacobs JL, Fasi AC, Ramette A, Smith JJ, Hammerschmidt R, Sundin GW. 2008. Identification and onion pathogenicity of Burkholderia cepacia complex isolates from the onion rhizosphere and onion field soil. Appl Environ Microbiol 74:3121-3129.

67. Ramos CG, Sousa SA, Grilo AM, Feliciano JR, Leitão JH. 2011. The second RNA chaperone, Hfq2, is also required for survival under stress and full virulence of Burkholderia cenocepacia J2315. Journal of bacteriology 193:1515-1526.

68. Ramos CG, da Costa PJ, Döring G, Leitão JH. 2012. The novel cis-encoded small RNA h2cR is a negative regulator of hfq2 in Burkholderia cenocepacia. PloS one 7:e47896.

69. Ramos CG, Grilo AM, da Costa PJ, Feliciano JR, Leitão JH. 2013. MtvR is a global small noncoding regulatory RNA in Burkholderia cenocepacia. Journal of bacteriology 195:3514-3523.

70. Ramos CG, Grilo AM, da Costa PJ, Feliciano JR, Leitão JH. 2014. Retraction for Ramos et al., MtvR Is a Global Small Noncoding Regulatory RNA in Burkholderia cenocepacia. Journal of bacteriology 196:3981.

71. Ramos CG, Sousa SA, Grilo AM, Feliciano JR, Leitão JH. 2014. Retraction for Ramos et al., the second RNA chaperone, Hfq2, is also required for survival under stress and full virulence of Burkholderia cenocepacia J2315. Journal of bacteriology 196:3980.

72. Kiekens S, Sass A, Van Nieuwerburgh F, Deforce D, Coenye T. 2018. The small RNA ncS35 regulates growth in Burkholderia cenocepacia J2315. mSphere 3:e00579-17.

73. Golanowska M, Potrykus M, Motyka-Pomagruk A, Kabza M, Bacci G, Galardini M, Bazzicalupo M, Makalowska I, Smalla K, Mengoni A. 2018. Comparison of highly and weakly virulent Dickeya solani strains, with a view on the pangenome and panregulon of this species. Frontiers in microbiology 9.

74. Mandin P, Gottesman S. 2010. Integrating anaerobic/aerobic sensing and the general stress response through the ArcZ small RNA. The EMBO journal 29:3094-3107.

75. Papenfort K, Said N, Welsink T, Lucchini S, Hinton JC, Vogel J. 2009. Specific and pleiotropic patterns of mRNA regulation by ArcZ, a conserved, Hfq-dependent small RNA. Molecular microbiology 74:139-158.

76. Yuan X, Zeng Q, Khokhani D, Tian F, Severin GB, Waters CM, Xu J, Zhou X, Sundin GW, Ibekwe AM. 2019. A Feed-forward signaling circuit controls bacterial virulence through linking cyclic di-GMP and two mechanistically distinct sRNAs; ArcZ and RsmB. Environmental microbiology.

77. Hoe C-H, Raabe CA, Rozhdestvensky TS, Tang T-H. 2013. Bacterial sRNAs: regulation in stress. International Journal of Medical Microbiology 303:217-229.

78. Andresen L, Sala E, Koiv V, Mäe A. 2010. A role for the Rcs phosphorelay in regulating expression of plant cell wall degrading enzymes in Pectobacterium carotovorum subsp. carotovorum. Microbiology 156:1323-1334.

79. Lu P, Zhang Y, Li L, Hu Y, Huang L, Li Y, Rayner S, Chen S. 2012. Small non-coding RNA SraG regulates the operon YPK_1206-1205 in Yersinia pseudotuberculosis. FEMS microbiology letters 331:37-43.

80. Mika F, Hengge R. 2013. Small regulatory RNAs in the control of motility and biofilm formation in E. coli and Salmonella. International journal of molecular sciences 14:4560-4579.

81. Schmidtke C, Findeiß S, Sharma CM, Kuhfuß J, Hoffmann S, Vogel J, Stadler PF, Bonas U. 2011. Genome-wide transcriptome analysis of the plant pathogen Xanthomonas identifies sRNAs with putative virulence functions. Nucleic acids research 40:2020-2031.

82. Schmidtke C, Abendroth U, Brock J, Serrania J, Becker A, Bonas U. 2013. Small RNA sX13: a multifaceted regulator of virulence in the plant pathogen Xanthomonas. PLoS pathogens 9:e1003626.

83. Kim J, Mannaa M, Kim N, Lee C, Kim J, Park J, Lee H-H, Seo Y-S. 2018. The Roles of Two hfq Genes in the Virulence and Stress Resistance of Burkholderia glumae. The plant pathology journal 34:412.

84. Lai JL, Tang DJ, Liang YW, Zhang R, Chen Q, Qin ZP, Ming ZH, Tang JL. 2018. The RNA chaperone Hfq is important for the virulence, motility and stress tolerance in the phytopathogen Xanthomonas campestris. Environmental microbiology reports 10:542-554.

85. Norelli J, Jones A, Aldwinckle H. 2003. Fire blight management in the twenty-first century - Using new technologies that enhance host resistance in apple. Plant Disease 87:756-765.

86. Sundin GW, Wang N, Charkowski AO, Castiblanco LF, Jia H, Zhao Y. 2016. Perspectives on the transition from bacterial phytopathogen genomics studies to

applications enhancing disease management: from promise to practice. Phytopathology 106:1071-1082.

87. Bayot RG, Ries SM. 1986. Role of motility in apple blossom infection by Erwinia amylovora and studies of fire blight control with attractant and repellent compounds. Phytopathology 76:441-445.

88. Raymundo A, Ries S. 1980. Motility of Erwinia amylovora. Phytopathology 70:1062-1065.

89. Nimtz M, Mort A, Domke T, Wray V, Zhang Y, Qiu F, Coplin D, Geider K. 1996. Structure of amylovoran, the capsular exopolysaccharide from the fire blight pathogen Erwinia amylovora. Carbohydrate research 287:59-76.

90. Gross M, Geier G, Rudolph K, Geider K. 1992. Levan and levansucrase synthesized by the fireblight pathogen Erwinia amylovora. Physiological and molecular plant pathology 40:371-381.

91. Castiblanco LF, Sundin GW. 2018. Cellulose production, activated by cyclic di-GMP through BcsA and BcsZ, is a virulence factor and an essential determinant of the three-dimensional architectures of biofilms formed by Erwinia amylovora Ea1189. Molecular plant pathology 19:90-103.

92. Koczan JM, McGrath MJ, Zhao Y, Sundin GW. 2009. Contribution of Erwinia amylovora exopolysaccharides amylovoran and levan to biofilm formation: implications in pathogenicity. Phytopathology 99:1237-1244.

93. Koczan JM, Lenneman BR, McGrath MJ, Sundin GW. 2011. Cell surface attachment structures contribute to biofilm formation and xylem colonization of Erwinia amylovora. Applied and environmental microbiology:AEM. 05138-11.

94. Bogdanove AJ, Bauer DW, Beer SV. 1998. Erwinia amylovora secretes DspE, a pathogenicity factor and functional AvrE homolog, through the Hrp (type III secretion) pathway. Journal of Bacteriology 180:2244-2247.

95. Kim JF, Wei Z-M, Beer SV. 1997. The hrpA and hrpC operons of Erwinia amylovora encode components of a type III pathway that secretes harpin. Journal of bacteriology 179:1690-1697.

96. Zhao Y, Qi M, Wang D. Evolution and function of flagellar and non-flagellar type III secretion systems in Erwinia amylovora, p 177-184. *In* (ed),

97. Maudet C, Mano M, Eulalio A. 2014. MicroRNAs in the interaction between host and bacterial pathogens. FEBS letters 588:4140-4147.

98. Padmanabhan C, Zhang X, Jin H. 2009. Host small RNAs are big contributors to plant innate immunity. Current opinion in plant biology 12:465-472.

99. Gupta OP, Sharma P, Gupta RK, Sharma I. 2014. Current status on role of miRNAs during plant–fungus interaction. Physiological and molecular plant pathology 85:1-7.

100. Brouns SJ, Jore MM, Lundgren M, Westra ER, Slijkhuis RJ, Snijders AP, Dickman MJ, Makarova KS, Koonin EV, Van Der Oost J. 2008. Small CRISPR RNAs guide antiviral defense in prokaryotes. Science 321:960-964.

101. Doudna JA, Charpentier E. 2014. The new frontier of genome engineering with CRISPR-Cas9. Science 346:1258096.

102. Georg J, Hess WR. 2011. cis-antisense RNA, another level of gene regulation in bacteria. Microbiol Mol Biol Rev 75:286-300.

103. Wagner EGH, Simons RW. 1994. Antisense RNA control in bacteria, phages, and plasmids. Annual review of microbiology 48:713-742.

104. Chao Y, Papenfort K, Reinhardt R, Sharma CM, Vogel J. 2012. An atlas of Hfq-bound transcripts reveals 3′ UTRs as a genomic reservoir of regulatory small RNAs. The EMBO journal 31:4005-4019.

105. Link TM, Valentin-Hansen P, Brennan RG. 2009. Structure of Escherichia coli Hfq bound to polyriboadenylate RNA. Proceedings of the National Academy of Sciences 106:19292-19297.

106. Brennan RG, Link TM. 2007. Hfq structure, function and ligand binding. Current opinion in microbiology 10:125-133.

107. Schumacher MA, Pearson RF, Møller T, Valentin-Hansen P, Brennan RG. 2002. Structures of the pleiotropic translational regulator Hfq and an Hfq–RNA complex: a bacterial Sm-like protein. The EMBO journal 21:3546-3556.

108. Möller P, Overlöper A, Förstner KU, Wen T-N, Sharma CM, Lai E-M, Narberhaus F. 2014. Profound impact of Hfq on nutrient acquisition, metabolism and motility in the plant pathogen Agrobacterium tumefaciens. PLoS One 9:e110427.

109. Piqué N, Miñana-Galbis D, Merino S, Tomás J. 2015. Virulence factors of Erwinia amylovora: a review. International journal of molecular sciences 16:12836-12854.

110. Cesbron S, Paulin J-P, Tharaud M, Barny M-A, Brisset M-N. 2006. The alternative σ factor HrpL negatively modulates the flagellar system in the phytopathogenic bacterium Erwinia amylovora under hrp-inducing conditions. FEMS microbiology letters 257:221-227.

111. Santander RD, Figàs-Segura À, Biosca EG. 2018. Erwinia amylovora catalases KatA and KatG are virulence factors and delay the starvation-induced viable but non-culturable (VBNC) response. Molecular plant pathology 19:922-934.

112. Slack SM, Zeng Q, Outwater CA, Sundin GW. 2017. Microbiological examination of Erwinia amylovora exopolysaccharide ooze. Phytopathology 107:403-411.

113. Hattingh M, Beer S, Lawson E. 1986. Scanning electron microscopy of apple blossoms colonized by Erwinia amylovora and E. herbicola. Phytopathology 76:900-904.

114. Zhao Y, Sundin GW, Wang D. 2009. Construction and analysis of pathogenicity island deletion mutants of Erwinia amylovora. Canadian journal of microbiology 55:457-464.

115. Wang D, Korban SS, Zhao Y. 2009. The Rcs phosphorelay system is essential for pathogenicity in Erwinia amylovora. Molecular plant pathology 10:277-290.

116. McNally RR, Toth IK, Cock PJ, Pritchard L, Hedley PE, Morris JA, Zhao Y, Sundin GW. 2012. Genetic characterization of the HrpL regulon of the fire blight pathogen Erwinia amylovora reveals novel virulence factors. Molecular Plant Pathology 13:160-173.

117. Wei Z-M, Beer SV. 1995. hrpL activates Erwinia amylovora hrp gene transcription and is a member of the ECF subfamily of sigma factors. Journal of Bacteriology 177:6201-6210.

118. Du Z, Geider K. 2002. Characterization of an activator gene upstream of lsc, involved in levan synthesis of Erwinia amylovora. Physiological and molecular plant pathology 60:9-17.

119. Zhao Y, Wang D, Nakka S, Sundin GW, Korban SS. 2009. Systems level analysis of two-component signal transduction systems in Erwinia amylovora: role in virulence, regulation of amylovoran biosynthesis and swarming motility. BMC genomics 10:245.

120. Datsenko KA, Wanner BL. 2000. One-step inactivation of chromosomal genes in Escherichia coli K-12 using PCR products. Proceedings of the National Academy of Sciences 97:6640-6645.

121. Bak G, Lee J, Suk S, Kim D, Lee JY, Kim K-s, Choi B-S, Lee Y. 2015. Identification of novel sRNAs involved in biofilm formation, motility, and fimbriae formation in Escherichia coli. Scientific reports 5:15287.

122. Abràmoff MD, Magalhães PJ, Ram SJ. 2004. Image processing with ImageJ. Biophotonics international 11:36-42.

123. Bellemann P, Bereswill S, Berger S, Geider K. 1994. Visualization of capsule formation by Erwinia amylovora and assays to determine amylovoran synthesis. International Journal of Biological Macromolecules 16:290-296.

124. Hildebrand M, Aldridge P, Geider K. 2006. Characterization of hns genes from Erwinia amylovora. Molecular genetics and genomics 275:310-319.

125. Santander RD, Biosca EG. 2017. Erwinia amylovora psychrotrophic adaptations: evidence of pathogenic potential and survival at temperate and low environmental temperatures. PeerJ 5:e3931.

126. Iwase T, Tajima A, Sugimoto S, Okuda K-i, Hironaka I, Kamata Y, Takada K, Mizunoe Y. 2013. A simple assay for measuring catalase activity: a visual approach. Scientific reports 3:3081.

127. Chung C, Niemela SL, Miller RH. 1989. One-step preparation of competent Escherichia coli: transformation and storage of bacterial cells in the same solution. Proceedings of the National Academy of Sciences 86:2172-2175.

128. Huynh TV, Dahlbeck D, Staskawicz BJ. 1989. Bacterial blight of soybean: regulation of a pathogen gene determining host cultivar specificity. Science 245:1374-1377.

129. Metsalu T, Vilo J. 2015. ClustVis: a web tool for visualizing clustering of multivariate data using Principal Component Analysis and heatmap. Nucleic acids research 43:W566-W570.

130. Dunn OJ. 1961. Multiple comparisons among means. Journal of the American statistical association 56:52-64.

131. Schachterle JK, Zeng Q, Sundin GW. 2019. Three Hfq-dependent small RNA s regulate flagellar motility in the fire blight pathogen Erwinia amylovora. Molecular microbiology.

132. Barny M-A. 1995. Erwinia amylovora hrpN mutants, blocked in harpin synthesis, express a reduced virulence on host plants and elicit variable hypersensitive reactions on tobacco. European Journal of Plant Pathology 101:333-340.

133. Baker CJ, Orlandi EW, Mock NM. 1993. Harpin, an elicitor of the hypersensitive response in tobacco caused by Erwinia amylovora, elicits active oxygen production in suspension cells. Plant Physiology 102:1341-1344.

134. Wei Z-M, Laby RJ, Zumoff CH, Bauer DW, He SY, Collmer A, Beer SV. 1992. Harpin, elicitor of the hypersensitive response produced by the plant pathogen Erwinia amylovora. Science 257:85-88.

135. Metzger M, Bellemann P, Schwartz T, Geider K. 1992. Site-directed and transposon-mediated mutagenesis with pfd-plasmids by electroporation of Erwinia amylovora and Escherichia coli cells. Nucleic acids research 20:2265-2270.

136. Bauer DW. 1991. Molecular genetics of pathogenicity of Erwinia amylovora: Techniques, tools and their application.

137. Geider K. 2000. Exopolysaccharides of Erwinia: amylovora: Structure, Biosynthesis, Regulation, Role in Pathogenicity of. Fire blight: the disease and its causative agent, Erwinia amylovora:117.

138. Zhang YF, Han K, Chandler CE, Tjaden B, Ernst RK, Lory S. 2017. Probing the sRNA regulatory landscape of P. aeruginosa: post-transcriptional control of determinants of pathogenicity and antibiotic susceptibility. Molecular microbiology 106:919-937.

139. Han K, Tjaden B, Lory S. 2017. GRIL-seq provides a method for identifying direct targets of bacterial small regulatory RNA by in vivo proximity ligation. Nature microbiology 2:16239.

140. Miya A, Albert P, Shinya T, Desaki Y, Ichimura K, Shirasu K, Narusaka Y, Kawakami N, Kaku H, Shibuya N. 2007. CERK1, a LysM receptor kinase, is essential for chitin elicitor signaling in Arabidopsis. Proceedings of the National Academy of Sciences 104:19613-19618.

141. Chinchilla D, Zipfel C, Robatzek S, Kemmerling B, Nürnberger T, Jones JD, Felix G, Boller T. 2007. A flagellin-induced complex of the receptor FLS2 and BAK1 initiates plant defence. Nature 448:497.

142. Kunze G, Zipfel C, Robatzek S, Niehaus K, Boller T, Felix G. 2004. The N terminus of bacterial elongation factor Tu elicits innate immunity in Arabidopsis plants. The Plant Cell 16:3496-3507.

143. Melotto M, Underwood W, Koczan J, Nomura K, He SY. 2006. Plant stomata function in innate immunity against bacterial invasion. Cell 126:969-980.

144. Heese A, Hann DR, Gimenez-Ibanez S, Jones AM, He K, Li J, Schroeder JI, Peck SC, Rathjen JP. 2007. The receptor-like kinase SERK3/BAK1 is a central regulator of innate immunity in plants. Proceedings of the National Academy of Sciences 104:12217-12222.

145. Thilmony R, Underwood W, He SY. 2006. Genome-wide transcriptional analysis of the Arabidopsis thaliana interaction with the plant pathogen Pseudomonas syringae pv. tomato DC3000 and the human pathogen Escherichia coli O157: H7. The Plant Journal 46:34-53.

146. Bolwell GP, Wojtaszek P. 1997. Mechanisms for the generation of reactive oxygen species in plant defence–a broad perspective. Physiological and Molecular Plant Pathology 51:347-366.

147. Guo M, Tian F, Wamboldt Y, Alfano JR. 2009. The majority of the type III effector inventory of Pseudomonas syringae pv. tomato DC3000 can suppress plant immunity. Molecular Plant-Microbe Interactions 22:1069-1080.

148. He SY. 1998. Type III protein secretion systems in plant and animal pathogenic bacteria. Annual review of phytopathology 36:363-392.

149. Jamir Y, Guo M, Oh HS, Petnicki-Ocwieja T, Chen S, Tang X, Dickman MB, Collmer A, R. Alfano J. 2004. Identification of Pseudomonas syringae type III effectors that can suppress programmed cell death in plants and yeast. The Plant Journal 37:554-565.

150. Toruño TY, Stergiopoulos I, Coaker G. 2016. Plant-pathogen effectors: cellular probes interfering with plant defenses in spatial and temporal manners. Annual review of phytopathology 54:419-441.

151. Berry MC, McGhee GC, Zhao Y, Sundin GW. 2009. Effect of a waaL mutation on lipopolysaccharide composition, oxidative stress survival, and virulence in Erwinia amylovora. FEMS microbiology letters 291:80-87.

152. Geier G, Geider K. 1993. Characterization and influence on virulence of the levansucrase gene from the fireblight pathogen Erwinia amylovora. Physiological and Molecular Plant Pathology 42:387-404.

153. Zhao Y, He S-Y, Sundin GW. 2006. The Erwinia amylovora avrRpt2EA gene contributes to virulence on pear and AvrRpt2EA is recognized by Arabidopsis RPS2 when expressed in Pseudomonas syringae. Molecular plant-microbe interactions 19:644-654.

154. Dellagi A, Brisset M-N, Paulin J-P, Expert D. 1998. Dual role of desferrioxamine in Erwinia amylovora pathogenicity. Molecular plant-microbe interactions 11:734-742.

155. Aldridge P, Metzger M, Geider K. 1997. Genetics of sorbitol metabolism in Erwinia amylovora and its influence on bacterial virulence. Molecular and General Genetics MGG 256:611-619.

156. Danhorn T, Fuqua C. 2007. Biofilm formation by plant-associated bacteria. Annu Rev Microbiol 61:401-422.

157. D'Haeze W, Holsters M. 2004. Surface polysaccharides enable bacteria to evade plant immunity. Trends in microbiology 12:555-561.

158. Kamber T, Buchmann JP, Pothier JF, Smits TH, Wicker T, Duffy B. 2016. Fire blight disease reactome: RNA-seq transcriptional profile of apple host plant defense responses to Erwinia amylovora pathogen infection. Scientific reports 6:21600.

159. Rivas R, Vizcaíno N, Buey RM, Mateos PF, Martínez-Molina E, Velázquez E. 2001. An effective, rapid and simple method for total RNA extraction from bacteria and yeast. Journal of microbiological methods 47:59-63.

160. Bolger AM, Lohse M, Usadel B. 2014. Trimmomatic: a flexible trimmer for Illumina sequence data. Bioinformatics 30:2114-2120.

161. Sebaihia M, Bocsanczy A, Biehl B, Quail M, Perna N, Glasner J, DeClerck G, Cartinhour S, Schneider D, Bentley S. 2010. Complete genome sequence of the plant pathogen Erwinia amylovora strain ATCC 49946. Journal of bacteriology 192:2020-2021.

162. Langmead B, Salzberg SL. 2012. Fast gapped-read alignment with Bowtie 2. Nature methods 9:357.

163. Li H, Handsaker B, Wysoker A, Fennell T, Ruan J, Homer N, Marth G, Abecasis G, Durbin R. 2009. The sequence alignment/map format and SAMtools. Bioinformatics 25:2078-2079.

164. Anders S, Pyl PT, Huber W. 2015. HTSeq—a Python framework to work with high-throughput sequencing data. Bioinformatics 31:166-169.

165. Anders S, Huber W. 2012. Differential expression of RNA-Seq data at the gene level–the DESeq package. Heidelberg, Germany: European Molecular Biology Laboratory (EMBL).

166. Livak KJ, Schmittgen TD. 2001. Analysis of relative gene expression data using real-time quantitative PCR and the 2− ΔΔCT method. methods 25:402-408.

167. Junglee S, Urban L, Sallanon H, Lopez-Lauri F. 2014. Optimized assay for hydrogen peroxide determination in plant tissue using potassium iodide. American Journal of Analytical Chemistry 5:730.

168. Urban JH, Vogel J. 2007. Translational control and target recognition by Escherichia coli small RNAs in vivo. Nucleic acids research 35:1018-1037.

169. García-Nafría J, Watson JF, Greger IH. 2016. IVA cloning: a single-tube universal cloning system exploiting bacterial in vivo assembly. Scientific reports 6:27459.

170. Miller WG, Leveau JH, Lindow SE. 2000. Improved gfp and inaZ broad-host-range promoter-probe vectors. Molecular Plant-Microbe Interactions 13:1243-1250.

171. Gama-Castro S, Salgado H, Peralta-Gil M, Santos-Zavaleta A, Muniz-Rascado L, Solano-Lira H, Jimenez-Jacinto V, Weiss V, Garcia-Sotelo JS, Lopez-Fuentes A. 2010. RegulonDB version 7.0: transcriptional regulation of Escherichia coli K-12 integrated within genetic sensory response units (Gensor Units). Nucleic acids research 39:D98-D105.

172. Blattner FR, Plunkett G, Bloch CA, Perna NT, Burland V, Riley M, Collado-Vides J, Glasner JD, Rode CK, Mayhew GF. 1997. The complete genome sequence of Escherichia coli K-12. science 277:1453-1462.

173. Camacho C, Coulouris G, Avagyan V, Ma N, Papadopoulos J, Bealer K, Madden TL. 2009. BLAST+: architecture and applications. BMC bioinformatics 10:421.

174. Kanehisa M, Goto S. 2000. KEGG: kyoto encyclopedia of genes and genomes. Nucleic acids research 28:27-30.

175. Fahnenstich H, Scarpeci TE, Valle EM, Flügge U-I, Maurino VG. 2008. Generation of hydrogen peroxide in chloroplasts of Arabidopsis overexpressing glycolate oxidase as an inducible system to study oxidative stress. Plant Physiology 148:719-729.

176. Rojas CM, Mysore KS. 2012. Glycolate oxidase is an alternative source for H2O2 production during plant defense responses and functions independently from NADPH oxidase. Plant signaling & behavior 7:752-755.

177. Rojas CM, Senthil-Kumar M, Wang K, Ryu C-M, Kaundal A, Mysore KS. 2012. Glycolate oxidase modulates reactive oxygen species–mediated signal transduction during nonhost resistance in Nicotiana benthamiana and Arabidopsis. The Plant Cell:tpc. 111.093245.

178. Carlioz A, Touati D. 1986. Isolation of superoxide dismutase mutants in Escherichia coli: is superoxide dismutase necessary for aerobic life? The EMBO journal 5:623-630.

179. Montillet J-L, Chamnongpol S, Rustérucci C, Dat J, Van De Cotte B, Agnel J-P, Battesti C, Inzé D, Van Breusegem F, Triantaphylides C. 2005. Fatty acid hydroperoxides and H2O2 in the execution of hypersensitive cell death in tobacco leaves. Plant physiology 138:1516-1526.

180. Krüger J, Rehmsmeier M. 2006. RNAhybrid: microRNA target prediction easy, fast and flexible. Nucleic acids research 34:W451-W454.

181. Hassan HM, Sun H. 1992. Regulatory roles of Fnr, Fur, and Arc in expression of manganese-containing superoxide dismutase in Escherichia coli. Proceedings of the National Academy of Sciences 89:3217-3221.

182. Niederhoffer EC, Naranjo CM, Bradley KL, Fee JA. 1990. Control of Escherichia coli superoxide dismutase (sodA and sodB) genes by the ferric uptake regulation (fur) locus. Journal of bacteriology 172:1930-1938.

183. Compan I, Touati D. 1994. Anaerobic activation of arcA transcription in Escherichia coli: roles of Fnr and ArcA. Molecular microbiology 11:955-964.

184. Benov L, Sequeira F. 2003. Escherichia coli Δ fur mutant displays low HPII catalase activity in stationary phase. Redox report 8:379-383.

185. Mettert EL, Kiley PJ. 2007. Contributions of [4Fe-4S]-FNR and integration host factor to fnr transcriptional regulation. Journal of bacteriology 189:3036-3043.

186. Tyson K, Bell A, Cole J, Busby S. 1993. Definition of nitrite and nitrate response elements at the anaerobically inducible Escherichia coli nirB promoter: interactions between FNR and NarL. Molecular microbiology 7:151-157.

187. Stojiljkovic I, Bäumler AJ, Hantke K. 1994. Fur regulon in gram-negative bacteria: identification and characterization of new iron-regulated Escherichia coli genes by a Fur titration assay. Journal of molecular biology 236:531-545.

188. Park DM, Akhtar MS, Ansari AZ, Landick R, Kiley PJ. 2013. The bacterial response regulator ArcA uses a diverse binding site architecture to regulate carbon oxidation globally. PLoS genetics 9:e1003839.

189. Iuchi S, Matsuda Z, Fujiwara T, Lin E. 1990. The arcB gene of Escherichia coli encodes a sensor-regulator protein for anaerobic repression of the arc modulon. Molecular microbiology 4:715-727.

190. Bekker M, Alexeeva S, Laan W, Sawers G, De Mattos JT, Hellingwerf K. 2010. The ArcBA two-component system of Escherichia coli is regulated by the redox state of both the ubiquinone and the menaquinone pool. Journal of bacteriology 192:746-754.

191. Venisse J-S, Malnoy M, Faize M, Paulin J-P, Brisset M-N. 2002. Modulation of defense responses of Malus spp. during compatible and incompatible interactions with Erwinia amylovora. Molecular Plant-Microbe Interactions 15:1204-1212.

192. Venisse J-S, Barny M-A, Paulin J-P, Brisset M-N. 2003. Involvement of three pathogenicity factors of Erwinia amylovora in the oxidative stress associated with compatible interaction in pear. FEBS letters 537:198-202.

193. Iakimova ET, Sobiczewski P, Michalczuk L, Węgrzynowicz-Lesiak E, Mikiciński A, Woltering EJ. 2013. Morphological and biochemical characterization of Erwinia amylovora-induced hypersensitive cell death in apple leaves. Plant physiology and biochemistry 63:292-305.

194. Gansert D. 2003. Xylem sap flow as a major pathway for oxygen supply to the sapwood of birch (Betula pubescens Ehr.). Plant, Cell & Environment 26:1803-1814.

195. Kim SJ, Han YH, Kim IH, Kim HK. 1999. Involvement of ArcA and Fnr in expression of Escherichia coli thiol peroxidase gene. IUBMB life 48:215-218.

196. Bouvier J, Gordia S, Kampmann G, Lange R, Hengge-Aronis R, Gutierrez C. 1998. Interplay between global regulators of Escherichia coli: effect of RpoS, Lrp and H-NS on transcription of the gene osmC. Molecular microbiology 28:971-980.

197. Shade A, McManus PS, Handelsman J. 2013. Unexpected diversity during community succession in the apple flower microbiome. MBio 4:e00602-12.